Advances in Capillary Electrophoresis Using Microfluidics

Inauguraldissertation

zur

Erlangung der Würde eines Doktors der Philosophie

vorgelegt der

Philosophisch-Naturwissenschaftlichen Fakultät

der Universität Basel

von

Israel Joel Koenka

von

Israel

Basel, 2017

Genehmigt von der Philosophisch-Naturwissenschaftlichen Fakultät

auf Antrag von

Prof. Peter C. Hauser

und

Prof. Wolfgang Thormann

Basel, den 18.04.2017

<div align="center">

Prof. Dr. Martin Spiess

Dekan

</div>

List of Abbreviations

ADC	analog-to-digital converter
API	application programming interface
BGE	background electrolyte
C4D	capacitively coupled contactless conductivity detection
CE	capillary electrophoresis
CZE	capillary zone electrophoresis
DAC	digital-to-analog converter
DETA	diethylenetriamine
EF	enhancement factor
EFGF	electric field gradient focusing
EKI	electrokinetic injection
EOF	electroosmotic flow
FASI	field amplified sample injection (also known as FESI)
FASS	field amplified sample stacking
GC	gas chromatography
GEMBE	gradient elution moving boundary electrophoresis
HDI	hydrodynamic injection
HPLC	high performance liquid chromatography
HV	high voltage
i.d.	inner diameter
IEF	iso-electric focusing
I^2C	inter-integrated circuit

I/O	input/output
ITP	isotachophoresis
LE	leading electrolyte
LOC	lab on chip
LOD	limit of detection
LPA	linear polyacrylamide
LVSS	large volume sample stacking
MEKC	micellar electrokinetic chromatography
μTAS	miniature total analysis system
o.d.	outer diameter
PACE	pressure assisted capillary electrophoresis
PAEKI	pressure assisted electrokinetic injection
PC	personal computer
PEEK	polyetheretherketone
PMMA	poly(methyl methacrylate)
SIA	sequential injection analysis
SPE	solid phase extraction
SPI	serial peripheral interface
TE	tailing electrolyte
TGF	temperature gradient focusing
tITP	transient isotachophoresis
TTL	transistor-transistor logic

Summary

This thesis focuses on instrumental advances in microfluidics-based capillary electrophoresis systems for achieving various goals.

Microfluidics systems and purpose-made scientific instruments in general may consist of many different hardware units, often made by different companies. This presents a challenge for system builders who want to efficiently build and use purpose-made instruments for conducting scientific experiments. As this challenge was relevant for all of the projects described in this thesis, it was the first one to be tackled by the development of the software package Instrumentino. The package allows system builders to build a useful graphical user interface (GUI) for their experimental setups, allowing automation of multiple components controlled by separate microcontrollers. A Code could be reused between projects using the same hardware units. Instrumentino was eventually used in all of the projects in this thesis, and while it required a lot of invested time for its development, it saved a lot of time in running experiments afterwards.

The first CE systems built for this thesis were for a collaborative project about the use of a C^4D cell array for following after separation processes, and comparing them to computer simulations. It was first (using 16 detectors) employed for CZE separations of inorganic anions and cations for the sake of demonstration, and later (using 8 detectors) for investigating CZE and ITP separations in linear polyacrylamide (LPA) coated silica capillaries, exhibiting a very low EOF.

Another issue discussed in this thesis is the implementation of concurrent CZE separations for anions and cations in portable systems. Two multi-channel portable CE instruments were built in collaboration with others and two review publications were written on the subject of concurrent determination of anions and cations (also a collaboration).

Relying on the experience gained from building the previous systems, a new approach for building electrophoretic separation systems was developed, based on a commercial breadboard system for miniaturized microfluidic parts, offering high design flexibility and small size as in lab-on-chip systems, yet using standard silica capillaries and obtaining comparable results to commercial CE instruments. The applicability of this

method was exemplified by the implementation of various electrophoretic experiments using the same building blocks. This approach proved to be very useful and was later employed for all following projects, enabling a quick realization of new designs in a miniaturized way.

A third multi-channel portable CE system was developed, offering a thermostated chamber in which separations took place and a new microfluidic design which employed a syringe pump for pressurization, enabling, among other things, a special semi-automatic mode for analyzing volume-limited samples. It was used to determine concentrations of target ions in groundwater and mine water samples in an abandoned mining site in Argentina, as well as the determination of inorganic ions in sediment porewater from Lake Baldegg in Switzerland. In parallel, another desktop system was developed for the semi-automatic analysis of volume-limited samples, employing a micro syringe for sample introduction.

Finally, a novel fully automated pre-concentration approach for CE was developed, employing a purpose-made microfluidic trapping block in which a hydrodynamic flow can be applied in a channel alongside an electric field that induces electrophoretic flow of the target ions in the opposite direction. A discontinuity in the target ions' electrophoretic flow in the channel results in a trapping point for these ions, to which their net flow is directed to from both sides (upstream and downstream). This is achieved by applying the trapping voltage through ion-exchange membranes, which only pass ions of opposite charge than that of the target ions. This trapping block was coupled to a capillary inlet, so that it could be injected and be separated in it, automatically. This approach was found to be applicable also for high conductivity samples (up to 0.1 M), which is unique as most pre-concentration approaches that are based on electrokinetic phenomena are limited to low conductivity samples. Furthermore, the system allows selectively trapping ions with mobilities over a certain level, determined by the relative strengths of the applied hydrodynamic flow and electric field.

Table of Contents

1   Introduction

1.1   Capillary zone electrophoresis

1.1.1   Basic principles

Capillary zone electrophoresis (CZE) belongs to a family of electrophoretic separation methods that employ narrow channels and a high voltage that is applied across them (ITP, IEF, MEKC, etc.). The narrow channel allows high voltages to be used without incurring high currents, which are undesirable as they heat up the capillary and deteriorate separation efficiency. The narrow channel also allows very small sample volumes to be analyzed, which is one of the hallmarks of capillary electrophoresis.

The basic operation mode of CZE is the following:

- Filling the capillary with background electrolyte (BGE)
- Injection of a sample plug to the capillary (normally around 1% of the capillary length)
- Placing the two capillary ends in BGE reservoirs and applying an electric field between them.

As the ions travel from the sample plug towards the opposite electrode, a detector, which is placed either somewhere along the capillary or at its end, records its signal as a function of time, to produce an electropherogram.

The applied electric field induces ion migration in the capillary towards the electrodes and ions are separated due to their different electrophoretic mobilities under the influence of the electric field, as shown by the equation:

$$(1) \; v = \mu_e \times E$$

v: electrophoretic velocity

μ_e: electrophoretic mobility

E: applied electric field

Electrophoretic mobilities depend on an ion's charge, as well as on the frictional force it experiences in solution, which depend on its effective size (including hydration shells) in

the capillary. For a steady state, where the electrokinetic force equals the frictional force (approximated by Stokes law), an ion's mobility is given by the following equation (for a spherical ion):

$$(2) \quad \mu_e = \frac{q}{6 \times \pi \times \eta \times r}$$

q : ion's charge

η : media viscosity

r : ion's effective radius

Therefore, the mobilities of ions depend on their charge to size ratio, and the bigger this ratio differs between ions, the easier and faster they separate. CZE is normally performed in narrow capillaries with diameters in the range of 10-100 µm. The surface properties of the capillary's inner wall have a considerable effect on transport phenomena such as electro-osmotic flow.

1.1.2   Electro-osmotic flow

In fused silica capillaries, which are most commonly used in CZE, the presence of silanol groups (SiO⁻) at the capillary wall make it negatively charged. Cations in solution are attracted to the walls and create a double layer together with the negatively charged silanol groups. The cation layer is composed of a Stern layer, which closely adheres to the surface and a diffuse layer (also called the Gouy-Chapman layer) [1, 2]. Upon application of an electric field, the cations in the diffuse layer migrate towards the cathode and drag with them the solution in the capillary, creating the so called electro-osmotic flow (EOF). As the driving force for EOF comes from the capillary walls, the flow profile is that of a plug, in contrast to laminar flow where friction with surrounding walls result in a parabolic flow profile. This is crucial for CZE operation, as flows with a non-flat profile contribute to band broadening, working against the separation process. EOF strength is determined by the capillary wall surface and the resulting double layer, and is described for the simple case of no externally applied pressure and uniform surface and solution properties by the Helmholtz-Smoluchowski equation [2] (more complicated cases require a different treatment [3-5]):

$$(3)\ v_{EOF} = (\varepsilon\zeta / \eta)E$$

$$(4)\ \mu_{EOF} = \varepsilon\zeta / \eta$$

v_{EOF} : EOF velocity

μ_{EOF} : EOF mobility

ε : dielectric constant

ζ : zeta potential

η : viscosity

E : electric field

The electrical potential diminishes exponentially in the diffuse layer and the potential difference across it is called the zeta potential. Its magnitude is determined by the solution and wall characteristics such as the solution concentration, its pH and the presence of surfactants. At high pH levels the silanol groups are all charged, resulting in a high zeta potential and a high EOF, while at low pH levels, the silanol groups are protonated, and therefore do not induce a high EOF. Dynamic or permanent coating of the capillary's inner walls may be used for modifying and even reversing the EOF by changing the effective wall charge (seen by the bulk solution) [2].

The EOF adds up to the flow of all ions in the capillary, sometimes even reversing their direction (as in the case of slow anions). The presence of EOF and the ability to change it adds another configuration dimension to CZE, and it may be used for altering analytes' mobilities intentionally. For example, a strong EOF (by using a high pH buffer) may be used to reverse the effective migration direction of slow anions, forcing them to travel towards the cathode and allowing their concurrent determination with the cations in the sample [6].

1.1.3   Broadening mechanisms

In CZE, analyte zones gradually separate from each other as they migrate and ideally, given a long enough capillary (and enough time) they would all separate from each other. Alas, there are mechanisms that act against the separation, broadening the zones

as they migrate, making it harder and sometimes even impossible to separate analyte zones.

One such mechanism is longitudinal diffusion. During the time of separation, diffusion also occurs and its longitudinal part (along the channel) broadens zone edges, making them more diffuse. As any diffusive process, this mechanism is more pronounced at higher temperatures and when the viscosity is lower.

Another temperature related broadening mechanism is Joule heating. Since electrical current passes through the capillary during separation, it heats up the solution and elevates the temperature in the capillary. Not only does this higher temperature increase the effect of longitudinal diffusion, it also creates temperature gradients inside the capillary since the temperature out of the capillary is normally lower. Temperature variations lead to viscosity variations, which in turn lead mobility variations in the capillary cross section.
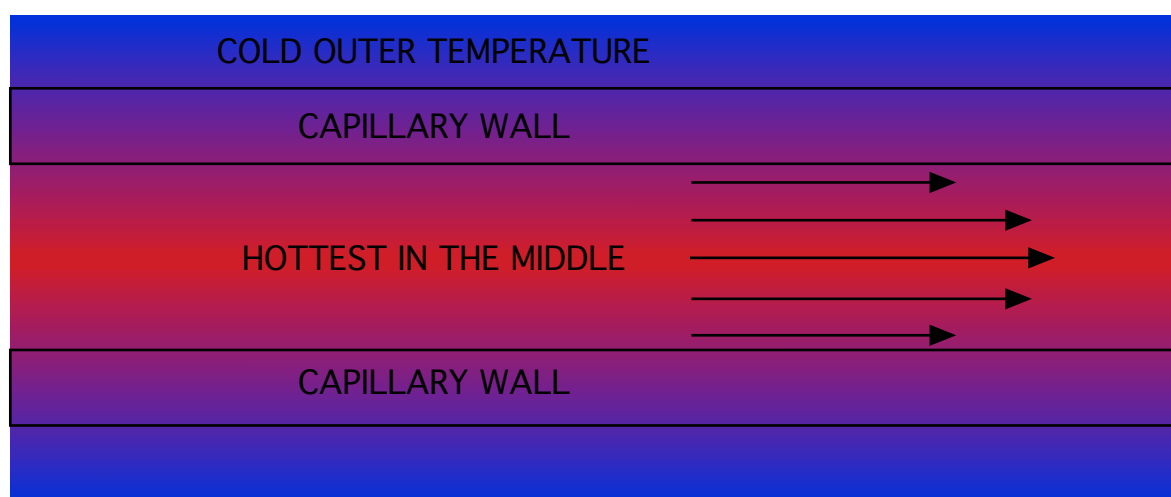
Fig. 1: Joule heating broadening. The arrows in the capillary depict the ion mobility variability due to differences in viscosity.

One way to reduce the effect of Joule heating broadening is to use very narrow capillaries (e.g. 10 μm i.d.). By shortening the capillary cross-section, smaller temperature gradients may evolve so less Joule heating broadening is observed. Moreover, the smaller cross-section allows less current to pass, which further reduces broadening by this mechanism.

In CZE, electro-neutrality is kept when analyte ions migrate through the capillary by the presence of the buffered BGE. Analyte ions "replace" background buffer co-ions as they migrate by acid-base reactions of the co-ions. This leads to higher or lower conductivities in analyte zones, for analytes that have a higher or lower mobility than the co-ion they're replacing respectively. These abrupt changes in conductivity cause proportional changes in the electric field strength, and is the cause for the phenomena called electrodispersion. Electrodispersion is the process in which analyte ions in low conductivity zones experience higher electric fields than out of the zone, forcing them to accelerate to the zone's end and to create so-called "tailed peaks", while analyte ions in high conductivity zones decelerate to the zone's beginning, creating "fronted peaks". In both cases the zones develop tails which broaden the zone and interfere with its separation from other zones.

MIGRATION DIRECTION
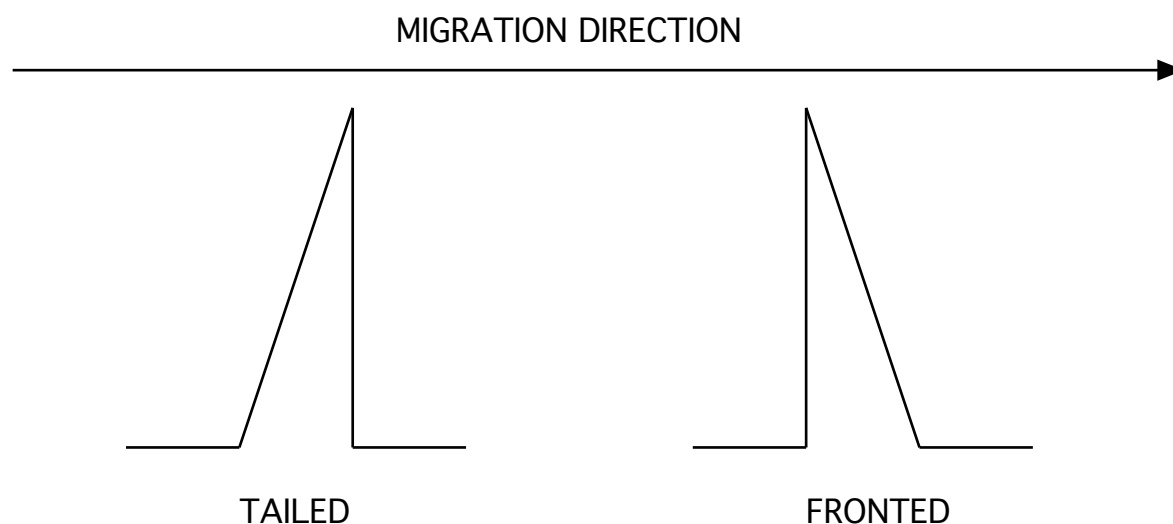
TAILED   FRONTED

Fig. 2: Tailed and fronted peaks in an electropherogram due to electrodispersion.

Another possible broadening mechanism is analyte adsorption to the capillary wall, causing the zones to tail. This is more common for proteins with positively charged sites, adsorbing on the negatively charged capillary walls [7]. The best way to avoid electrodispersion is to choose the buffer co-ion to have a similar mobility to the target analytes. Yet it's important to keep it not too close when using conductivity detection, as it's exactly this difference that the detector measures (more below).

Zone broadening may also happen due to the existence of a laminar flow. This might happen unintentionally when the two BGE reservoirs in which the capillary ends are dipped are not leveled and gravitation creates a pressure difference across the capillary,

inducing a laminar flow through the capillary. As laminar flow has a parabolic flow profile, all of the zones in the capillary become broader at the same time. One way to avoid that is to make sure buffer levels on both containers are even. Another way which reduces the impact of laminar flow broadening is to use a very narrow capillary, as the narrower the capillary i.d. is, the smaller the resulting flow gradients across the capillary diameter [8].

Analyte zones may be broadened because of complexation equilibria because the complexed and non-complexed species have different mobilities. This effect is less prominent when the complexing agent's concentration is high enough (compared to the target analyte) "to saturate" almost all of the analytes [9].

Last but not least, the detector itself has a strong impact on the apparent width of analyte zones. A detector that probes a large area may produce a very high signal, but at the same time effectively lower the separation resolution. The probing window of a detector should be just as big to let produce enough signal strength but small enough to allow the separate detection of neighboring zones.

1.1.4 Detection methods

The most popular detection methods for CE are optical detection such as absorption and fluorescence detection, as well as capacitively coupled contactless conductivity detection (C^4D). There are also others such as mass spectrometry (MS) and other electrochemical detection methods, yet only C^4D will be described here at length as it's the only method used for the works presented herein. Both C^4D and optical detection methods have the advantage that physical contact with the liquids in the capillary is not required. This helps to avoid complications with chemical interactions between detector parts (e.g. electrodes) and the capillary's content and is generally quite comfortable since the detector can be placed anywhere along the capillary. Optical detection has the advantage of being selective for absorbing analytes and therefore usually produces a straight baseline, but it has the disadvantage that very narrow capillaries (i.d. < 50 μm) can't be used due to the shortened light path length in them (Beer-Lambert's law). The selectiveness of optical detectors may also be a disadvantage as not all analytes can be detected directly.

C^{4}D cells, on the other hand, are considered as "bulk" detectors because they provide a signal to any conductivity change, not only due to analyte zones. It allows to detect all ionic species but may also lead to baseline drifts, for example due to electrolysis products migrating from the outlet BGE vial. When using C^{4}D, it's important to choose the BGE co-ion so that its mobility is different enough from the target analytes. If it's too similar, the conductivities of analyte zones, in which BGE co-ions are replaced with analyte ions, will be too similar to that of the BGE, and the resulting detector signal will be very low. On the other hand, choosing a co-ion that is too different would make electromigration more pronounced, and indeed having electromigration dispersion when using C^{4}D is unavoidable.

In C^{4}D, the conductivity of the solution between the two electrodes is indirectly measured by applying an AC field between in the excitation electrode and reading the AC current in the pick-up electrode (using an operational amplifier). The inter-electrode distance is usually in the order of 1 mm to assure enough spatial resolution yet have a strong enough signal [10]. A schematic representation of the C^{4}D principle is shown in Fig. 3. A Faraday shield between the two electrodes, through which the capillary passes reduces direct coupling between the electrodes (through the air). Such coupling is called stray capacitance and it severely affects the behavior of C^{4}D cells.
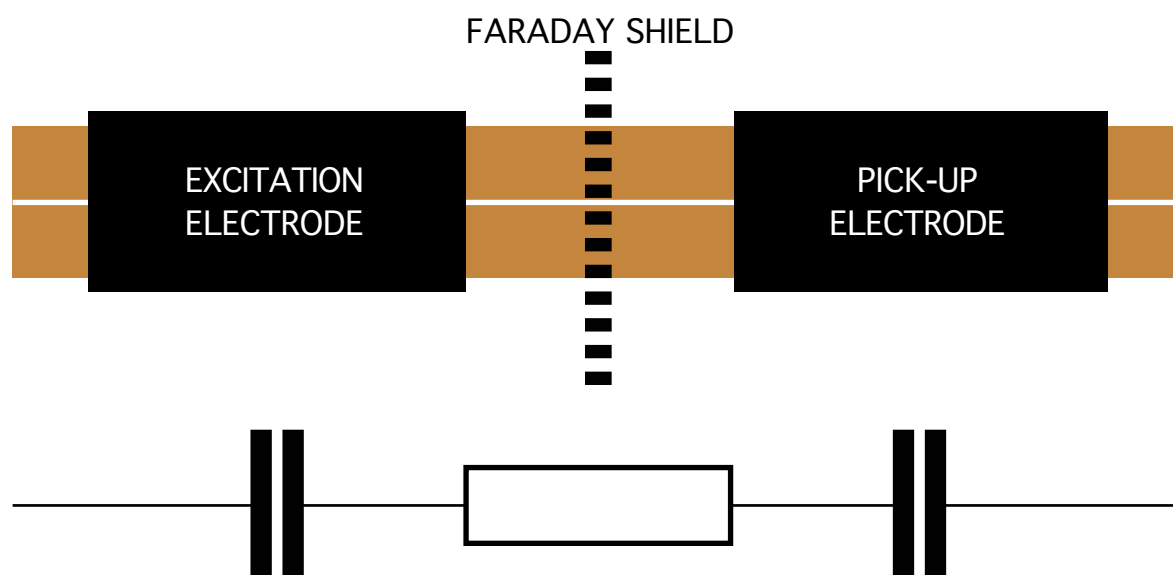

Fig. 3: Schematic drawing of C^{4}D electrodes around a capillary and an equivalent electrical circuit below.

The tubular electrodes are separated from the conductive solution by the insulating capillary wall, which can be simply modeled as a tubular capacitor. A resistor can be used for modeling the solution in the capillary between the electrodes, the conductivity of which is of interest for the sake of detection. The resulting model circuit for this setup (which of course is only a simplified model) is a resistor in series to two capacitors, as seen in Fig. 3. Applying Ohm's law for AC gives the following equation:

$$(5) \ I = \frac{V}{\sqrt{R^2 + \left(\dfrac{1}{2\pi f C}\right)^2}}$$

I : measured current

V : applied voltage amplitude

f : applied voltage frequency

R : resistance of the probed solution

C : equivalent capacitance of the two tubular capacitors

From the equation, it is apparent that for higher frequencies, the capacitive term diminishes and the measured current becomes more sensitive to changes in the probed solution's resistance. Indeed, frequencies in the range of hundreds of kHz are regularly used in C^4D cells.

C^4D is very fit for use with CZE since its sensitivity doesn't suffer as other methods do for the small scales of the capillary (e.g. optical methods). This happens because both the signal and the noise decrease, leaving the signal-to-noise ratio almost unchanged. This is an important advantage as the narrower the capillary, the less Joule heating related band broadening occurs and higher separation resolutions may be reached. Furthermore, in capillaries with narrow inner diameter, the broadening effect of laminar flow is less pronounced, and it was shown that when using capillaries with inner diameters as low as 10 μm, pressure may be successfully used without a significant penalty in separation resolution. An example where pressure application may be beneficial is when the required ions for analysis contain a group of fast ions that quickly separate and reach the detector and some slower ions that reach the detector considerably later. Applying a pressure step after the first group of ions was detected

can be used to "fast forward" empty or uninteresting parts of the electropherogram, pushing the slower ions faster towards the detector [8, 11, 12].

1.1.5   Injection methods in CE

One of the critical aspects for performing CE properly and reproducibly is the sample injection. Any issue with the injected sample plug, such as diffuse boundaries, or inability to reproduce the injected plug in consecutive separation has detrimental effects on the results' quality. Technically, it is very easy to control electronically the applied high voltage and the amount of time it is applied, but handling such small amounts of liquid is more tricky and demands special attention.

There are principally two ways for injecting sample in CE: electrokinetic injection (EKI) and hydrodynamic injection (HDI). In EKI, a high voltage (but not as high as the separation voltage) is applied for a short time in order to pull ions into the capillary. This is very easily implemented as every CE system has the ability to apply high voltages and it can be fully automated and electronically controlled. But this injection method has the disadvantage that ions are injected into the capillary according to their electrophoretic mobility (more high mobility ions are injected than low mobility ions). Low mobility target ions require long injections and in this time higher amounts of high mobility ions are injected, which can later disturb the separation.

In hydrodynamic injection however, a plug of sample solution is pushed into the capillary by creating a pressure difference between the two capillary ends, and with it all of the target ions in equal amounts. This can be done either by raising the pressure on the injection end (positive pressure injection), lowering the pressure on the detection end (negative pressure injection) or by elevating the injection end relative to the detection end (siphoning injection). As injection is critical for reproducibility, it is normal to allow injection times of several seconds at least since very short times are harder to reproduce with low variability. At the same time, if the same pressure source is used for capillary flushing, it should be high enough to flush the capillary within a reasonable time (normally a few minutes). This dictates which pressure range is suitable for which capillary, considering its i.d. and its length. Long and narrow capillaries can be used with high pressure sources while short and wide capillaries can be only used with low pressure sources.

Siphoning injection is the simplest way for performing HD injection, as it requires no special equipment and can be done manually. The disadvantage of this approach is that only small pressure differences are achievable, and therefore very narrow capillaries (below 50 μm) are not suitable. Furthermore, when performed manually, siphoning injection has only modest reproducibility and results highly depend on the operator's skills [11]. It is possible however to perform this automatically, either by using a robotic arm which lifts a container with the injection end for a given time, or by coupling the detection end to a lower fluidic level [13].

Positive/negative pressure injections are performed by coupling one of the capillary ends with a pressure/vacuum source while the other end is open to the atmosphere. The technical challenge in these injections depend on the pressure source, as will be discussed in the next section.

1.2   Building automated CE instruments using microfluidics

The field of microfluidics deals with the manipulation of fluids in confined spaces, having at least one dimension between 100 nm and several hundred μm. The first attempts to manipulate such small amounts of liquid happened in the 1950s, and resulted among other things in the ink-jet technology [14]. Since then, many developments have been made in the field, but it was only in the middle of 1990 when interest in this field rose exponentially, much thanks to the article by Manz, Graber and Widmer that coined the term μTAS, standing for miniaturized total analysis systems [15]. This later developed to be part of the lab-on-chip (LOC) concept, as people realized these technologies could be applied for other laboratory purposes other than chemical analysis. One of the earliest applications of μTAS was the use of glass (and later polymer [16]) rectangular chips for performing electrophoretic separations [17] and its still the most common separation techniques performed on chips. An example for such a chip is the well-known cross design, as seen in Fig. 4. Sample injection in the cross chip is done by passing sample solution between the two sample wells, filling a pre-defined part of the longer channel with sample solution. A high voltage is then applied between the two BGE reservoirs to initiate the separation [18].
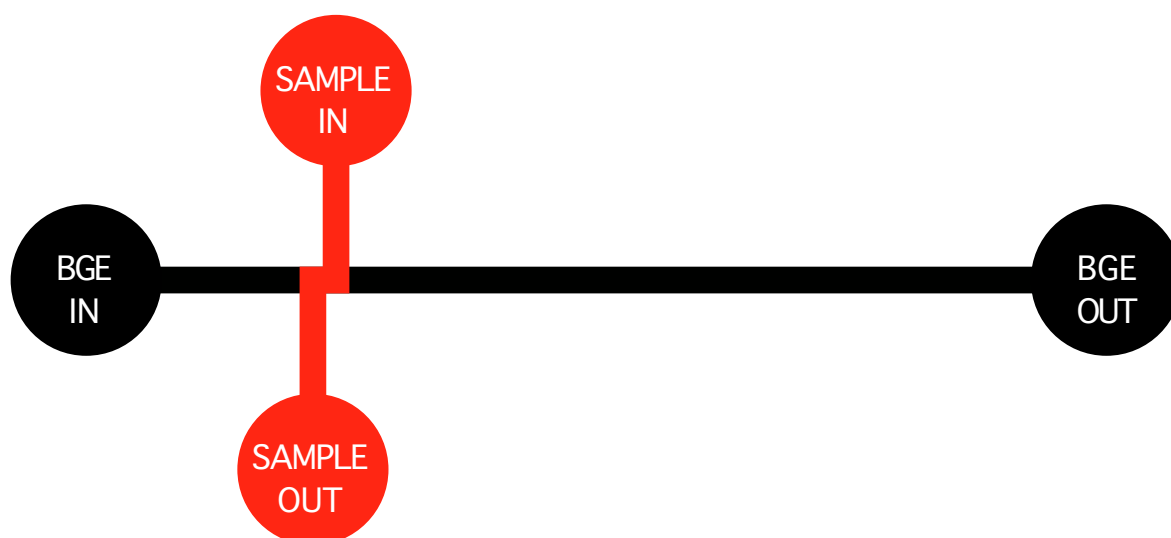
Fig. 4: The basic cross design for microchip electrophoresis. Lines are channels engraved in a the chip and circles are wells for liquid placement.

The μTAS and LOC ideas ignited the imaginations of many researchers as they were promised to open the way to lower the cost and size of lab instruments. Indeed, the chips themselves became cheaper and cheaper, as new production methods were established such as embossing and injection molding. But for a chip based system to be automated, auxiliary hardware is needed (such as pumps and valves for sample introduction) which may not be cheap or small. Chip based electrophoresis also has some practical issues such as siphoning effects when the chip is placed on an uneven plain, geometrical constraints for efficient detection and the need for printing a new chip for every small change needed, such as changing the separation channel length [12]. This lack of flexibility makes electrophoretic microchips less attractive for scientific research, which led to the development of interlocking microfluidic blocks by several groups [19-21].

Another approach to build CE instruments, which doesn't involve the use of microchips is the traditional use of capillaries and periphery hardware, which predated the μTAS and LOC concepts. Capillary-based CE instruments are by far more common on the market than chip based ones and the ability to miniaturize and automate such instruments have been widely demonstrated [22-26].

The efforts required for building an automated capillary-based CE system can be divided to three parts:

- Microfluidic design
- Electronics
- Software development

1.2.1 Microfluidic design

1.2.1.1 Basic concepts

The microfluidics framework is very useful for building CE instruments, as it offers the tools for handling fluids in small amounts and to move them from place to place automatically. The most basic building block in a microfluidic circuit is the channel, which may be engraved in a bulk material in the case of microchips or be simply a tube (usually made of an inert polymer material) or a capillary (usually made of silica and having a smaller i.d. then tubes in the system).

When connecting two microfluidic elements, it is important to make sure that the inner dimensions of the elements fit, to make sure liquids may flow sequentially and avoid turbulences. When a mismatch occurs, dead volumes are created. Volumes are termed "dead" if they are difficult or impossible to flush with new incoming liquids, and their occurrence may disturb the operation of the microfluidic system by reducing the sharpness of liquid-liquid interfaces. Two examples for dead volumes are presented in the figure 5.
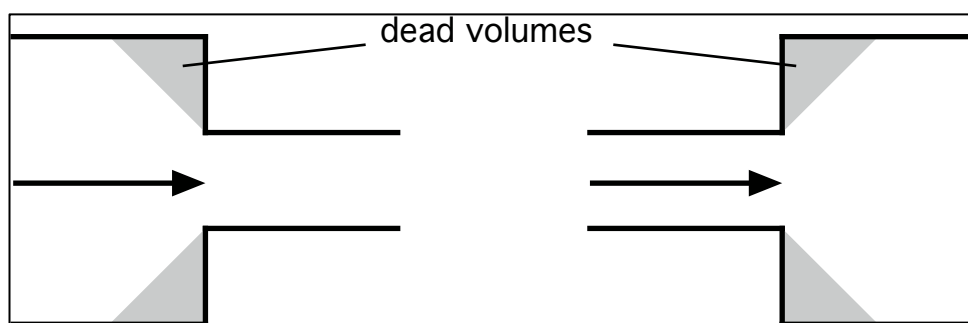

Fig. 5: Examples of dead volumes (marked in grey).

Tubes can be connected to each other by using passive component as interconnects (see Fig. 6A-C) or active components such as valves (see Fig. 6D-F). There are many types of valves, mostly offering 2 states but sometimes more. Syringe pumps provide the driving force to displace liquids in the tubes in a useful manner (see Fig. 6E).
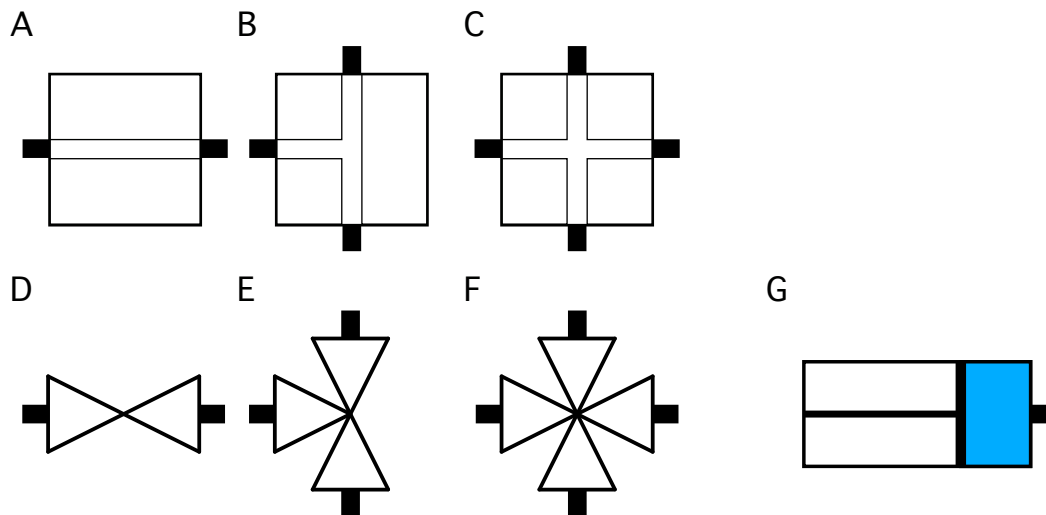
Fig. 6: Different passive and active microfluidics components. Interconnect of types union (A), Tee (B) and cross (C). Schematic symbols for a 2-way (D) 3-way (E) and 4-way (F) valves, and for a syringe pump (G).

Tubes are connected to components by the use of fittings (mostly also made of polymer material). There are several technologies for ensuring a leak-free connection between a tube, a fitting and an interconnect. One of them is to bend (by applying heat) the end of the tube around the flat end of a fitting, so that when the fitting is screwed in tightly, the flat end will press the tube against the interconnect wall, providing a tight fit (as seen in Fig. 7A). The advantage in this technology is that the tube is directly pressed to the interconnect, leaving no route for fluids to leak, but this comes at the cost of widening the tube's ending, which may lead to dead volumes. Moreover, makes tube recycling more difficult when changing a design and it is not so comfortable to use since tubes made of hard polymers, like Polyetheretherketone (PEEK), are harder to bend that way. Another one is to use a flat-end fitting to press a conical ferrule to the interconnect wall, and by that pressing the fitting-ferrule-tube ensemble together (as seen in Fig. 7B). The tight fit in this technology is between the ferrule's flat end and the interconnect's flat wall in front of it, which may result in a dead volume between the tube's end and the interconnect wall. In a third technology, the coned ferrule principle was used to create a single-piece coned fitting (as seen in Fig. 7C). This is the most comfortable one to use as only one piece is needed, and this also enables the miniaturization of the fitting (very small ferrules would be hard to deal with), as was shown by the company LabSmith (www.labsmith.com). The disadvantage of this type of fittings is that more dead volume may occur at the tube-interconnect interface. Furthermore, miniaturized fittings are less

robust and may fail mechanically (for example when over-tightening using a tightening tool).

Inner channels in commercial interconnects usually come at standard sizes (e.g. 0.02" or 0.01") but it isn't always possible to use tubes with the same i.d. so dead volumes may occur at such junctions, regardless of the fitting technology used (as seen in Fig. 7D). Furthermore, it is sometimes required to dip a narrow capillary in a larger channel. Such is the case when a fused silica separation capillary needs to be coupled to a microfluidic circuit in which tube i.d. are necessarily larger (to ensure the capillary can be fitted in). One way to make this coupling is using a standard tube fitting and a sleeve to bridge the gap between the capillary's o.d. (usually around 360 μm) and the i.d. of the interconnect's inner channel (as seen in Fig. 7E). In such cases, many possible dead volumes may occur, depending on how deep the sleeve and the capillary are inserted.
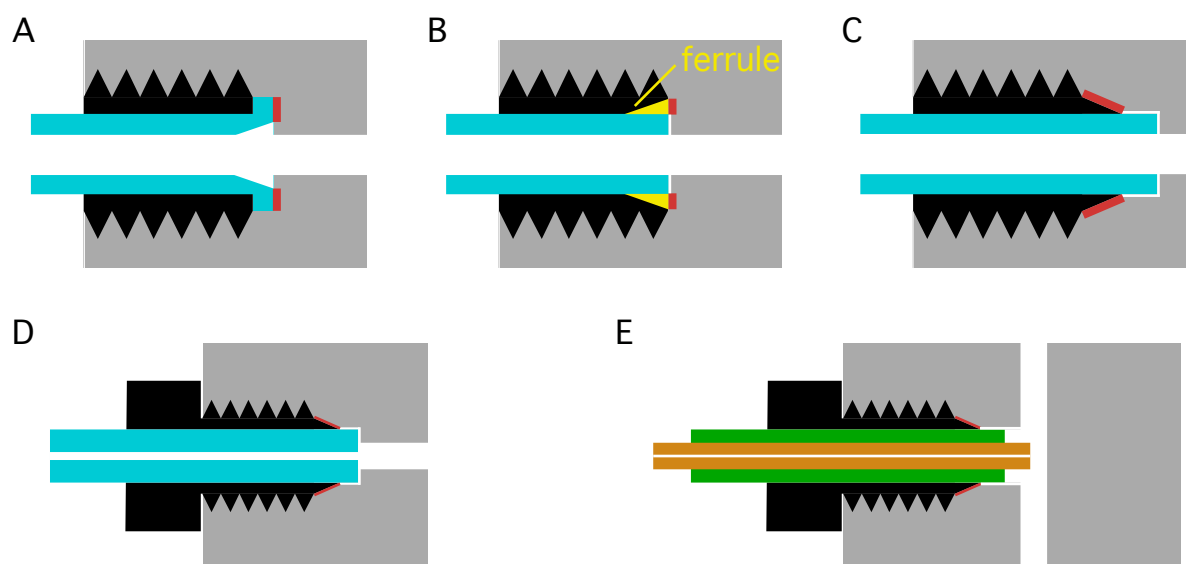
Fig. 7: Possible dead volumes in tube-interconnect junctions for the technologies of heat-bending (A), using a ferrule (B), using a single-piece coned fitting (C) and for cases where the inner diameter of the tube is different than that of the interconnect (D) or when a sleeve is needed (E). Places where the ensemble's tightness prevents leaks are marked in red and possible dead volumes are marked in white. Different passive and active microfluidics components. Close up on the connection between an interconnect and a tube, using a screw fitting (in black) for the cases when the tube has the appropriate o.d. (D) and when its i.d. is too small, requiring the use of a sleeve (in green) for a tight fit (E).

Another point requiring attention is the presence of gas in a microfluidic system. Even when gas is not actively introduced, it may appear when liquids that contain dissolved gasses are exposed to high temperatures or low pressures. This is why it is important to evacuate all of the liquids that are used in a microfluidic system prior to their introduction. Another way for gas to be introduced in a microfluidic system is when electrolysis products are created in a closed system and can't be flushed out. Usually it is water that undergoes electrolysis, producing O_2 and H_2 in the anode and cathode respectively. Hydrogen gas, having a much lower solubility in water than Oxygen, is the first to appear as bubbles in a microfluidics system, and measures should be taken to remove it from the system.

1.2.1.2 *Design considerations for CE*

The microfluidic design for a CE instruments generally has two parts, namely the inlet and the capillary area.

The inlet is where solutions are introduced to the system. In its simplest form, it is a single vial where the injection side of the capillary is dipped and changing vials allows the injection and flushing of the capillary with different liquids. This process may be also done automatically with the use of valves and a pump. One of the well-known approaches for automatically dispensing different fluids is the sequential injection analysis (SIA) design [3, 27-29], as can be seen in Fig. 8A. In SIA, a 3-way valve is connected to the head of a syringe pump. One port of the valve is connected with tubes to a vial containing the carrier solution (S_0) and the second is connected, through a loading coil (a long narrow tube) to the inlet of a multi-position valve. One of the multi-position valve's ports is connected to the rest of the system (where the capillary inlet is dipped) and serves as an outlet while the rest are connected to different solution vials. The loading coil is there for loading solutions from the multi-position valve (pulling them inside), in order to dispense them to the outlet. The i.d. of the loading coil must be narrow enough to prevent turbulent flow and the mixing of fluids in the system and the it should hold enough volume to flush at least once (but preferably twice or more) the tubes between the multi-position valve and the capillary's end. As multi-position valves can be quite expensive, and sometimes bulky, SIA can be implemented by using 3-way valves in series, as seen in Fig. 8B. For a single run of CE, without special additives, only two different vials (Sample and BGE) are needed. More vials are required for different

cases such as ITP where a leading electrolyte (LE) and a tailing electrolyte (TE) are needed instead of the BGE.
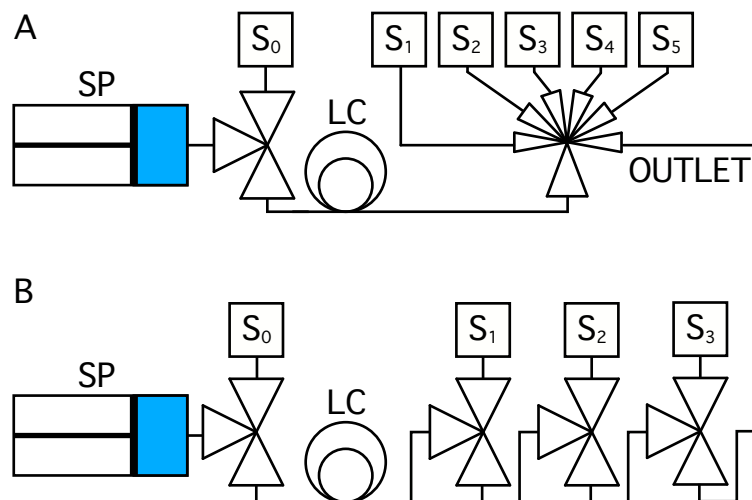
Fig. 8: Two SIA implementations, using a mutli-position valve (A) and a series of 3-way valves. SP: syringe pump, LC: loading coil, S_X: vial containing solution X.

The capillary area is where the injection end of the capillary is dipped, as well as a ground electrode for the separation voltage application. When coupling capillaries and ground electrodes to a microfluidic system (as shown in Fig. 7E) it is important that the electrode is downstream from the capillary inlet, and preferably distanced by a tube with narrow diameter. This is to avoid electrolysis products from entering the capillary and influencing the separation process and the detector signal. When possible, it is good practice to flush the channel in which the capillary and the electrode are dipped with a small flow (large flows may introduce laminar flow in the capillary). The i.d. of channels in a microfluidic CE circuit should be at least one order of magnitude bigger than the i.d. of the capillary itself in order to minimize pushing liquids into the capillaries when this is not needed (this is called "stray injection"). When possible, it's better practice to apply negative pressures for flushing the microfluidic channels, as this only has the potential to draw liquids out of the capillary, which isn't bad as the other end of the capillary is dipped in a BGE reservoir, together with the HV electrode. The capillary must be the only path for current to pass from the HV electrode to the ground electrode so special care has to be taken to ensure the isolation of the HV vial. A common way is to enclose it in a cage made of poly(methyl methacrylate) (PMMA). Fitting the cage door with a safety switch gives the option to disrupt the power to the HV unit, offering a further safety precaution.

1.2.1.3 Pressurization techniques

As discussed above, sample injection is one of the most crucial steps on the way for a good reproducible separation, and HDI is usually preferred over EKI. In microfluidics, the Reynolds number is usually low and therefore a pressure gradient over a narrow channel leads to laminar flow. The relation between the pressure gradient and the flow rate is given in such cases by the Hagen–Poiseuille law:

$$(6) \quad \Delta P = \frac{8\eta L Q}{\pi r^4}$$

ΔP : pressure difference in a channel

η : liquid viscosity

L : channel length

r : channel radius

Q : volumetric flow rate

In order to control injection, it would be most straightforward to apply a pressure difference to exactly control the flow rate for a few seconds, in which the sample injection takes place. Pressure application and its release should ideally be instantaneous, resulting in a straight pressure step. There are several ways to achieve pressurization, the simplest of which is syphoning, which may be done either manually or automatically, as discussed above. Other automated techniques for pressurization include dynamically creating the desired pressure by using a pump and using a regulated pressure (or vacuum) reservoir. The latter may be used to create exact pressure steps (for example by opening and closing valves to couple the regulated pressure to the microfluidic circuit for a defined time) yet this allows only a single pressure to be used, and in CE at least two pressures should be available: low pressure for exact injection and high pressure for fast flushing. One way for employing regulated pressure reservoirs for CE is to use two of them (one high and the other low), but this limits the capillary i.d. range to be used with the system. Another way is to use an electronic pressure controller, which controls a proportional 1-way valve according to pressure readout. Pressure controllers may have or not an internal venting valve, which means they are able or not to reduce the pressure when it is too high, respectively. For

the latter case, an external venting valve must be employed to release pressure for the system when injection should be stopped. The applicability of a syringe pump for injection pressure mainly depends on the pump's volumetric step size (taking into account the syringe i.d. and the motor's linear resolution). The smaller the volumetric step size is, the better can the pressure be controlled. As the volumes to be injected are usually measured in nL, most (if not all) of the syringe pumps to date don't have a small enough step size (which would have to be at least one order of magnitude smaller) for exact injection simply by moving a few steps. But regardless of the step size, a pressure sensor is necessary in order to control injection accurately for all cases. Employing an electronic feedback loop (similar to that in a pressure controller) it is possible to control applied pressures with very high precision, for both positive and negative (vacuum) values. As a pump is normally needed for flushing the microfluidic circuit with different fluids, it is good if the same pump can also perform exact injection. It is also possible to calibrate the number of steps a pump should take according to the pressure buildup, but such calibration don't take into account the possible occurrence of gasses in the system (different gas amounts would need separate such calibrations). Nevertheless, when gas is made sure to be out of the system, this method can be employed and has been demonstrated [27]. It is also possible to reduce the effective pressure produced by a pump by splitting the flow (this is known as split injection). A needle valve can control what portion of the pressure is applied to the capillary, and with fine-tuning it is possible to achieve reproducible injections as well.

1.2.2 Electronics

The hardware units needed for performing a capillary electrophoresis experiment mostly offer electrical control, using some standard electrical interface, for which an electronic circuit needs to be built. The units in turn control experimental variables which can be divided to digital variables which have a discrete limited number of options for setting (like setting the state of a valve) and analog variables, which can be set within a given range (such as setting a voltage or a pressure in a given range), for both of which standard control interfaces have been developed throughout the years.

The simplest way for controlling variable is by setting a voltage level. A very common interface for controlling a two-state digital variable is called transistor-transistor logic (TTL), in which a voltage between 0 and 5 volts is used to communicate low (voltage

between 0-0.8 V) and high (voltage between 2-5 V) logic states. Similarly, a very common interface for controlling analog variables is setting a voltage in a certain range, and in response the hardware unit sets the analog variable proportionally within its range. The translation between the input voltage and the output value of the variable is given by the following equation:

$$(7) \ X = X_{min} + \frac{V - V_{min}}{V_{max} - V_{min}} \cdot \left(X_{max} - X_{min} \right)$$

V_{max}, V_{min} : The maximal and minimal input voltage values

X_{max}, X_{min} : The maximal and minimal variable values

V, X : The input voltage and the output variable value

Since 5 V is widely used for TTL, the range 0-5 V for controlling analog variables is quite popular, yet manufacturers also use lower voltages for control circuits, such as 3.3 V and 1.8 V in order to reduce power consumption.

In some cases, a hardware unit implements the direct control of several variables internally, exposing the user a more specific interface. For example, the purpose of a syringe pump is to pull and dispense liquids, so it makes sense to ask the user for the amount of liquid to be dispensed rather than asking for the next requested plunger position. This is where more elaborate interfaces are needed, such as data busses (e.g. I^2C, SPI) and communication protocols (e.g. RS232, USB, TCP/IP). Bus interfaces and networked communication protocols have the advantage of being able to connect many hardware units on the same bus and to address them in the same way.

Direct voltages control mechanisms can be easily implemented on an electronic breadboard, and can be then controlled manually with switches and potentiostats, and while this approach requires the least work for setting up a system, it requires manual handling of the instrument. Another approach is to use a microcontroller, which can implement the necessary interfaces in the control circuitry, and to program it to perform the needed tasks. Such a program can be triggered by the user manually (again, using switches) or through a user interface program on a PC connected to the microcontroller.

In recent years, the field of microelectronics was widely popularized by the release of simple and well documented microcontroller boards such as Arduino (www.arduino.cc), Raspberry Pi (www.raspberrypi.org) and others. These offer a variety of boards with varying capabilities. Almost all of them allow at least reading and writing TTL signals (some with 0-5 V ranges, some with others) and many also allow reading analog voltages, by including analog-to-digital converters (ADC) on the board. Creating an output analog voltage is much less common, and can be done by connecting a digital-to-analog converter (DAC) to the board and programming it to output the requested voltage.

1.2.3 Software development

Microcontrollers always include a programmable microprocessor. Each microprocessor has its own machine code (also called assembler code), giving access to the basic abilities implemented in the microprocessor (e.g. turning TTL signals on and off). In order to ease the process of programming, microprocessor manufacturers implement in the microprocessor a standardized input/output (I/O) design, for which a compiler program exists, or alternatively, the write a new compiler program for their new design. This enables programmers to write code in higher-level languages, C/C++ being the most common. The manufacturers of popular microcontroller boards provide a C/C++ software library that enables control of the board resources, and by that making it easier to develop software for their boards. Additionally, a loading program is provided so that a PC connected to the board can upload newly written programs. This is usually done with the help of a small program called a "boot-loader" which is delivered with each board.

Writing code for the microcontroller board alone doesn't allow to control the system interactively from the PC, and for that a separate software needs to be prepared, to run on the PC and communicate the user's wishes to the board. This is the way popular instrument control solutions work, such as LabView (www.ni.com/labview).

For the sake of automation, all of the electrical units in a system should be controlled by a single microcontroller. This is, however, not always possible, for example when a manufacturer does not report the electrical interface for a hardware unit but rather provides a proprietary microcontroller that connects directly to a PC, where a proprietary software controls it. In such cases, it is common that the manufacturer also

exposes an application programming interface (API), which is an alternative way for accessing the microcontroller from a PC. The API can be then interfaced by the control software running on the PC, allowing the whole system to be monitored from a single place.

1.3 Enhancing limits of detection (LOD) in CE

Capillary electrophoresis is a very attractive analytical method since it can be performed with relative ease and requires very small amounts of sample and consumables. However, CE is currently only secondary in importance to competing separation methods such as HPLC and GC, which is mostly because limits of detection in CE are not as low as in these methods. Using CE, it is usually possible to detect analytes in the low micromolar levels, which isn't sufficient in many cases such as heavy metal contaminations. Therefore, LOD enhancement has been the focus of many research groups in the past years. The general approach is to introduce a concentration phase prior to the normal CE separation and detection, and thus effectively lowering the detection limits in CE.

Concentration methods in CE are divided into two major categories [30, 31]:

1. Methods that involve partitioning into a distinct phase. These are referenced as extraction methods.
2. Methods that happen in the liquid phase alone and rely on velocity changes of target ions due to electrophoretic phenomena. These are referred to in the literature by the general term "stacking". This may be confusing as the term "stacking" is also used to describe a set of in-line concentration methods.

A concentration method is called off-line when the stacking happens outside of the capillary, and on-line if it's fully coupled to the rest of the separation process. When the concentration process occurs inside the separation capillary it is called an in-line method. In-line methods are very popular as they happen in the capillary and no further engineering effort is needed for coupling the pre-concentration process to the separation process. Some of the most common methods are described below.

1.3.1 Field amplified sample stacking (FASS)

FASS is a stacking technique in which the target ions' velocity in the sample matrix is enhanced due to a higher electrical field in that zone. This is simply achieved by having

the sample zone's overall conductivity to be at least 10 times lower than that of the BGE [30, 32]. This technique doesn't fit samples, which inherently have a high conductivity (such as some biological or environmental samples). The maximal volume that can be injected in FASS is around 5% of the capillary length [30]. Larger injection volumes do not enhance sensitivity induce due to EOF mismatches between the sample plug and the BGE, which cause hydrodynamic dispersion. Sensitivity enhancement less than 50 may be achieved [33].

1.3.2   Field amplified sample injection (FASI)

Also referred to as field-enhanced sample injection (FESI), this technique also applies to situations where the sample's conductivity is much lower than that of the BGE. It only differs from FASS by the fact that instead of injecting the sample hydrodynamically, it is injected electrokinetically. As the BGE conductivity is much higher, the injected ions don't travel so fast in it and long injections may be used. FASI has a higher potential for sensitivity enhancement than FASS (1000 fold and more [30]), but has the disadvantage that the sample matrix conductivity must be constant. If it isn't, reproducibility suffers and the technique becomes too cumbersome to use. Another limiting factor in FASI is that EOF may force some of the sample matrix to enter the capillary, which disturbs the process and reduces reproducibility. Artificial EOF reduction in the capillary may allow longer injections.

1.3.3   Pressure assisted electrokinetic injection (PAEKI)

PAEKI is FASI with an addition of pressure from the inlet or outlet reservoirs to exactly cancel the EOF, allowing long injections. Like in FASI and FASS, it is necessary that the sample's conductivity will be lower than that of the BGE. Several publications on PAEKI have been published using anions, and recently on cations as well [34]. Enhancement factors as high as 10,000 were reported. [35-42]

1.3.4   Large volume sample stacking (LVSS)

LVSS was developed by Chien and Burgi [43] as a way to overcome the 5% injection limitation of FASS and FASI, allowing sample injection of up to 100% of the capillary. The sample matrix is then removed from the capillary by EOF pumping and as almost all of it leaves through the capillary inlet, the polarity is reversed and separation can begin. As the target ions are stacked in the end of the sample zone, they leave the capillary last

so careful operation can ensure they all stay inside for analysis (timing the polarity reversal is done by examining the current signal). An alternative for polarity reversal was later introduced by Burgi [44], where the direction change is done chemically (termed "LVSS using EOF pump") by adding EOF suppressing agents to the BGE, such as diethylenetriamine (DETA). As the sample matrix is pumped out of the inlet by the EOF, more and more of the capillary is filled with the DETA containing BGE and more and more is the EOF suppressed. Eventually the BGE fills the capillary completely and the ions start separating. Several alternatives for controlling this transition where later developed by others [45].

1.3.5   Transient ITP (tITP)

In ITP, sample ions are sandwiched between a high-mobility leading electrolyte (LE) and a low-mobility terminating electrolyte (TE). The mobility and concentration of the LE determines the concentration effect on the sample. ITP can also be performed transiently by using short TE and LE zones, so after equilibrium is reached, the sample zone enters a larger zone of BGE, where it continues to separate in CZE mode. Several modification to tITP exist, where either a constituent of the BGE or the sample itself act as LE, or where a low conductivity plug replaces the TE (this is also called pseudo-ITP) [33]. ITP-based concentration is has the special attribute that low target analyte concentrations can be increased even in the presence of other large concentration ions. While the presence of high concentration background electrolytes renders many stacking methods useless by increasing the sample's conductivity (e.g. FASS), their presence doesn't disturb the concentration mechanism in ITP [46].

1.3.6   Dynamic pH junction

The focusing principle in the dynamic pH junction method is velocity changes due to different pH levels in neighboring zones, resulting in the focusing of analytes between them. For example, Aebersold and Morrison [47] who introduced this method, increased the pH of a protein containing sample above the proteins' pI level, making them negatively charged, while using a BGE with a pH level below pI. After the sample plug injection, the injection end was dipped back in the acidic BGE solution and was applied a positive voltage. The anionic proteins in the sample plug migrated towards the injection end but reversed after crossing the interface to the low pH BGE zone, which resulted in their focusing around this interface. When the pH level of the sample plug was low

enough (due to interaction with the acidic surrounding), the cationic proteins along the interface started moving towards the cathode.

1.3.7 Sweeping techniques

The focusing principle in sweeping techniques is adding an additive to the BGE (but not to the sample solution) to which the target analytes have a higher affinity. These additives, which are usually referred to as a pseudostationary phase (PSP) may be charged or neutral and include surfactants, microemulsions, polymers, dendrimers etc. When charged, target analytes are "swept" along the interface between the BGE zone (from the injection end) and the sample zone as the PSP penetrate the sample zone and pick up target ions. When neutral, the it is the target analytes that penetrate the PSP [48].

1.3.8 pH-mediated field-amplification stacking (pH mediated sample stacking)

In this method, a low conductivity zone is created chemically. Sample is electrokinetically injected to a buffer containing a conjugate ion (such as acetate) [49, 50]. Immediately after the sample was injected, a strong acid is also injected electrokinetically. This injected acid neutralizes the base in the area where the sample was injected, and lowers the conductivity there. Sample ions can then stack on the transition area between the newly created low conductivity zone and the rest of the BGE.

1.3.9 Isoelectric focusing (IEF)

This is a very old method that was developed to separate and concentrate proteins according to their pI values. In this method, a pH gradient is applied along a channel where a mixture of proteins resides and an electric field is applied across it. The proteins migrate according to their charge state until they reach the point in the channel in which the pH equals their pI,. This is their focus point as their electrophoretic velocity vanishes. Given enough time, proteins are concentrated in bands along the channel and can be then detected.

1.3.10 Counter-flow gradient electrofocusing

This is a set of methods, in which the combination of electrophoresis and a bulk solution counter-flow are used to focus analytes along the separation column. Given a constant bulk flow at one direction, an electric field is used to migrate target analytes to the

opposite direction. A gradient in the electric field is necessary so that at some point along the channel, the total velocity of an analyte is zero, where it can focus. Examples are electric field gradient focusing (EFGF) where a set of electrodes are used to pattern the electric field across the channel, and temperature gradient focusing (TGF) where a buffer system is chosen so that a temperature gradient changes its ionic strength, and therefore results in an electrophoretic velocity gradient [51]. These methods are similar to IEF by that in all of them, analytes are concentrated in stationary points along the channel. They have also been used mainly to concentrate and detect proteins and have the advantage over IEF since the proteins are not focused in their pI, so less precipitation occurs (a common problem in IEF) [52].

1.3.11 Methods using membranes

The process of pre-concentration has to do with the preferential transport of target ions to a defined space. In on-line methods, where the pre-concentrated solution needs to be automatically injected to the separation capillary, the exact definition (in space) and manipulation of this solution is detrimental. The use of membranes is common in pre-concentration methods, both in-line (e.g. EFGF) and on-line. One example for the use of membranes is to use it as a gate between a volume of sample solution and a smaller volume into which the target ions should migrate. This is the case in the method electromembrane extraction (EME), where an electric field is used to migrate target analytes from a reservoir (or a stream) of sample solution through an ion-exchange membrane to a smaller compartment for enrichment [53, 54].

2   Results and Discussion

The majority of the results presented in this thesis have been published in or submitted to different scientific journals for analytical chemistry and computer science. The "Results and Discussion" chapter is therefore compiled of sections, each of which contains a brief summary of the main work, and the reprints of the relevant published publications or manuscripts follow.

2.1   Projects

The projects described below are divided into five parts. The first part describes work on dynamic processes in electrophoretic separations, studied by using an array C^4D cells. The second part describes the development of Instrumentino, a software framework for controlling purpose-made instruments. The third part includes several purpose-made CE instruments, built for different purposes, employing Instrumentino. The fourth part includes two review publications written about the concurrent determination of anions and cations in CE. The fifth part describes the development of a novel way for enhancing the LOD in CE, using pre-concentration.

2.1.1   Studying dynamic processes in electrophoretic separations by using an array of contactless conductivity detectors

Studying the dynamics of electrophoretic separations and processes is of importance both for understanding the basic physical phenomena and for developing better models to help optimizing configurations for electrophoretic analyses. An array of C^4D cells built in-house was used for probing conductivity signals along separation capillaries, while performing either CZE or ITP, and the results were then compared to computer simulations, using the GENTRANS software [4, 55-57]. This project was done in collaboration with the group of Prof. Wolf Thormann from the University of Bern, and our part of the project was to provide the experimental setting for Prof. Thormann to check his computational models using a detector array.

First results were obtained from an array of 16 detectors (publication #1 [29]) showing the separation dynamics in CZE of inorganic ions, and by placing the first detector very close to the inlet it was possible to exhibit the effect of FASS in the initial steps of the separation process. In one experiment, a sample plug containing two anions and two

cations was placed in the middle of the capillary (between the 8th and the 9th detectors) and the separation of both species were monitored simultaneously.

In a follow up publication (publication #2 [3]), an array of 8 detectors was used to validate computational models of EOF behavior in LPA coated capillaries. Experimental results from CZE separations with an applied co-flow were compared to simulations, and where found to agree well, including the prediction of system peaks' behavior. The EOF dependency on ionic strength was investigated by repeating the experiment with two BGE concentrations (high and low) and it was found that the EOF and its dependency on ionic strength could be modeled with a previously used model for the case of fused-silica capillaries dynamically double coated with Polybrene and poly(vinylsulfonate) [58]. The electroosmotic mobility in the case of LPA coated capillaries was found to be 17-fold smaller than for dynamically double coated capillaries. ITP experiments were also conducted and compared to simulation and further corroborated these findings. By having the first detector very close to the inlet, it was possible to observe sigmoidal transitions related to the injection boundary that migrates with the EOF. It was found that the EOF velocity was increasing during the experiment, in agreement with the dynamically double-coated capillary model, which was successfully applied for the CZE data. Models not exhibiting EOF ionic strength dependency did not fit well to the experimental data.

The results of this project were published in two publications:

- Publication #1: "Contactless conductivity detector array for capillary electrophoresis" [29]
- Publication #2: "Validation of CE modeling with a contactless conductivity array detector" [3]

My participation in the publication #1 was to fix and modify an existing experimental system to fit it to the needs of the experiments (fixing all of the detectors, changing the injection manifold and adding the gas pressure parts), to conduct all of the experiments described in the publication and to analyze the outcome data.

My participation in publication #2 was to build the experimental system (fluidics, hardware and software) and to jointly conduct the experiments described in the publication, together with Prof. Thormann's assistant, Mrs. Jitka Caslavska.

2.1.2 Instrumentino: an open source Python framework for controlling scientific experiments

In the process of scientific research, it is often needed to build purpose-made systems to create the exact conditions for certain experiments. Universities normally hold permanent technical staff for helping researchers in such endeavors, usually with the mechanical and electrical aspects. Necessary software development, however, needs to be done within the research group, which may present difficulties for students that are not familiar with programming. Instrumentino was created to try and alleviate such difficulties by providing a solid framework for sequencing experimental steps and acquiring relevant signals. It is a Python framework that lets system builders set up a custom GUI for their experimental systems with relative ease, and for some cases, presents an alternative solution for commercial programs like LabVIEW (www.ni.com/labview). It currently includes support for experimental systems employing Arduino boards (www.arduino.cc) and LabSmith (www.labsmith.com) controllers, and various hardware units such as thermometers, pressure sensors and controllers, valves, pumps, HV controllers, etc. One of the big advantages of Instrumentino is that it enables the concurrent use of different controllers for a single experiment, allowing all of the devices in the system to participate in automated operation sequences. Hinted by its name, Instrumentino was first developed as a customizable GUI for Arduino based experimental setups, following their rising popularity in the scientific community. Arduino boards popularized microelectronics and made it more accessible for novices, and Instrumentino attempts to do the same for automated purpose-made instrumental control.

Instrumentino was used for various experimental setups, both within our group and others, including all of the experimental systems described in this thesis but one, as it was realized prior to the development of Instrumentino. Some of the works published by collaborators using Instrumentino for system automation include a portable dual-channel CE system [59], a triple-channel CE system [25] and an optical gas detector [60].

Instrumentino was released as an open-source project and its source code is managed and further developed in GitHub (www.github.com).

The results of this project were published in two publications, the second of which is an extension of the first one, providing additional clarifications as to how the system works and giving usage examples:

- Publication #3: "Instrumentino: An open-source modular Python framework for controlling Arduino based experimental instruments" [61]
- Publication #4: "*Instrumentino*: An Open-Source Software for Scientific Instruments" [62]

2.1.3   Purpose-made CE systems

Capillary Electrophoresis can be used to determine many kinds of ions and be employed for various analytical applications. During my PhD period I was involved in building several CE systems, made for different purposes.

A portable dual channel CE instrument was built and used for environmental detection of inorganic ions in water samples in collaboration with the groups of Prof. Bernhard Wehrli and Prof. Beat Müller from EAWAG (publication #5 [Koenka, 2016 #445]). The system introduced a thermostated chamber in which the separation took place, the use of only off-the-shelf components for building the microfluidics circuit and the use of a miniaturized syringe pump for pressure creation in the system, employing a feedback loop between the pump and a pressure sensor. This could replace the bulky and heavy gas containers formerly used as a pressure source for the other portable CE systems. The use of the syringe pump was found to provide the most accurate and reproducible pressure source (compared to sources used in the earlier works) and enabled the application of a wide range of pressures, both positive and negative. The possibility of negative pressure application opened the way for a special semi-automatic mode for analyzing volume-limited samples, in which sample is introduced by dipping the HV end of the capillaries in a sample vial, performing the vacuum injection and then placing the capillaries back in the HV reservoirs for the separation. It is an easy way to introduce automation for low-volume samples. The addition of a thermostated chamber was shown to provide comparable peak areas and migration times for a separation when

done at room temperature and when placed in a cooled room (6-10 °C), in contrast to very different results when the thermostat wasn't active.

The system was used to determine concentrations of target ions in groundwater and mine water samples in an abandoned mining site in Argentina, as well as the semi-automatic determination of inorganic ions in sediment porewater from Lake Baldegg in Switzerland.

In publication #6 [63], a CE system employing a micro-injector block was built and tested together with Dr. Jorge Sáiz to semi-automatically handle sample volumes as small as 300 nL. This was an improvement on earlier systems where the use of microfluidics for injection automation limited the minimal volume of sample that could be handled. In the new system, sample was manually placed in a small cavity to which the capillary was fixed, and following that everything else was done automatically, namely: precise injection, separation and capillary conditioning as preparation for the next sample. Collaborating with the group of Prof. Beat Müller, the micro-injector was used for the determination of inorganic cations in porewater samples withdrawn from a sediment core from lake Baldegg in Switzerland. This was to exemplify the improvement over previous measurements that had to be done with manual siphoning injection [64, 65], due to the limited sample volume available.

Publication #7 presents a way for building electrophoretic experimental systems by employing a miniature microfluidic breadboard, offering high design flexibility such as in lab-on-chip devices, but using standard capillaries and plastic tubing. To exemplify the flexibility of the system, several very diverse configurations and modes of electrophoresis were implemented: a standard CZE separation of 6 inorganic cations, a fast separation (35 seconds) of the same cations, pressure assisted CZE for the efficient determination of both fast and slow anions, dual capillary CZE for the simultaneous separation of anions and cations, a separation of cationic amino acids by ITP and a separation of small carboxylic acids by GEMBE.

The results of these projects were published in five publications:

- Publication #5: "Thermostatted dual-channel portable capillary electrophoresis instrument" [Koenka, 2016 #445]
- Publication #6: "Micro-injector for capillary electrophoresis" [63]
- Publication #7: "A microfluidic breadboard approach to capillary electrophoresis" [12]

My participation in publication #6 was to prepare the software and electronics for operating the experimental system and to jointly build the fluidics system, conduct the experiments described in the publication, analyze the results and write the manuscript, together with Dr. Sáiz.

2.1.4 Reviews about concurrent determination of anions and cations in CE

In its simplest use, it is possible to detect either anions or cations in a single CE separation. There are, however, several ways to conduct CE separations so that both species can be detected at the same time. This is very desirable in many cases, as by doing so both time and money can be substantially saved. In publication #8, the different methods known to date, for simultaneously determining cations and anions, were reviewed, including the use of complexing agents, micelles, two injectors, dual detectors, and two capillaries, and their benefits and drawback were discussed. In publication #9, recent applications (in the years 2011-2015) comprising simultaneous determination of anions and cations were reviewed.

Two reviews were written in collaboration with Dr. Jorge Sáiz:

- Publication #8: "Concurrent determination of anions and cations in consumer fireworks with a portable dual-capillary electrophoresis system" [6]
- Publication #9: "Simultaneous separation of cations and anions in capillary electrophoresis - Recent applications" [66]

2.1.5 Enhancing detection limits in CE by pre-concentration

One of the greatest shortcoming of CE in comparison to other separation methods like HPLC or GC is its higher detection limits, resulting from the capillary's narrow inner diameter. Therefore, concentration enhancement methods have been of great interest in the past 10 years [31] and various approaches have been developed, though most of them are limited for low conductivity samples (in comparison to the BGE concentration). In this work, a new approach was reported, which was successfully tested on high concentration samples (as high as 0.1 M). The pre-concentration principle was based on balancing the hydrodynamic and electrokinetic flows, applied opposed to each other, with the aid of ion-exchange membranes. By choosing the right flows, high mobility ions could be selectively pre-concentrated while low mobility ions wouldn't. Furthermore, the principle was shown to be applicable in a fully automated way, built as an add-on interface to an existing automated microfluidic-based CE system. In this work, pre-concentration of anions was demonstrated using a cation-exchange membrane but the principle is expected to work for cations, employing anion-exchange membranes instead and using reversed polarities.

A single short communication manuscript was published online in the journal *Electrophoresis*.

- Publication #10: "Background conductivity independent counter flow pre-concentration method for capillary electrophoresis" [67]

2.2 Publication reprints

This section contains the reprints of all of the publications mentioned above.

Publication #1:

Contactless conductivity detector array for capillary electrophoresis

Marko Stojkovic[1]
Israel Joel Koenka[1]
Wolfgang Thormann[2]
Peter C. Hauser[1]

[1]Department of Chemistry, University of Basel, Basel, Switzerland
[2]Clinical Pharmacology Laboratory, Institute for Infectious Diseases, University of Bern, Bern, Switzerland

Short Communication

Contactless conductivity detector array for capillary electrophoresis

A CE system featuring an array of 16 contactless conductivity detectors was constructed. The detectors were arranged along 70 cm length of a capillary with 100 cm total length and allow the monitoring of separation processes. As the detectors cannot be accommodated on a conventional commercial instrument, a purpose built set-up employing a sequential injection manifold had to be employed for automation of the fluid handling. Conductivity measurements can be considered universal for electrophoresis and thus any changes in ionic composition can be monitored. The progress of the separation of Na^+ and K^+ is demonstrated. The potential of the system to the study of processes in CZE is shown in two examples. The first demonstrates the differences in the developments of peaks originating from a sample plug with a purely aqueous background to that of a plug containing the analyte ions in the buffer. The second example visualizes the opposite migration of cations and anions from a sample plug that had been placed in the middle of the capillary.

The elucidation of the dynamics of electrophoretic separations and processes is of high interest to explore and understand the basic phenomena occurring under the influence of the electric field applied to a liquid medium and to optimize configurations for electrophoretic analyses. Dynamic changes along the electrophoretic column can be investigated by computer simulation and experimental means [1]. Dynamic simulation provides plentiful data for any given electrophoretic system, namely the separation dynamics of sample components together with the ongoing changes of buffer components, pH, ionic strength, conductivity, and electric field strength along the separation column, and effects of fluid flow, including electroosmosis [2, 3]. Experimentally, dynamic processes can be explored with sensors that repeatedly scan the electrophoretic column [4], array or multiple detectors placed along part of or the entire separation space [5, 6], and whole column imaging [7].

Monitoring of the electric field strength or conductivity along the separation space can be considered universal for electrophoresis as it visualizes changes in ionic composition encountered in moving boundary electrophoresis, isotachophoresis, zone electrophoresis, and isoelectric focusing. The use of an array of 255 potential gradient sensors that were in contact with the liquid medium of a 10 cm capillary column of rectangular cross-section led to the visualization of the evo-lution of zone patterns in moving boundary electrophoresis [5], isotachophoresis [5, 8, 9], and zone electrophoresis [5] and a similar device with 100 sensors was employed to study the dynamics of the electric field strength distribution in isoelectric focusing of simple buffer systems [6] and synthetic carrier ampholytes [10]. Different types of conductivity detectors for CE were developed over the years, the most appealing being those based on capacitively coupled contactless sensing, an approach that is not subject to corrosion and other deleterious surface phenomena that can occur at electrodes in contact with a liquid medium. Recent reviews are available [11–16]. A contactless conductivity detector cell (the method is often referred to as C^4D for "capacitively coupled contactless conductivity detection") is simple in construction, compact in size and inexpensive. The concurrent employment of more than one detector is therefore feasible. Indeed, Saito et al. [17] and Mai and Hauser [18] have made use of two cells placed on the same capillary. This allowed the independent optimization of the detector positions for the simultaneous determination of anions and cations in CZE. In a further development, Gaudry et al. [19] not only used two detectors but also two capillaries for concurrent separation. In another effort, Caslavska and Thormann employed two contactless conductivity detectors to follow bidirectional isotachophoretic zone patterns in double coated fused-silica capillaries that feature a strong EOF toward the cathode [20].

The detector design used in our research group has now been modified to allow placement of individual cells directly side by side on a capillary. This was enabled by appropriate sideways positioning of the cabling for external connections.

Correspondence: Professor Peter C. Hauser, Department of Chemistry, University of Basel, Spitalstrasse 51, 4056 Basel, Switzerland
E-mail: Peter.Hauser@unibas.ch
Fax: +41-61-267-10-13

Abbreviation: SIA, sequential injection analysis
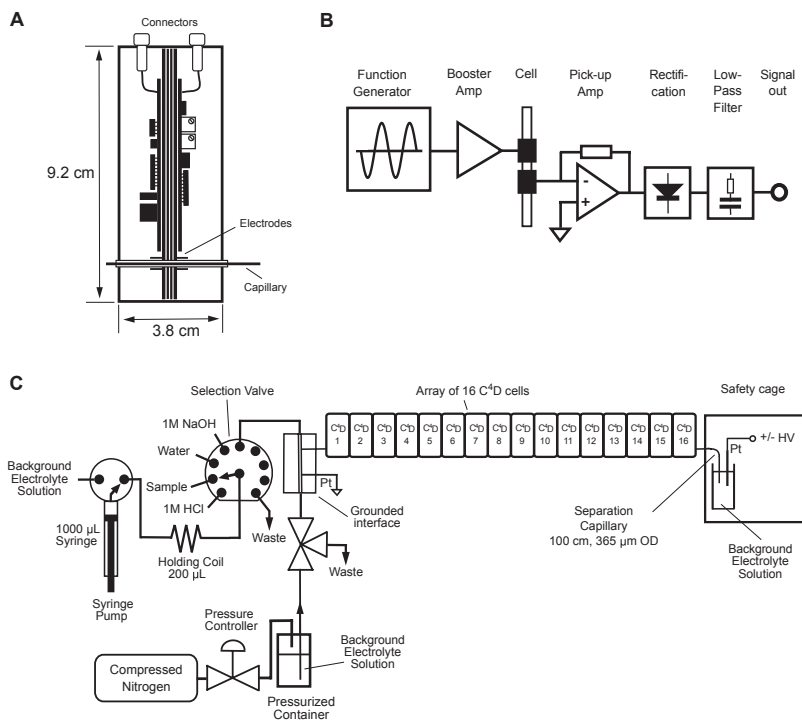
Figure 1. Schematic drawings of (A) geometry of each C⁴D-cell, (B) circuitry of the C⁴D-cells, (C) SIA-CE-C⁴D system with an array of 16 detectors.

Furthermore, the system was miniaturized overall by building the circuitry in the surface mount technology format. Therefore the entire electronic circuitry could be included in the same housing that contains the electrodes, rather than having part of it in an external housing as had previously been the case. In addition, due to the number of units required, the detector was designed for ease of fabrication. The printed circuit boards were etched in our laboratory, the components soldered by hand, and the mechanical work was limited to the cutting of the boards to size and the drilling of holes.

A schematic drawing of a cell is shown in Fig. 1A. The case is divided into two parts by a stack of four printed circuit boards, similar to the arrangement reported by Francisco and do Lago [21]. The two boards on the inside with a thickness of 0.5 mm each are completely covered by copper layers that are facing each other and are electrically grounded to form a Faradaic shield between the two cell halves. A hole of 0.4 mm diameter allows passage of the capillaries with external diameters of 365 μm. The two outer boards contain the electrodes consisting of metallic wire ferrules and some basic electrical connections. The spacing between the electrodes is defined by the total thickness of the two inner boards and is thus 1 mm. The excitation and pick-up circuitries are built on separate smaller printed circuit boards that are mounted on either side of the sandwich of the four boards. A block diagram of the circuitry is given in Fig. 1B. The excitation part consists of an integrated circuit sine wave generator and an operational amplifier that brings the amplitude to 20 V peak-to-peak. On the pick-up side the cell current is converted to a voltage that is then rectified and low-pass filtered and passed directly to an external data-acquisition system. More general details on the circuitry can be found in earlier publications [22, 23].

Each cell has a width of about 40 mm. This allowed the placement of 16 individual detectors on a capillary of 100 cm total length. The detectors occupy a space of about 70 cm with sensing locations being about 4.4 cm apart. Some extra capillary length is required at the two ends to allow injections and to accommodate buffer reservoirs and high voltage electrodes. The assembly is illustrated in Fig. 1C. Due to space limitations and as the capillary has to be stretched linearly for placement of the detectors the use of a conventional commercial CE instrument was not possible. Instead,

a system based on a sequential injection analysis (SIA) manifold was employed [18, 24–28]. The conventional SIA setup with a holding coil consisting of a syringe pump (Cavro XLP 6000, Tecan, Crailsheim, Germany) and a 9-port channel selection valve (Cavro Smart Valve, Tecan), serves for aspiration and transport of solutions, including sample plugs, to the capillary interface. However, in departure to earlier systems that utilized the syringe pump to achieve pressurization for flushing with sodium hydroxide solution, water and buffer and for injection this was implemented with compressed nitrogen utilizing an electronic pressure controller (VSO-BT, Parker Hannifin, Etoy, Switzerland). While this requires an additional component, the control of pressurization is more easily achieved and more precise with this approach. The three-way valve needed for directing the flow was obtained from NResearch (Gümligen, Switzerland). The SIA-CE interface is made of Perspex and is connecting the liquid channel with the capillary and a grounded electrode, which are mounted through two T-junctions. Polyimide coated fused silica capillaries were obtained from Polymicro (Phoenix, AZ, USA). The capillary ending was placed into a vial, which was filled with the electrolyte solution together with the platinum wire serving as the high voltage electrode. A dual polarity high voltage power supply (±30 kV, Spellman CZE2000, Pulborough, UK) was employed for application of the separation voltage. The assembly at the high voltage end was insulated in a safety box made from Perspex that was equipped with a micro switch to disrupt the high voltage on opening. All parts of the system were operated under computer control. The detector signals were captured with a 16-channel e-corder (EDAQ, Denistone East, NSW, Australia) and processed with the Chart software package (EDAQ).

The application of the detector array is illustrated in Fig. 2 for the simple example of the separation of Na^+ and K^+. The stacked plots shows the signals recorded on all of the 16 detectors. In this case, the two ions happened to be already separated at the first detector located 4.5 cm from the injection end, but the further progress of zone electrophoresis is shown very clearly by comparing the traces obtained by the detectors at increasing distances on the separation channel. Note that the electropherograms have been normalized against the baseline signal. This is readily possible, as the circuitry does not have an offset facility. The reason for the normalization is a variation in the sensitivity of the detectors (with maximum deviations of approximately ±60% from the average), which is thought to be due to small differences in the geometry of the cell arrangement. The cells were produced by hand, so that the achievable mechanical precision was limited. The peaks are negative going, indicating a reduction in conductivity when the analyte ions are passing. This is mainly due to the difference in equivalent conductivity between the cations and the co-ion (H^+) from the acetic acid BGE employed for this separation. Negative peaks are a common feature of C^4D, and are often inverted in order to show them in the commonly expected sense, but they were left in the raw state in this case. The figure
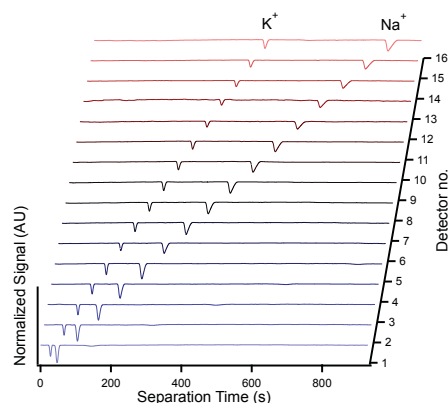
Figure 2. A 100 μM of Na^+ and K^+ separated in a BGE of 500 mM acetic acid in a capillary of 25 μm internal diameter and 100 cm length at 20 kV. The analytes were injected as NaCl and KNO_3 dissolved in pure water as a plug of 1 cm length (20 psi for 2873 ms).

very nicely demonstrates the capability of the detector array to directly monitor and study dynamic electrophoretic processes.

Examples of the potential benefits in examining electrophoretic separations are given in Fig. 3. The separation of the same cations is shown again in the panels of Fig. 3A and B. Hydrodynamic injection was employed in both cases, but for Fig. 3A the two model analytes were contained in pure water, while for Fig. 3B they were contained in the BGE. The length of the injected plug was 2 cm in both cases. For clarity, only the signals of the first four detectors are shown. Clearly, the peaks for the two ions injected in water are sharper and separation occurs faster. The reason for this is the transient stacking effect taking place at the cathodic buffer interface when the high voltage is turned on. As is the case with the shorter initial zone length (Fig. 2), separation of the two compounds is already complete at the location of the first detector. Also apparent in Fig. 3A is a change of peak shape from a nearly Gaussian shape to a nonsymmetrical appearance. This is particularly clear for the slower ion, Na^+. The increasing skewedness of the peak, and its expanding width at baseline, can be ascribed to electrodispersion. The peaks of Fig. 3B did not experience the stacking effect as the sample plug did not have a lower conductivity compared to the BGE and are thus wider. Furthermore, as separation of the two cations progresses more slowly compared to the case of Fig. 3A, a transient-mixed zone is monitored at the location of the first detector. The interesting shape of the conductivity signal reveals three zones, the first representing K^+, the second a transient-mixed zone containing both cations and the third one Na^+. At the location of the second detector, the two cations are almost completely separated,
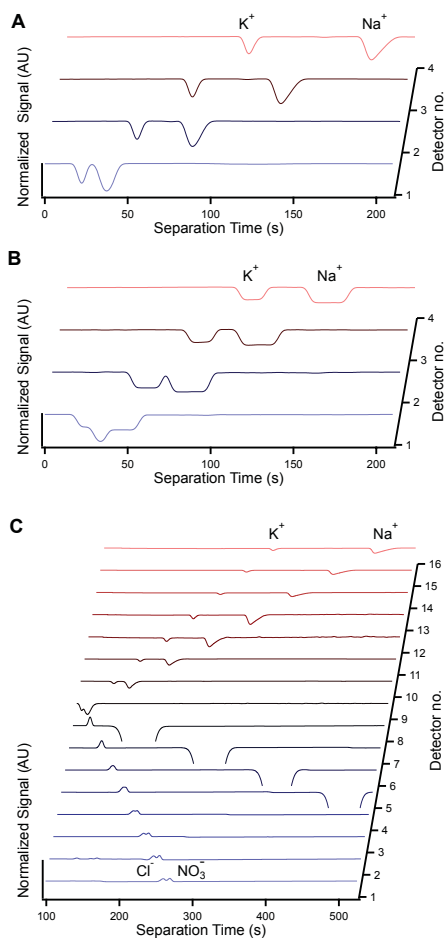
Figure 3. (A) A 100 µM of Na^+ and K^+ injected as purely aqueous solution. Sample plug: 2 cm (20 psi for 5746 ms). Other conditions are as for Fig. 2. (B) A 100 µM of Na^+ and K^+ injected dissolved in BGE. Sample plug: 2 cm. Other conditions are as for Fig. 2. (C) A sample plug of 1 cm length of 100 µM of NaCl and KNO_3 injected as a purely aqueous solution was placed by hydrodynamic pumping between detectors 8 and 9 before applying the separation voltage. Other conditions are as for Fig. 2.

highly conducting co-ion (H^+) from the BGE. The separation dynamics and conductivity distributions of the two configurations shown in Fig. 3A and B were found to be in complete agreement with those obtained by dynamic computer simulation using the SIMUL5 code of Hruška et al. [2] (data not shown).

In Fig. 3C the concurrent separation of cations and anions is monitored. A 1 cm long plug of a mixture of 100 µM each of KNO_3 and NaCl in pure water was injected hydrodynamically and then placed half-way down the separation capillary, i.e. exactly between detectors 8 and 9. This was possible by precise control and timing of the applied pressure for hydrodynamic pumping. The detector array also enables the operator to follow the movement of the sample plug through the capillary during this manipulation. When the desired position of the sample plug was reached the application of pressure was stopped and the electrophoretic separation started by turning on the high voltage. The electropherograms obtained with the 16 detectors show the subsequent progress of the separation. The cations migrate toward the cathodic capillary end and their movement and separations can be followed on the detector cells 9–16. The anions move in the opposite direction, i.e. toward the injection end of the capillary, and the progress of their separation can also be followed with chloride being slightly faster than nitrate. In contrast to the cationic part, conductivities across the anionic zones are higher compared to the conductivity of the background electrolyte. This and the entire dynamics were again found to be in agreement with computer simulations (data not shown). Note that a dilute acetic acid solution was employed as BGE. At the low pH value of 2.5, a strongly reduced EOF toward the cathode was expected, and thus the fast migrating inorganic anions were not expected to be swept with an appreciable cathodic EOF as would be the case with a buffer of neutral or alkaline pH. In fact, it was found that there was a small flow toward the anode under the conditions used, as evidenced by the large, partly covered, negative going conductivity peak visible for detectors 8 to 4 that represents the fluid element originally occupied by the sample prior to power application. The origin of this anodic flow is not clear and was not yet further investigated.

In conclusion, an SIA manifold for injection was used to construct a CE system with an array of contactless conductivity detectors along the separation capillary. This was possible, as the injection approach does not require the movement of the capillary. The new system allows the simultaneous monitoring of electrophoretic processes throughout a large part of the separation channel and is deemed to have a high potential as a tool to study the fundamental processes underlying the evolution of separations as well as the shapes of peaks and boundaries. C^4D features a universal response to any changes in ionic composition of the liquid medium in the capillary. Therefore, it is possible to also monitor background processes exhibiting conductivity changes that are not accessible by optical detection. It should furthermore prove useful for the study of reaction kinetics.

whereas complete separation is monitored with detectors 3 and 4. Conductivities across the cationic sample zones are again lower compared to the conductivity of the BGE, and the mixed zone has a lower conductivity then the K^+ and Na^+ zones, presumably because of the displacement of the

References

[1] Mosher, R. A., Saville, D. A., Thormann, W., *The Dynamics of Electrophoresis*, VCH Publishers, Weinheim 1992.

[2] Hruška, V., Jaroš, M., Gaš, B., *Electrophoresis* 2006, *27*, 984–991.

[3] Thormann, W., Breadmore, M. C., Caslavska, J., Mosher, R. A., *Electrophoresis* 2010, *31*, 726–754.

[4] Hjertén, S., *Chromatogr. Rev.* 1967, *9*, 122–219.

[5] Thormann, W., Arn, D., Schumacher, E., *Electrophoresis* 1984, *5*, 323–337.

[6] Thormann, W., Mosher, R. A., Bier, M., *J. Chromatogr.* 1986, *351*, 17–29.

[7] Wu, X.-Z., Huang, T., Liu, Z., Pawliszyn, J., *Trends Anal. Chem.* 2005, *24*, 369–382.

[8] Thormann, W., Arn, D., Schumacher, E., *Sep. Sci. Technol.* 1984, *19*, 995–1011.

[9] Thormann, W., Arn, D., Schumacher, E., *Electrophoresis* 1985, *6*, 10–18.

[10] Thormann, W., Egen, N. B., Mosher, R. A., Bier, M., *J. Biochem. Biophys. Methods* 1985, *11*, 287–293.

[11] Kubáň, P., Hauser, P. C., *Electrophoresis* 2013, *34*, 55–69.

[12] Mai, T. D., Hauser, P. C., *Chem. Record* 2012, *12*, 106–113.

[13] Coltro, W. K. T., Lima, R. S., Segato, T. P., Carrilho, E., de Jesus, D. P., do Lago, C. L., da Silva, J. A. F., *Anal. Methods* 2012, *4*, 25–33.

[14] Kubáň, P., Hauser, P. C., *Electrophoresis* 2011, *32*, 30–42.

[15] Kubáň, P., Hauser, P. C., *Electrophoresis* 2009, *30*, 176–188.

[16] Trojanowicz, M., *Anal. Chim. Acta* 2009, *653*, 36–58.

[17] Saito, R. M., Brito-Neto, J. G. A., Lopes, F. S., Blanes, L., da Costa, E. T., Vidal, D. T. R., Hotta, G. M., do Lago, C. L., *Anal. Methods* 2010, *2*, 164–170.

[18] Mai, T. D., Hauser, P. C., *J. Chromatogr. A* 2012, *1267*, 266–272.

[19] Gaudry, A. J., Guijt, R. M., Macka, M., Hutchinson, J. P., Johns, C., Hilder, E. F., Dicinoski, G. W., Nesterenko, P. N., Haddad, P. R., Breadmore, M. C., *Anal. Chim. Acta* 2013, *781*, 80–87.

[20] Caslavska, J., Thormann, W., *Electrophoresis* 2006, *27*, 4618–4630.

[21] Francisco, K. J. M., do Lago, C. L., *Electrophoresis* 2009, *30*, 3458–3464.

[22] Tanyanyiwa, J., Galliker, B., Schwarz, M. A., Hauser, P. C., *Analyst* 2002, *127*, 214–218.

[23] Zhang, L., Khaloo, S. S., Kubáň, P., Hauser, P. C., *Meas. Sci. Technol.* 2006, *17*, 3317–3322.

[24] Mai, T. D., Schmid, S., Müller, B., Hauser, P. C., *Anal. Chim. Acta* 2010, *665*, 1–6.

[25] Mai, T. D., Hauser, P. C., *Talanta* 2011, *84*, 1228–1233.

[26] Mai, T. D., Hauser, P. C., *Electrophoresis* 2011, *32*, 3000–3007.

[27] Mai, T. D., Hauser, P. C., *Electrophoresis* 2013, *34*, 1796–1803.

[28] Stojkovic, M., Mai, T. D., Hauser, P., *Anal. Chim. Acta* 2013, *787*, 254–259.

Publication #2:

Validation of CE modelling with a contactless conductivity array detector

Jitka Caslavska[1]
Israel Joel Koenka[2]
Peter C. Hauser[2]
Wolfgang Thormann[1]

[1]Clinical Pharmacology
Laboratory, Institute for
Infectious Diseases, University
of Bern, Bern, Switzerland
[2]Department of Chemistry,
University of Basel, Basel,
Switzerland

Research Article

Validation of CE modeling with a contactless conductivity array detector

Dynamic computer simulation data are compared for the first time with CE data obtained with a laboratory made system comprising an array of 8 contactless conductivity detectors (C^{4}Ds). The experimental setup featured a 50 μm id linear polyacrylamide (LPA) coated fused-silica capillary of 70 cm length and a purpose built sequential injection analysis manifold for fluid handling of continuous or discontinuous buffer configurations and sample injection. The LPA coated capillary exhibits a low EOF and the manifold allows the placement of the first detector at about 2.7 cm from the sample inlet. Agreement of simulated electropherograms with experimental data was obtained for the migration and separation of cationic and anionic analyte and system zones in CZE configurations in which EOF and other column properties are constant. For configurations with discontinuous buffer systems, including ITP, experimental data obtained with the array detector revealed that the EOF is not constant. Comparison of simulation and experimental data of ITP systems provided the insight that the EOF can be estimated with an ionic strength dependent model similar to that previously used to describe EOF in fused-silica capillaries dynamically double coated with Polybrene and poly(vinylsulfonate). For the LPA coated capillaries, the electroosmotic mobility was determined to be 17-fold smaller compared to the case with the charged double coating. Simulation and array detection provide means for quickly investigating electrophoretic transport and separation properties. Without realistic input parameters, modeling alone is not providing data that match CE results.

Keywords:

Array detector / Capillary electrophoresis / Computer simulation / Electroosmosis / LPA coated capillary   DOI 10.1002/elps.201500424

1 Introduction

In a recent publication, the construction of a CE system featuring an array of 16 contactless conductivity detectors (C^{4}Ds) was reported [1]. In that instrument, the detectors were arranged along 70 cm length of a capillary with 100 cm total length and the capillary was interfaced to a setup with a sequential injection analysis (SIA) manifold for automation of fluid handling. The new system allows the simultaneous monitoring of electrophoretic processes throughout a large part of the separation channel and its use was demonstrated via following of the progress of the separation of simple ions by zone electrophoresis [1]. Monitoring of the conductivity or electric field strength at multiple locations along the capillary

can be considered universal for electrophoresis as it visualizes changes in ionic composition and thereby provides a tool to study the dynamics of boundaries, peaks and zones in all electrophoretic modes, including moving boundary electrophoresis, isotachophoresis, zone electrophoresis and isoelectric focusing [2–6]. Different types of conductivity detectors for CE were developed over the years, the most appealing being those based on capacitively coupled contactless sensing, an approach which is not subject to corrosion and other deleterious surface phenomena which can occur at electrodes in contact with a liquid medium [7–12]. The first contactless conductivity detector was built for zone detection in capillary isotachophoresis [13].

The elucidation of the dynamics of electrophoretic separations and processes is of high interest to explore and understand the basic phenomena occurring under the influence of the electric field applied to a liquid medium and to optimize configurations for electrophoretic analyses. Dynamic changes along the electrophoretic column can be investigated experimentally using conductivity [1], electric field strength [2–6] or optical [14–18] detection principles, or by computer simulation [19–28]. Dynamic simulation provides plentiful data

Correspondence: Professor Dr. W. Thormann, Clinical Pharmacology Laboratory, Institute for Infectious Diseases, University of Bern, Murtenstrasse 35, 3008 Bern, Switzerland
E-mail: wolfgang.thormann@ifik.unibe.ch
Fax: +41 31 632 4997

Abbreviations: C^{4}D, contactless conductivity detector; **HV**, high voltage; **LE**, leading electrolyte; **LPA**, linear polyacrylamide; **NPE**, norpseudoephedrine; **PFA**, perfluoroalkoxy alkane; **SIA**, sequential injection analysis; **TE**, terminating electrolyte

www.electrophoresis-journal.com
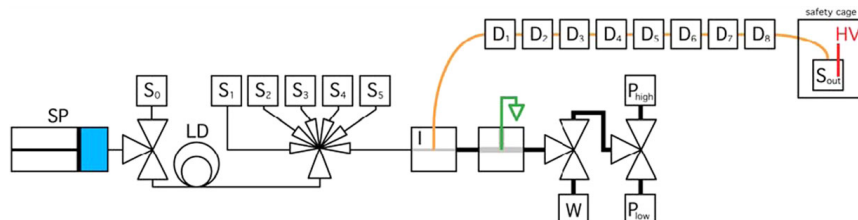
Figure 1. Schematic representation of the CE setup with an SIA manifold and a separation capillary with eight contactless conductivity detectors. Key: HV: high voltage, S: solution, D: detector, W: waste, P: pressure regulator, SP: syringe pump, I: injector interface, LD: loading coil.

for any given electrophoretic system, namely, the separation dynamics of sample components together with the ongoing changes of buffer components, pH, ionic strength, conductivity and electric field strength along the separation column, and effects of fluid flow, including electroosmosis. Comprehensive simulators, including GENTRANS [19–22], SIMUL5 [23, 24] and SPRESSO [25], are available for that task. They are 1D transient electrophoresis models which allow high-resolution, real-power simulations for any electrolyte arrangements, including those associated with zone electrophoresis, isotachophoresis and IEF [26–28].

CE is typically associated with fluid flow, mostly electroosmosis. Imposed hydrodynamic flow is used in special applications [29]. The EOF is an electrokinetic phenomenon associated with the surface charge at the inner capillary wall and the composition of the solution, including pH and ionic strength. GENTRANS permits the combined simulation of the temporal behavior of electrophoresis and electroosmosis under constant voltage or current conditions and was previously used to estimate the pH and ionic strength dependent EOF in uncoated fused-silica [21, 30] and polymethylmethacrylate (PMMA) capillaries [30]. In another effort, the pH independent EOF in dynamically double coated fused-silica capillaries featuring a charged surface was studied in the same way [31]. Furthermore, this dynamic CE model which uses material or surface property specific input data for estimation of electroosmosis was applied to investigate fundamental aspects of isoelectric focusing in capillaries or microchannels made from bare fused-silica, fused-silica coated with a sulfonated polymer, PMMA and poly(dimethylsiloxane) [32]. In GENTRANS, EOF is treated as plug flow with no contribution to dispersion, whereas the impact on zone and boundary dispersion caused by hydrodynamic flow is calculated with the Taylor-Aris equation [29].

The main focus of this paper is the validation of computer simulation data generated by GENTRANS with a CE setup featuring eight C^4Ds along a 50 μm id fused-silica capillary coated with linear polyacrylamide (LPA), an approach that is reported here for the first time. The previously described laboratory made CE system with C^4D array detection [1] was modified to allow (i) application of hydrodynamic flow during an electrophoretic run and (ii) handling of configurations with

continuous and discontinuous buffer systems. The changes in the experimental setup are described and computer predicted electropherograms using the GENTRANS software are compared to those obtained experimentally. Examples studied include (i) the migration and separation dynamics of cationic and anionic analyte and system zones in CZE with imposed hydrodynamic buffer flow, and (ii) the following of electrophoretic boundaries formed in a discontinuous buffer system and of an ITP sample zone in configurations without pressure driven hydrodynamic flow. The setup used allows the placement of C^4Ds detectors close to the sample inlet such that comparison of experimental and simulation data can be employed to characterize transient zone patterns formed around the sampling compartment of the capillary and the temporal behavior of EOF in an LPA coated capillary under ITP conditions.

2 Materials and methods

2.1 Reagents

If not stated otherwise, all chemicals used were of analytical or research grade. Sodium acetate anhydrous, DL-mandelic acid, nicotinic acid, glycolic acid and L-arginine were purchased from Fluka (Buchs, Switzerland). Acetic acid, formic acid, sodium hydroxide solution Titripur 0.1 mol/L and benzoic acid were from Merck (Darmstadt, Germany). (1S,2S)-(+)-norpseudoephedrine (+NPE), (1R,2R)-(-)-norpseudoephedrine (–NPE) and tryptamine were from Sigma-Aldrich (St. Louis, MO, USA).

2.2 Instrumental setup

An overall schematic representation of the CE instrument is depicted in Fig. 1. The setting comprises a pressure assisted SIA system [1, 33–37] designed to deliver solutions to the capillary inlet and into it using hydrodynamic pressure. The heart of the system is a syringe pump with a 3-way valve (Cavro XLP 6000, Tecan, Crailsheim, Germany) which is connected to a 6-port channel selection valve (Cavro Smart Valve,

Tecan) via a 400 μL holding coil. The holding coil's volume was set to be much larger than the volume between the selection valve and the capillary entrance (<10 μL). All tubes of the system are made of perfluoroalkoxy alkane (PFA) and have a 1/16" od (Idex, Wertheim-Mondfeld, Germany). One of the 3-way valve ports is connected to solution S_0, which is the only solution allowed in the syringe pump. Solutions S_1 to S_5 are connected to ports 1 to 5 of the selection valve and are transferred to the capillary entrance via use of the holding coil. For CZE, S_0 was the BGE and S_5 was the sample solution. For ITP, S_0 was the terminating electrolyte (TE), S_5 was the leading electrolyte (LE) and S_4 was the sample. Port 6 of the selection valve is connected to an injection interface to which the CE capillary and the ground electrode are connected. The injection interface was built by connecting two 1/16" T-interconnects made from solvent resistant ULTEM resin (T116-203, LabSmith, Livermore CA, USA) with a short 0.04" id PFA tubing in between. One T-interconnect was used as is (inner channels of 0.02") and one was machined to have wider channels (0.06") such that the fluid volume around the electrode is large enough to avoid the interference of electrolysis products with the CE separation.

All tubes upstream to the capillary are 0.01" id, while all tubes downstream and the second T to which the ground electrode is connected are 0.04" id (thin and thick lines in Fig. 1, respectively). This reduces post-capillary flow resistance in order to minimize undesired diversion of solutions into a capillary when passing by its inlet. Furthermore, the injection interface is connected to a 3-way valve (AV201-T116, LabSmith) which permits selection of the waste container (W) or one of two pressure regulators (P_{high} or P_{low}, controlled by another 3-way valve (AV201-T116, LabSmith)). The high pressure regulator can provide pressures between 10 and 100 psi (VSO-BT, Parker Hannifin, Etoy, Switzerland) and is used to flush the capillary between separations, while the low pressure regulator can provide pressures between 0.2 and 2 psi (OEM-EP, Parker Hannifin), which is used for sample plug injection and for applying hydrodynamic co-flow during a separation. Both regulators are fed from a pressurized 4.5 nitrogen cylinder (PanGas, Dagmersellen, Switzerland). The separation capillary used was a 70 cm long, 50 μm id fused-silica capillary coated with LPA (Polymicro Technologies, Phoenix, AZ, USA), and was passed through eight purpose-made C⁴Ds [1]. The centers of the eight detectors were positioned 2.7, 8.2, 13.2, 18.4, 23.5, 28.5, 33.5 and 38.5 cm away from the capillary's injection end (distance between detectors was about 5 cm). The capillary end was dipped into a 50 mL plastic vial (Falcon tube, Corning, Amsterdam, The Netherlands) containing the outlet solution S_{out} (BGE for CZE separations and LE for ITP) and a stainless steel electrode which was connected to a dual polarity ±30 kV supply (CZE2000, Spellman, Pulborough, UK). As a precaution, the outlet container was placed in a Perspex safety box equipped with a micro switch to disrupt high voltage (HV) on opening. All system parts (syringe pump, valves, pressure regulators and HV supply) were connected to a purpose made control box and were operated from a PC. The

control box included an Arduino Nano 3.0 microcontroller (Gravitech, Minden, NV, USA) which was tethered to a purpose made GUI software on the PC based on the open-source framework Instrumentino [38, 39]. This enabled to control each experiment and easily execute long run sequences for optimizing experimental parameters such as sample plug injection conditions. Detector data were recorded with a 16-channel e-corder (eDAQ, Denistone East, NSW, Australia) and processed with the Chart software package (eDAQ). Applied voltage and current as function of time were monitored by Instrumentino. The current reading provided a noisy signal which was smoothed by regression analysis.

2.3 Experimental procedures

New capillaries were rinsed with water, 0.1 M NaOH and BGE or LE (for a few minutes each). Between runs capillaries were rinsed with BGE for CZE and with LE in the case of ITP. Overnight or when not in use, capillaries were stored filled with 70% isopropanol. Each experiment was executed by a sequence of system-defined actions comprising (i) initialization, (ii) interface flushing, (iii) capillary flushing, (iv) sample injection and (v) application of voltage with or without co-flow. For CZE separations, the interface was flushed with 400 μL of BGE, followed by a capillary flush for 3 min using 20 psi. The sample was injected at 0.70 psi for 12 s. The interface was flushed again with 400 μL of BGE followed by application of a constant 20 kV using a co-flow produced by application of pressure between 1 and 2 psi. For ITP, the interface was flushed with 400 μL of LE. This flush was performed three times, with short capillary flushes (10 s) in between, to ensure that any TE left from the previous run was completely removed. The cleaning progress was verified by checking the conductivity level which had to reach the expected level for pure LE. After this initial washing procedure, the capillary was flushed with LE for 3 min using 20 psi. Sample (or LE in case of blank runs) was introduced by application of 1.6 psi for 13 s. The interface was flushed with 600 μL of TE followed by application of constant voltage of 20 kV or constant current of about 3 μA. No imposed co-flow was applied.

For measuring the low EOF and the imposed flow generated via application of pressure during electrophoresis in an LPA coated capillary, a setup with a C⁴D as described elsewhere [29, 31] was employed. Briefly, it comprised a PrinCE sampler (model 560, Prince Technologies, Emmen, The Netherlands), a 50 μm id capillary of 90 cm total length and the detector at 47 % of capillary length. BGEs of 10 mM ionic strength, a sample composed of arginine and benzoic acid (1 mM each in 50% BGE, hydrodynamically injected at anodic capillary end) and a voltage of 20 kV were applied. The temperature was ambient (around 24°C). Flow properties were assessed by variation of applied pressure between 0 and 100 mbar (0–1.45 psi) at a 20 mbar interval and the detected non-migrating system peak (referred to as EOF or flow peak in case of absence and presence of imposed flow, respectively) was used for data evaluation. Detector data were

Table 1. Physico–chemical input parameters used for simulation[a]

Compound	pKa	Mobility (x 10^{-8} m^2/Vs)
Acetic acid	4.75	4.24
Formic acid	3.75	5.66
Benzoic acid	4.20	3.36
Glycolic acid	3.89	4.24
Tryptamine	9.25	3.00
Arginine	8.92, 12.48	2.69[b]
Norpseudoephedrine	8.9	2.65[c]
Na$^+$	–	5.19

a) From data base of PeakMaster and SIMUL5.
b) Equal mobilities were assigned to all species.
c) Estimated value.

collected at a sampling rate of 100 Hz and stored using an e-corder 401 (eDAQ, Denistone East, NSW, Australia) as described elsewhere [29].

2.4 Computer simulations with GENTRANS and data presentation

GENTRANS was executed on Windows 7 based PCs featuring i5 processors running at 2.4 GHz. Configurations under normal polarity with or without an imposed buffer flow towards the cathode were investigated. Electroosmosis was calculated as function of ionic strength according to the model described for fused-silica capillaries that were dynamically double coated with Polybrene and poly(vinylsulfonate) [31] and having an electroosmotic mobility determined for an LPA coated capillary. The component's input data for simulation are summarized in Table 1. If not stated otherwise, the impact of ionic strength on electrophoretic mobilities was not considered. For CZE simulations with imposed flow, the program featuring Taylor-Aris dispersion was used [29]. A 35 cm capillary divided into 35 000 segments of equal length ($\Delta x = 10.0\ \mu$m) and a constant voltage of 5000 V (80 V/cm) were used. For constructing detector plots, simulation data storage occurred at 2 Hz. Simulations for 12.5 min of electrophoresis could thereby be executed in about 4 h. Samples were applied at the anodic capillary end as a plug with a length of 1.0% of column length (initially placed between 1.0 and 2.0% of column length) and a boundary width of 0.001%. The composition of the BGE and sample is given in the description of each example. For ITP simulations, a 17.5 cm separation space divided into 35 000 segments of equal length ($\Delta x = 5.0\ \mu$m) and a constant current density of 370 A/m^2 or a constant voltage of 1500 V were employed. Sample was applied at the anodic capillary end as a plug with a length of 2.5% of column length (initially placed between 5.0 and 7.5% of column length). For 10 min of electrophoresis, this required simulation times between 4 and 9 h. The composition of LE and TE are given in the description of each

example. All simulations were executed with data smoothing as described elsewhere [28].

2.5 Additional simulation tools and data presentation

CZE simulation data produced with GENTRANS were compared to those predicted using PeakMaster 5.2 software [40] which can be downloaded for free from http://www.natur.cuni.cz/Gas. Sample plug lengths and the velocity of the imposed applied flow were estimated with the CE Expert Lite software (Beckman Coulter, Fullerton, CA, USA). For smoothing of experimental current data and making plots of experimental and simulation electropherograms, data were imported into SigmaPlot 12.5 (Systat Software, San Jose, CA, USA).

3 Results and discussion

3.1 Electroosmosis and applied hydrodynamic flow in an LPA coated capillary

In this paper, simulation data are compared to those obtained experimentally in LPA coated fused-silica capillaries. For CZE, hydrodynamic flow was applied in order to be able to detect cationic and anionic zones in one run. For the simulation of electrophoretic processes in capillaries, it is necessary that EOF and applied hydrodynamic flow are known. Thus, using a conventional CE setup with conductivity detection [29], EOF and hydrodynamic flow as function of applied pressure in an LPA coated 50 μm id capillary were determined first. BGEs with ionic strength of 10.02 mM comprising 12 mM HIBA and 10 mM NaOH (measured pH 4.66) or 20 mM nicotinic acid and 10 mM NaOH (measured pH 4.76) were employed. For the two buffers, evaluation of the velocity of the non-migrating system peak as function of applied pressure revealed linear relationships (R^2 of 0.9999 and 0.9996, respectively) with the y-intercepts reflecting EOF (53.7 and 52.2 μm/s, respectively). The electroosmotic mobilities could thereby be calculated as 2.42×10^{-9} and 2.35×10^{-9} m^2/Vs, respectively, values that are considerably smaller than those observed in uncoated capillaries at that pH (about 25×10^{-9} m^2/Vs) and capillaries dynamically double coated with Polybrene and poly(vinylsulfonate) (about 41×10^{-9} m^2/Vs) [31]. For LPA coated capillaries and buffer pH < 8, the EOF is assumed to be essentially independent of pH [41]. Thus, EOF as function of ionic strength was estimated according to the model described for fused-silica capillaries dynamically double coated with Polybrene and poly(vinylsulfonate) via use of an electroosmotic mobility of 2.4×10^{-9} m^2/Vs instead of 41.1×10^{-9} m^2/Vs. The slopes of the linear relationships revealed the imposed flow velocity per unit pressure (9.83 and 9.89 μm/mbar, respectively). For a pressure of 80 mbar (1.16 psi), the flow was about 788 μm/s, a value that compares well to 780 μm/s

estimated with the CE Expert Lite calculator for a temperature of 25°C. The CE Expert Lite calculator is based on the Poiseuille equation which describes how fluid under pressure is flowing through a cylindrical vessel. Experiments with array detection were made with a capillary of 70 cm total length. Corresponding flow values calculated for 25 and 30°C are 1000 and 1120 μm/s, respectively. Thus, as the intracapillary temperature was assumed to be slightly above room temperature, the imposed pressure driven flow in our experiments at 1.16 psi (80 mbar) was taken as 1050 μm/s and EOF was estimated by subtraction of 1050 μm/s from the total flow value which was determined from the flow peak in the experimental data.

3.2 Capillary zone electrophoresis with array detection

CZE in an LPA coated capillary was studied in order to validate the electrokinetic simulation model for configurations with constant column properties, including the small EOF encountered in this type of capillary. The example studied comprised a two-component BGE composed of 20 mM formic acid and 10 mM NaOH together with four sample components (two cationic, two anionic) in a 70 cm long, 50 μm id fused-silica capillary whose inside wall was coated with LPA. Ionic strength, conductivity and pH of the BGE were calculated to be 10.17 mM, 0.112 S/m and 3.77, respectively. The sample was applied at the anodic capillary end and was transported along the capillary by the concomitant actions of electromigration, electroosmosis and hydrodynamic flow. According to the prediction of the PeakMaster software, this configuration produces two system peaks. The first one is migrating towards the cathode (calculated mobility: 12.00×10^{-9} m^2/Vs without correction of ionic strength, 13.53×10^{-9} m^2/Vs with correction of ionic strength), the second does not migrate and is thus also referred to as the EOF peak (or flow peak in case of a configuration with hydrodynamic flow). Both system peaks are characterized by a conductivity change and are thus recognizable with a conductivity detector. The sample was composed of benzoic acid, tryptamine, glycolic acid and L-arginine (1 mM each in BGE).

Simulation data generated with GENTRANS and application of Taylor-Aris diffusivity to account for dispersion caused by the imposed flow are depicted in Fig. 2A. As was discussed in a previous paper [29], electropherograms can be properly predicted by dynamic simulation using half of the column length together with half of imposed flow and current density (quarter of applied voltage). The time scales of predicted and experimental electropherograms are thereby identical but simulation time is much shorter compared to simulations with the full capillary length. Thus, simulations were performed with a 35 cm capillary (35 000 segments, $\Delta x = 10.0$ μm) at a constant 5000 V, an imposed hydrodynamic flow of 525 μm/s towards the cathode and a sample occupying 1% of capillary length at the anodic capillary end (placed between 1 and 2% of the capillary length with boundary widths

of 0.001). Initial current density and EOF were calculated to be 1597.19 A/m^2 and 44.12 μm/s, respectively. The execution time was 4.17 h. The simulated electropherograms of all eight detectors obtained with a sampling frequency of 2 Hz are presented in Fig. 2A. The selected positions for detectors 1 to 8 were 4.86, 12.71, 19.86, 27.29, 34.57, 41.71, 48.86 and 56.00% of simulation column length, respectively, and correspond to those used in the experimental setup with the adjustment for the 1% initial shift of the sample position used in the simulation. The predicted detector data reveal that all four sample components provide zones which have a lower conductivity compared to the conductivity of the BGE. The opposite is true for the two system peaks. Furthermore, the two anionic sample components (glycolic acid and benzoic acid) and the two system peaks are quickly separated (see signal of second detector). On the other hand, the two cationic sample components separate slowly and are not completely separated when they are transported across the last detector (top graph in Fig. 2A). In CZE configurations analyte and system peaks are the only discontinuities present. Thus, transport properties through the capillary should essentially be constant. The dynamic simulation approach of GENTRANS revealed this behavior. The computer predicted current density at 12 min is 1594.57 A/m^2 which is almost identical to that at the beginning of the run. The net buffer flow (sum of imposed flow and EOF) remains constant which indicates that the predicted EOF is constant. Both flows correspond to those monitored experimentally in the 70 cm capillary (see below).

For experimental validation, the sample was injected for 12 s at 0.70 psi thereby occupying a capillary segment of about 1% of capillary length (calculated with CE Expert Lite software). After sample application, the interface was flushed with 400 μL of BGE followed by application of 20 kV and a co-flow produced by a pressure of 1.16 psi which generated a constant imposed flow towards the cathode (1050 μm/s, see Section 3.1). Conductivity electropherograms obtained with the eight detectors are presented in Fig. 2B and compare well with those predicted by simulation shown in Fig. 2A. Electropherograms of the eight C^{4}Ds were not normalized to the response of a selected detector. It is apparent that simulation is correctly predicting analyte and system peaks. Evaluation of the detector position for detectors 2 to 8 as function of the detection time of the flow peak (peak S2 in Fig. 2B) revealed a perfect linear relationship ($r^2 = 1.000$) with a slope representing the total flow (1139 μm/s) and an intercept (2.56 mm) indicating the imprecision of detector mounting in relation to the beginning of the capillary and placement of the initial sample plug. These data indicate that the EOF was 89.0 μm/s which corresponds to an electroosmotic mobility of 3.12×10^{-9} m^2/Vs, a value that is comparable to that obtained during flow calibration experiments reported in Section 3.1. Measured voltage was constant throughout the experiment and the current was 6.7 μA which compares well to that predicted for a 50 μm ID capillary of 70 cm length at 20 kV (6.27 μA). The applied power level was low (0.193 W/m).

The characteristics of system peaks are known to be dependent on buffer concentration and composition [42]. Thus,
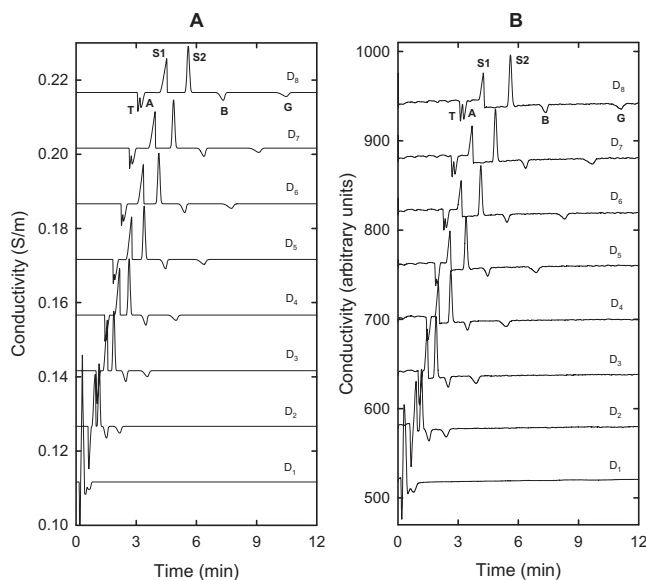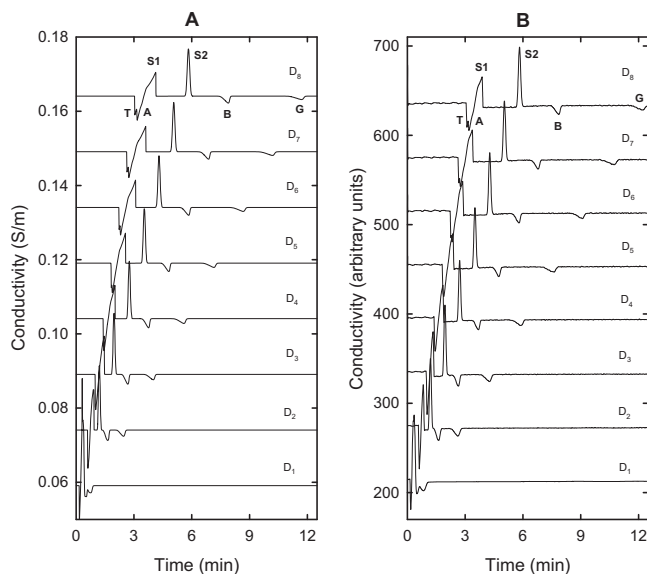
Figure 2. (A) Simulated and (B) experimental conductivity electropherograms of detectors D_1 to D_8 (presented with a y-scale offset) for a zone electrophoretic separation of two cations and two anions in an LPA coated fused-silica capillary using a BGE composed of 20 mM formic acid and 10 mM NaOH under conditions of constant voltage and a constant imposed buffer flow towards the cathode. The sample (1 mM of each component in BGE) was applied as a 1% pulse at the anodic capillary end. For information about applied voltage and flow see text. Key of peaks: A: arginine, B: benzoic acid, G: glycolic acid, T: tryptamine, S1: cationic migrating system peak, S2: system peak with no migration (flow marker).

in order to visualize this aspect, the same sample was also analyzed in the BGE with half the concentration of the two buffer components (10 mM formic acid and 5 mM NaOH) and otherwise identical conditions. Ionic strength, conductivity and pH of the BGE were calculated to be 5.17 mM, 0.0590 S/m and 3.78, respectively. According to the prediction of the PeakMaster software, this configuration produces two system peaks. The first one is migrating towards the cathode (calculated mobility: 21.56×10^{-9} m^2/Vs without correction of ionic strength, 23.27×10^{-9} m^2/Vs with correction of ionic strength), the second does not migrate and is thus also referred to as the flow peak. Dilution of the BGE compared to that used for Fig. 2 has an impact on the migration velocity of system peak S1. Its mobility becomes higher and the system peak is predicted to interfere with the two cationic sample ions. This is nicely seen in the GENTRANS simulation data presented in Fig. 3A. Tryptamine and arginine do not separate properly and system peak S1 is broader compared to the data of Fig. 2A. The same behavior could be verified experimentally (Fig. 3B). Separation of the two anionic sample components (benzoic acid and glycolic acid) are unaffected by the buffer change. Both simulation and experimental data indicate that transport properties through the capillary are essentially constant. Evaluation of the detector position for detectors 2 to 8 as function of the detection time of the flow peak (peak S2 in Fig. 3B) revealed a perfect linear relationship ($r^2 = 1.000$) with a slope representing the total flow (1092 µm/s) and an intercept (4.45 mm) indicating the imprecision of detector mounting and/or sample position in

relation to the beginning of the capillary. EOF could thus be calculated as being 42.4 µm/s. This value is smaller compared to that observed in Fig. 2B. It is important to mention that according to the EOF simulation model applied, the EOF should be 13.6 % higher compared to the case of Fig. 2. Reasons for this discrepancy were not investigated and the EOF input for the simulation data of Fig. 3A was adjusted to match the experimental EOF as mentioned at the end of Section 3.1.

3.3 Electrophoretic boundaries formed in a discontinuous buffer system

After having followed analyte and system peaks in CZE, the dynamics of a discontinuous buffer system in an LPA coated capillary was investigated under constant current and constant voltage conditions. The catholyte (also referred to as LE) was composed of 10 mM NaOH and 24.6 mM acetic acid (calculated pH and conductivity of 4.60 and 0.0920 S/m, respectively) and the anolyte (TE) comprised 10 mM acetic acid (calculated pH and conductivity of 3.39 and 0.0160 S/m, respectively). In this configuration, the sodium ion of the catholyte is the leading component, H_3O^+ the terminating ion and acetic acid the counter component [4,43]. Upon power application a moving steady-state boundary between the LE and the adjusted TE (in this case 30.87 mM HAc with a pH of 3.14 and a conductivity of 0.0283 S/m) is formed which migrates towards the cathode. The migration velocity in absence of any electroosmotic and hydrodynamic buffer flow is given by the
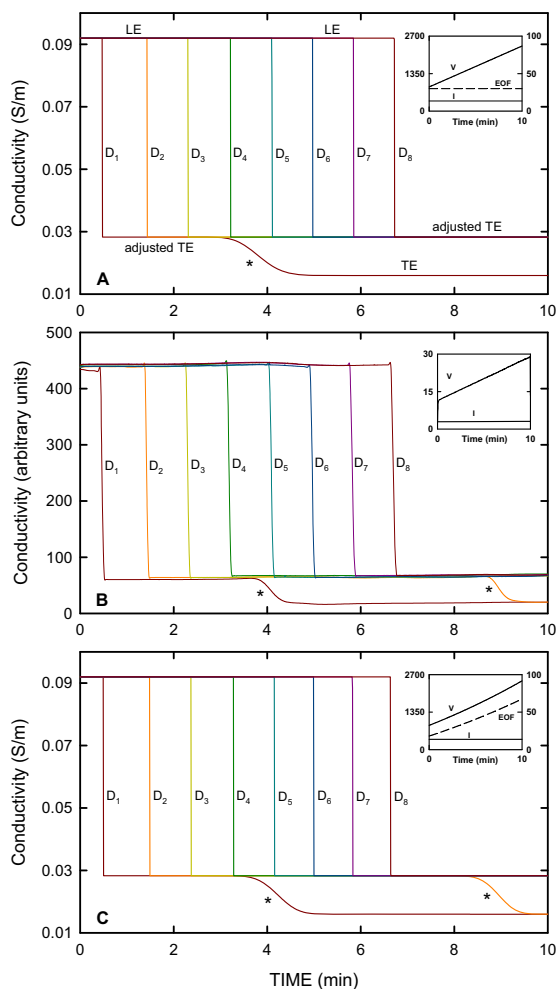
Figure 3. (A) Simulated and (B) experimental conductivity electropherograms of detectors D_1 to D_8 (presented with a *y*-scale offset) for a zone electrophoretic separation of the same sample in a BGE composed of 10 mM formic acid and 5 mM NaOH and otherwise identical conditions as in Fig. 2. Key of peaks as for Fig. 2.

relationship $v = (T_{Na+} \, I)/(F \, C_{Na+})$ where T_{Na+} and C_{Na+} refer to the transfer number and concentration of sodium in the catholyte (mol/m^3), *F* is the Faraday constant (96487 As/mol) and *I* the current density (A/m^2) [4]. For the given example, T_{Na+} equals 0.55 ($T = m_{Na+}/(m_{Na+} + m_{Ac^-})$ where m_j are the mobilities of sodium and acetate given in Table 1) and $v = 5.70 \times 10^{-7} \, I$ (m/s). Furthermore, at the location of the initial interface between catholyte and anolyte, a non-migrating, diffusing transition between 10 mM and 30.87 mM HAc is formed [4, 43].

GENTRANS predicted conductivity detector data of that system at a sampling rate of 2 Hz and having the eight detectors are depicted in Fig. 4A. The selected detector positions were 8.86, 16.71, 23.86, 31.29, 38.57, 45.71, 53.86 and 60.00% of simulation column length and correspond to those used in the experimental setup corrected for the 5% initial shift of the sample used in the simulation (cf. Section 2.4). The computer predicted data reveal the sharp decrease between the conductivity of the LE and the adjusted terminator together with the expected advancement of the migrating boundary. Simulations were performed with a 17.5 cm capillary (35 000 segments, $\Delta x = 5.0 \, \mu$m) at a constant 370 A/m^2 (initial voltage: 871.4 V; voltage at 10 min: 2344 V, see data in insert of Fig. 4A) and without imposed flow. A constant EOF of 30 μm/s was assumed to mimic the presence of a small EOF. The simulation could be executed in about 7 h. Simulations with the capillary length used for the experiment together with the applied power would require a much higher mesh

and would result in simulation time intervals of up to several weeks. The predicted current for a 50 μm id capillary of 70 cm length would be 2.91 μA. This value compares well to that monitored in the experiment (see below). Furthermore, the response of detector D_1 shows a sigmoidal conductivity decrease around 3.8 min (marked with asterisk). This transition comprises the detection of the diffusing boundary which was formed at the location of the initial buffer interface between catholyte and anolyte and does not migrate in the electric field but is transported by buffer flow.

Experimental data obtained with the 8-detector setup using a 70 cm long, 50 μm id fused-silica capillary whose inside wall was coated with LPA are depicted in Fig. 4B. Electropherograms of the eight C^{4}Ds were normalized to the response of detector eight such that comparable signal changes were obtained for all detectors. Correction factors for the data of Fig. 4B varied between 1.000 (detector 8) and 1.141 (detector 1) and were used to normalize all other ITP data presented in this work. Data of Fig. 4B were recorded under constant current conditions (3 μA) and without application of a hydrodynamic flow. They reveal the sharp decrease between the conductivity of the LE and the adjusted terminator together with the advancement of the migrating boundary. During the experiment, the voltage increased from 10.0 to 28.9 kV (insert in Fig. 4B) and the applied power level increased within 10 min from 0.043 to 0.124 W/m. The migration velocity of the boundary was calculated to be 870.9 μm/s using the relationship $v = 5.70 \times 10^{-7}$ I (m/s) where *I* is the current density (A/m^2) as is discussed above. The thereby estimated

Figure 4. (A, C) Simulated and (B) experimental conductivity electropherograms of detectors D_1 to D_8 for detection of a cationic ITP boundary between sodium as leading component and H_3O^+ as terminating component under constant current conditions in an LPA coated fused-silica capillary. The LE (catholyte) was composed of 10 mM NaOH and 24.6 mM acetic acid and the TE (anolyte) was 10 mM acetic acid. Simulations were performed with (A) a constant EOF and (C) an ionic strength dependent EOF. For details refer to text. The inserts in panels A and C comprise computer predicted temporal behavior of voltage *V* (V, left *y*-axis scale), current density *I* (A/m², left *y*-axis) and EOF (µm/s, right *y*-axis scale). The insert in panel B represents recorded current (µA) and voltage (kV). The asterisks mark the transitions between adjusted TE and TE (EOF marker).

boundary velocity compares well to the mean (SD) net velocity of 960.0 µm/s (4.0 µm/s) elucidated from detector position and detection time of the ITP boundaries, a value which includes migrational transport and buffer flow, i.e. EOF. Furthermore, the responses of detectors D_1 (placed at 2.7 cm) and D_2 (at 8.2 cm) show a sigmoidal conductivity decrease around 4.0 and 8.9 min, respectively (marked with asterisks). These transitions comprise the detection of the diffusing boundary which was formed at the location of the initial buffer interface between catholyte and anolyte and thus represent buffer flow. As no hydrodynamic flow was applied, these data

suggest that there was a small EOF. Based on the data of the first detector, the average velocity was estimated at 112.5 µm/s, for the second detector at 153.6 µm/s, values which suggest that the EOF is increasing with time. Furthermore, with constant EOF, the sigmoidal transition detected by detector 2 should be significantly broader compared to that of detector 1. The broadening is not observed in the experiment (Fig. 4B) which is in support of the increasing EOF. Not surprisingly, the use of a constant EOF (around 30 µm/s) for the simulation did not reveal data that matched those monitored experimentally. Within the investigated 10 min
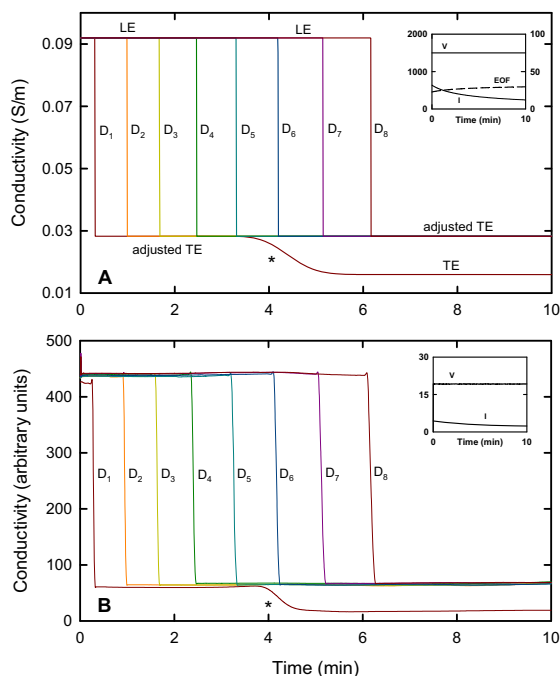
Figure 5. (A) Simulated and (B) experimental conductivity electropherograms of detectors D_1 to D_8 for detection of a cationic ITP boundary between sodium as leading component and H_3O^+ as terminating component under constant voltage conditions. The configuration was the same as for Fig. 4. Simulations were performed with an ionic strength dependent EOF as for Fig. 4C. For details refer to text. The insert in panel A comprises computer predicted temporal behavior of voltage V (V, left y-axis scale), current density I (A/m^2, left y-axis) and EOF ($\mu m/s$, right y-axis scale). The insert in panel B represents recorded current (μA) and voltage (kV). The asterisks mark the transitions between adjusted TE and TE (EOF marker).

runs, the transition was only predicted for the first detector (Fig. 4A). The transition would have reached the second detector after 10 min which is not in agreement with the experiment (compare data of Fig. 4A with those of Fig. 4B).

Simulation data for the system of Fig. 4A with ionic strength dependent EOF and otherwise identical conditions are depicted in Fig. 4C. Electroosmosis was calculated as function of ionic strength according to the model first described for fused-silica capillaries which were dynamically double coated with Polybrene and poly(vinylsulfonate) [31]. An electroosmotic mobility of 2.4×10^{-9} m^2/Vs instead of 41.1×10^{-9} m^2/Vs was used (see Section 3.1) and the predicted EOF increased from 18.04 to 67.47 $\mu m/s$ within 10 min of power application (insert in Fig. 4C). Using these conditions, the time scales of predicted and experimental electropherograms became nearly identical and predicted electropherograms, including the positions of the sigmoidal flow marker transitions of detectors 1 and 2, were qualitatively in agreement with those monitored experimentally. The simulation could be executed in about 9 h. The EOF model used predicts a higher pumping rate in regions of lower ionic strength and higher electric field. The ionic strength of adjusted TE and the TE were predicted to be 0.73 and 0.41 mM, respectively, values that are much smaller compared to the 10.02 mM ionic strength of the LE. Furthermore, the electric field in

these zones is much higher compared to that within the LE. Thus, the prediction of a steadily increasing EOF (insert in Fig. 4C) makes sense. In ITP, the LE is gradually replaced by adjusted TE and TE and the used EOF model appears to take into account that fact in a reasonable way for an LPA coated capillary.

The data depicted in Fig. 5 were obtained under constant voltage conditions, at 1.5 kV for the simulation data (Fig. 5A) and at 20 kV in the experiment (Fig. 5B). The same boundary was observed. However, due to the decreasing current, it migrated with gradually decreasing velocity. Using the same configuration and EOF model as for Fig. 4C, matching simulation data were obtained (compare data of Fig. 5A and B). Within the 10 min time interval, the predicted current density decreased from 637.00 to 243.18 A/m^2. The predicted current for a 50 μm id capillary of 70 cm length would accordingly decrease from 5.00 to 2.39 μA. This change is comparable to that observed experimentally (4.41–2.32 μA). The predicted EOF increased from 22.78 to 29.64 $\mu m/s$. This change is smaller compared to that predicted under constant current conditions.

It was interesting to find that predicted conductivity changes are somewhat different to those monitored with contactless conductivity detection. This is best seen with the sigmoidal transitions predicted for and detected with detectors 1
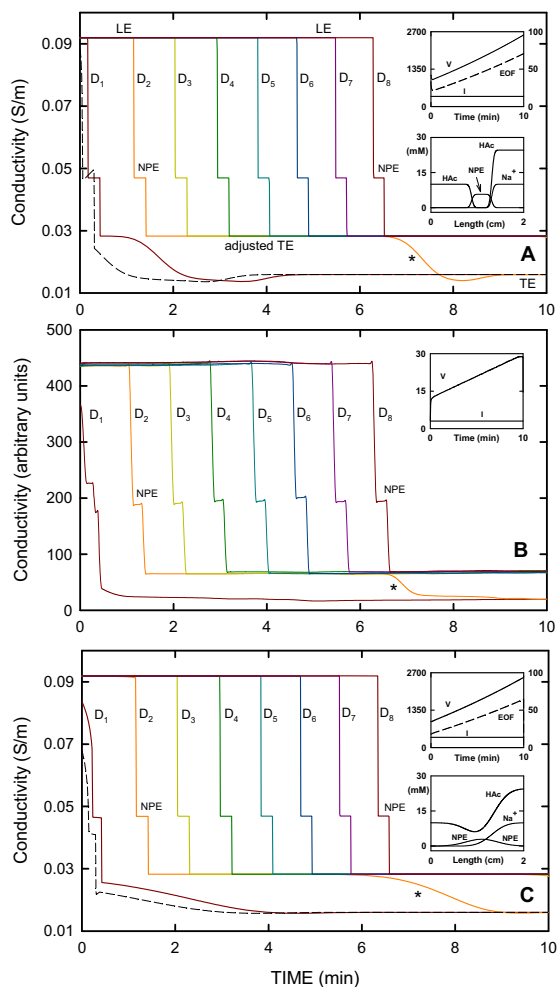
Figure 6. (A, C) Simulated and (B) experimental conductivity electropherograms of detectors D_1 to D_8 for detection of a cationic ITP zone formed by NPE between sodium as leading component and H_3O^+ as terminating component under constant current conditions. Simulations were performed with an ionic strength dependent EOF as was used for Fig. 4C having (A) sample boundary widths of 0.02 % shown as lower insert of panel A and (C) very diffuse boundaries which are depicted in the lower insert of panel C. The dashed line graphs in panel A and C were obtained for a position of detector 1 corresponding of 2.0 instead of 2.7 cm. Upper inserts in panels A and C depict the temporal behavior of voltage *V* (V, left *y*-axis scale), current density *I* (A/m², left *y*-axis scale) and EOF as dashed line graph (μm/s, right *y*-axis scale). The insert in panel B represents recorded current (μA) and voltage (kV). For details refer to text. The asterisks mark the transitions between adjusted TE and TE. Other conditions as for Fig. 4.

(Figs. 4 and 5) and 2 (Fig. 5). Simulation provides a conductivity change of 0.0637 S/m across the migrating ITP boundary whereas that of the sigmoidal transition is 0.0123 S/m. This indicates that the conductivity change across the ITP boundary is predicted to be 5.2 times larger compared to the change across the sigmoidal transition. The corresponding signal ratio in the experiments is about 8.5. Efforts in using input values for simulation that were corrected for ionic strength (*p*Ka and mobility values, as described in [29]) revealed an even lower ratio of 4.4 and did not provide an explanation of the discrepancy between simulation and experiment. Thus,

it is assumed that contactless conductivity detection as used in this work is providing a non-linear response for the conductivity changes encountered in the ITP boundary example. More work is required to assess this difference.

3.4 Isotachophoretic sample zone followed by array detection

After studying the behavior of a migrating and a non-migrating boundary of a discontinuous buffer system in a

LPA coated capillary, work was directed towards the formation of an ITP sample zone. A sample composed of +NPE and −NPE (2.85 mM each) was applied to the same LE and TE system as described in Section 3.3. It represents the same sample as was used in a separate project dealing with the study of the stereoselective ITP separation process. Without a suitable chiral selector in the LE, the two analytes cannot be separated by ITP and thus form a homogeneous cationic sample zone between the LE and the adjusted TE. Figure 6A depicts computer simulated data at constant current density of 370 A/m^2 and using the same EOF model as for Fig. 4C. The initial sample zone length was 2.5% of column length with a boundary width of 0.02% (for initial component distribution see lower insert in Fig. 6A). The sample zone is demarcated with sharp conductivity changes and migrates along the capillary as ITP zone of constant length and with an electrophoretic transport rate of 211 μm/s calculated with $v = 5.70 \times 10^{-7}$ I (m/s) as described in Section 3.3 [4,43,44]. The EOF is predicted to increase from 33.21 to 77.77 μm/s within the 10 min time interval (dashed line graph in upper insert of Fig. 6A) and is smaller compared to the electrophoretic transport. Thus, the net transport rate is slightly increasing with time. Experimental results obtained at a constant current of 3 μA are depicted in Fig. 6B. The sample was introduced by application of 1.6 psi for 13 s, thereby occupying a capillary segment of about 2.5% of capillary length (calculated with CE Expert Lite software). Experimentally monitored detector profiles of detectors 2 to 7 correspond well with those predicted by GENTRANS. For the chosen conditions under a constant current density, the voltage is predicted to increase in a similar fashion as was predicted by simulation (compare voltage graphs in upper insert of Fig. 6A with insert of Fig. 6B).

For detector 1 and the transition marked with asterisk detected with detector 2, the predicted detector profiles are somewhat different compared to those monitored experimentally. With detection at an earlier position than that of detector 1 provided a predicted detector signal which compares better to that monitored with detector 1. This is shown with the dashed line graph in Fig. 6A which corresponds to a detector placed at 2.0 instead of 2.7 cm of the 70 cm long capillary. At this location, however, the first detector could not be placed in the used setup. Thus, other sources with impact on detector profiles at early column locations were investigated. Transient states occurring prior to the formation of the ITP zone are dependent on the initial composition of the sample. Broader initial boundaries between sample and its surrounding electrolytes (LE and TE on cathodic and anodic side, respectively) were found to have an impact on the predicted detector signal of the first detector and the buffer transition of detector 2 marked with an asterisk in Fig. 6. This is illustrated with the data of Fig. 6C which were obtained with very diffuse initial sample boundaries (lower inset in Fig. 6C). Better agreement between experimental and simulation data for detector 1 and for the buffer transition of detector 2 was thereby found. These findings suggest that the initial sample plug produced by the SIA setup does not comprise sharp boundaries between sample and the two electrode solutions. More work is required to study this phenomenon.

4 Concluding remarks

Data obtained with dynamic simulation and the laboratory made CE system featuring an array of eight C^{4}Ds along an LPA coated fused-silica capillary were found to be in agreement for various configurations, including CZE with a small constant EOF and ITP with a varying EOF. The techniques provide means for quickly investigating the zone electrophoretic separability of components and the required capillary length for that task under specified experimental conditions. Furthermore, in the case of CZE, the discussed data demonstrate that system peaks and interferences between system peaks and analytes can be properly recognized. The same would be true for separations and analyses based on electrokinetic capillary chromatography, including those using monolithic columns for which contactless conductivity detection was demonstrated to be feasible [45]. All experiments were made in a setup which permits positioning of the first C^{4}D as close as 2.7 cm from the sample inlet such that basic phenomena, including the visualization of EOF and transient patterns in ITP, could be explored. Data obtained demonstrate that modeling alone is not sufficient for cases without realistic input parameters. This was found to be true for the prediction of (i) EOF in an LPA coated capillary under ITP conditions and (ii) formed transient configurations around the sampling compartment of the capillary. Gathering of simulation and experimental data led to the elucidation of the temporal behavior of EOF and, for the first time, finding of a reasonable model to estimate the EOF in an LPA coated capillary. EOF can be estimated with an ionic strength dependent model similar to that previously used to describe EOF in fused-silica capillaries dynamically double coated with Polybrene and poly(vinylsulfonate) and is not constant for configurations with discontinuous buffer systems such as ITP. All data demonstrate that it is beneficial to have multiple detectors along CE columns for studying the separation processes. A detector array can quickly give a lot of information useful in the development of an application or, as in the cases reported here, in the improvement of input parameters for simulation. Dynamic simulation, on the other hand, is rather slow but provides insight into basic phenomena of ion transport and EOF. Furthermore, a detector position close to the sampling compartment provides information that can be used for the improvement of the instrumental setup. Dynamic computer simulation and CE with an array of C^{4}Ds are currently used to follow isotachophoretic enantiomer separations and results will be reported in a second contribution. The same technology will also be employed to study formation and migration behavior of a variety of other electrophoretic boundaries in discontinuous buffer systems, including those associated with IEF.

5 References

[1] Stojkovic, M., Koenka, I. J., Thormann, W., Hauser, P. C., *Electrophoresis* 2014, *35*, 482–486.

[2] Thormann, W., Arn, D., Schumacher, E., *Electrophoresis* 1984, *5*, 323–337.

[3] Thormann, W., Arn, D., Schumacher, E., *Sep. Sci. Technol.* 1984, *19*, 995–1011.

[4] Thormann, W., Arn, D., Schumacher, E., *Electrophoresis* 1985, *6*, 10–18.

[5] Thormann, W., Mosher, R. A., Bier, M., *J. Chromatogr.* 1986, *351*, 17–29.

[6] Thormann, W., Egen, N. B., Mosher, R. A., Bier, M., *J. Biochem. Biophys. Methods* 1985, *11*, 287–293.

[7] Kubáň, P., Hauser, P. C., *Electrophoresis* 2013, *34*, 55–69.

[8] Mai, T. D., Hauser, P. C., *Chem. Record* 2012, *12*, 106–113.

[9] Coltro, W. K. T., Lima, R. S., Segato, T. P., Carrilho, E., de Jesus, D. P., do Lago, C. L., da Silva, J. A. F., *Anal. Methods* 2012, *4*, 25–33.

[10] Kubáň, P., Hauser, P. C., *Electrophoresis* 2011, *32*, 30–42.

[11] Kubáň, P., Hauser, P. C., *Electrophoresis* 2009, *30*, 176–188.

[12] Trojanowicz, M., *Anal. Chim. Acta* 2009, *653*, 36–58.

[13] Gaš, B., Demjanenko, M., Vacík, J., *J. Chromatogr.* 1980, *192*, 253–257.

[14] Hjertén, S., *Chromatogr. Rev.* 1967, *9*, 122–219.

[15] Hirokawa, T., Nakahara, K., Kiso, Y., *J. Chromatogr.* 1989, *463*, 39–49.

[16] Wang, T., Hartwick, R. A., *Anal. Chem.* 1992, *64*, 1745–1747.

[17] Beale, S. C., Sudmeier, S. J., *Anal. Chem.* 1995, *67*, 3367–3371.

[18] Wu, X.-Z., Huang, T., Liu, Z., Pawliszyn, J., *Trends Anal. Chem.* 2005, *24*, 369–382.

[19] Bier, M., Palusinski, O. A., Mosher, R. A., Saville, D. A., *Science* 1983, *219*, 1281–1287.

[20] Mosher, R. A., Saville, D. A., Thormann, W., *The Dynamics of Electrophoresis*, VCH Publishers, Weinheim 1992.

[21] Thormann, W., Zhang, C.-X., Caslavska, J., Gebauer, P., Mosher, R. A., *Anal. Chem.* 1998, *70*, 549–562.

[22] Breadmore, M. C., Kwan, H. Y., Caslavska, J., Thormann, W., *Electrophoresis* 2012, *33*, 958–969.

[23] Hruška, V., Jaroš, M., Gaš, B., *Electrophoresis* 2006, *27*, 984–991.

[24] Hruška, V., Beneš, M., Svobodová, J., Zusková, I., Gaš, B., *Electrophoresis* 2012, *33,* 938–947.

[25] Bercovici, M., Lele, S. K., Santiago, J. G., *J. Chromatogr. A* 2009, *1216*, 1008–1018.

[26] Thormann, W., Caslavska, J., Breadmore, M. C., Mosher, R. A., *Electrophoresis* 2009, *30*, S16–S26.

[27] Thormann, W., Breadmore, M. C., Caslavska, J., Mosher, R. A., *Electrophoresis* 2010, *31*, 726–754.

[28] Mosher, R. A., Breadmore, M. C., Thormann, W., *Electrophoresis* 2011, *32*, 532–541.

[29] Caslavska, J., Mosher, R. A., Thormann, W., *Electrophoresis* 2015, *36*, 1529–1538.

[30] Caslavska, J., Thormann, W., *J. Microcol. Sep.* 2001, *13*, 69–83.

[31] Caslavska, J., Thormann, W., *Electrophoresis* 2006, *27*, 4618–4630.

[32] Thormann, W, Caslavaska, J., Mosher, R. A., *J. Chromatogr. A* 2007, *1155*, 154–163.

[33] Mai, T. D., Schmid, S., Müller, B., Hauser, P. C., *Anal. Chim. Acta* 2010, *665*, 1–6.

[34] Mai, T. D., Hauser, P. C., *Talanta* 2011, *84*, 1228–1233.

[35] Mai, T. D., Hauser, P. C., *Electrophoresis* 2011, *32*, 3000–3007.

[36] Stojkovic, M., Mai, T. D., Hauser, P., *Anal. Chim. Acta* 2013, *787*, 254–259.

[37] Mai, T. D., Hauser, P. C., *J. Chromatogr. A* 2012, *1267*, 266–272.

[38] Koenka, I. J., Sáiz, J., Hauser, P. C., *Comput. Phys. Commun.* 2014, *185*, 2724–2729.

[39] Koenka, I. J., Sáiz, J., Hauser, P. C., *Chimia* 2015, *69*, 172–175.

[40] Gaš, B., Jaroš, M., Hruška, V., Zusková, M. S., Štědrý, M., *LC-GC Eur.* 2005, *18*, 282–288.

[41] Nakatani, M., Shibukawa, A., Nakagawa, T., *Electrophoresis* 1995, *16*, 1451–1456.

[42] Gaš, B., Hruška, V., Dittmann, M., Bek, F., Witt, K., *J. Sep. Sci.* 2007, *30*, 1435–1445.

[43] Boček, P., Gebauer, P., Deml, M., *J. Chromatogr.* 1981, *217*, 209–224.

[44] Snopek, J., Jelínek, I., Smolková-Keulemansová, E., *J. Chromatogr.* 1988, *438*, 211–218.

[45] Mai, T. D., Pham, H. V., Hauser, P. C., *Anal. Chim. Acta* 2009, *653*, 228–233.

www.electrophoresis-journal.com

Publication #3:

Instrumentino: An open-source modular Python framework for controlling Arduino based experimental instruments

Instrumentino: An open-source modular Python framework for controlling Arduino based experimental instruments[☆]

Israel Joel Koenka [a,*], Jorge Sáiz [b], Peter C. Hauser [a]

[a] Department of Chemistry, University of Basel, Spitalstrasse 51, 4056 Basel, Switzerland
[b] Department of Analytical Chemistry, Physical Chemistry and Chemical Engineering - University of Alcalá, Ctra. Madrid–Barcelona Km 33,6, Alcalá de Henares 28871, Madrid, Spain

ARTICLE INFO

ABSTRACT

Instrumentino is an open-source modular graphical user interface framework for controlling Arduino based experimental instruments. It expands the control capability of Arduino by allowing instruments builders to easily create a custom user interface program running on an attached personal computer. It enables the definition of operation sequences and their automated running without user intervention. Acquired experimental data and a usage log are automatically saved on the computer for further processing. The use of the programming language Python also allows easy extension. Complex devices, which are difficult to control using an Arduino, may be integrated as well by incorporating third party application programming interfaces into the Instrumentino framework.

Program summary

Program title: Instrumentino, Controlino

Catalogue identifier: AETJ_v1_0

Program summary URL: http://cpc.cs.qub.ac.uk/summaries/AETJ_v1_0.html

Program obtainable from: CPC Program Library, Queen's University, Belfast, N. Ireland

Licensing provisions: GNU General Public License, version 3

No. of lines in distributed program, including test data, etc.: 17 097

No. of bytes in distributed program, including test data, etc.: 3 425 023

Distribution format: tar.gz

Programming language: Python, C.

Computer: i386, x86-64.

Operating system: Linux, Mac OS X, Windows.

RAM: 60 MB

Classification: 16.4.

External routines: wxPython, pySerial, matplotlib, agw (Instrumentino), SoftwareSerial (Controlino)

Nature of problem:
Control and monitor purpose-made experimental instruments

Solution method:
Modular Graphical User Interface for hardware control

Running time:
Depends on the user.

1. Introduction

In the process of scientific research, many laboratories around the world face the need to build their own purpose-made experimental systems. Indeed, this is an inherent feature of scientific research, in which new and unknown phenomena require new experimental set-ups. While some instruments are too complicated to be developed in-house and require professional assistance and ready-made tools from industry, many are simple enough to be realized with limited engineering capabilities available within research groups and from university support staff. In recent years, the scientific community has discovered the open-source electronics platform "Arduino" for monitoring and controlling experimental hardware [1,2]. An Arduino consists of a microcontroller located on a small printed circuit board (PCB) which is fitted with sockets to allow easy connection of external devices to digital and analog input and output (I/O) pins. The success of this particular hardware package stems from the dedicated integrated development environment (IDE), running on a personal computer (PC) under Windows, Mac OS X or Linux, which was designed for the non-expert user and integrates and significantly simplifies the different steps of editing, compiling, and uploading software to the microcontroller. An Arduino can be connected to a separate PCB or a breadboard equipped with interface circuitry to adapt the signals to different components of an experimental system, and thus gain control and monitor abilities. As an open-source project, the Arduino ecosystem offers a significantly cheaper alternative to other hardware control solutions, such as LabVIEW (National Instruments, Austin TX, USA); Arduino boards are available for as little as about 10$.

The popularity of Arduino controllers took off with hobby projects such as wall-avoiding robots and drones [3,4], 3D printers [5], musical instruments [6,7], cellular phones [8], and scientific applications were not late to follow. To date, Arduino controllers have been reported to control various scientific experimental set-ups. Xoscillo [9], for example, is an Arduino-based oscilloscope and logical analyzer. Do Lago and da Silva [10,11] used an Arduino to control their capacitively coupled contactless conductivity detector (C^4D) for capillary electrophoresis (CE) and high performance liquid chromatography (HPLC). Anzalone et al. [12] reported on an Arduino controlled low-cost colorimeter. Kamogawa et al. [13] have used Arduino to control valves in a flow analysis system. Several Arduino based portable CE instruments were built and successfully used to analyze various samples [14–16]. Several research groups have used the Arduino to monitor ambient conditions such as temperature, humidity and radiation [17–26], as well as pressure and force [19,27–30]. Indeed, many detectors and actuators can be controlled using an Arduino, the possibilities are endless.

The Arduino tool-set provides all the bits and bytes to set up physical control of hardware components. However, it provides only a limited way to interactively control them and there is much room to improve in terms of user interface. The most common and straightforward way to control an Arduino based system is to use the existing Universal Serial Bus (USB), which also powers the Arduino, to exchange information between the Arduino and the PC connected to it. This is easily done using the Arduino *Serial* library and any terminal program on the PC side, but provides only basic capabilities (textual commands and lack of automation and data acquisition). A more sophisticated approach is to write a Graphical User Interface (GUI) that runs on the PC and communicates with the Arduino. Several examples of commercial and free GUIs, built to operate Arduino controlled setups, have been reported. For example, it is possible to create a *MATLAB* (MathWorks, Natick MA, USA) based GUI for Arduino [31] or to use the inherent GUI abilities of *LabVIEW* [32] to control an Arduino. Both of these approaches can produce powerful and customized GUIs for experiments, which are

stand-alone or a part of a more complicated control mechanism. Powerful as they are, a clear disadvantage of these approaches is that they require the purchase of expensive commercial products. Open source alternatives exist as well. For example, *DueGUI* [33], offers Arduino GUI libraries for direct connection to a touch screen, instead of an external PC. Another example is *Guino* [34], which employs a fixed GUI environment on a PC, which receives commands from an Arduino. Both of these packages allow the user to create custom GUI with direct control and monitoring capabilities. The problem is that the GUI customization is done in the Arduino sketch and the Arduino microcontrollers have fairly limited resources in terms of memory and processing power. Moreover, such approaches do not easily allow the interaction with other hardware directly connected to the PC, in order to control more complicated instrumentation. A better approach would be to run a small slave program on the Arduino, and control it via a custom-made GUI on a PC. Such slave programs are available [35,36], yet a fully customizable GUI program is still missing.

In this work we present *Instrumentino*, an open-source modular GUI framework, written in Python, to control and monitor Arduino based experimental systems. It communicates with a program running on the Arduino called *Controlino* (a *sketch* in the Arduino world), via a textual master/slave serial protocol (see next sections). One of the advantages is that this sketch is constant between projects and serves only as a mediator between *Instrumentino* on the PC and the physical I/O pins. All of the GUI implementation is done on the PC, and the effort of programming an Arduino is replaced by writing a system description file in Python.

2. Overview

The information flow in an *Instrumentino* controlled experimental system is depicted in Fig. 1. The I/O pins of an Arduino interface different hardware parts via some glue circuitry to properly convert electrical signals, voltage and power levels. The Arduino board is connected via a USB to a PC which is running *Instrumentino* and provides the GUI. Connection to more complex hardware parts can be made via another USB port of the PC (or a legacy interface such as the RS232, a parallel port etc.). These will be controlled by their matching Application Programming Interfaces (APIs), which in turn, are governed by the *Instrumentino* software.

To clarify, a simple example is given in Fig. 2. It consists of an electronic 0–100 psi pressure controller (Parker–Hannifin, Cleveland OH, USA), which is connected to Arduino, and a 3-way valve (LabSmith, Livermore CA, USA), controlled by a dedicated LabSmith controller. The pressure is set with an analog voltage created using the pulse width modulation (PWM) Arduino output pin, and it is monitored with an analog to digital converter (ADC) input channel. The valve is operated using a LabSmith API, integrated into *Instrumentino*.

3. The *Controlino* sketch

The *Controlino* sketch (controlino.ino, see extra material) provides a simple way to control and monitor an Arduino board via the USB cable. It implements the slave side of a textual master/slave protocol (described below), over a 115 200 bps serial connection. On startup, the sketch initializes and begins listening to the serial port for incoming commands. Each command is an ASCII string, terminated by a carriage return (CR) character (ASCII code: 0x0D). Each command starts with a word (*set*, *read*, etc.), followed by a few parameters. The self-explanatory nature of the commands enables a user to directly control the Arduino using any terminal program for debugging purposes. When a CR character is received, *Controlino* parses the received string and acts upon it. When the execution of a command is finished, it replies with a "done!" string, preceded by other relevant data.

Table 1
The available commands in the Controlino sketch. Arguments are given in parenthesis with possible options separated by vertical lines.

set [pin number] [in\out]	Set a digital pin mode to input or output
reset	Set all digital pins to input mode
read [pin1] [pin2]…	Read the values of a list of pins. Pins are given as "A1" or "D1" for analog and digital pins respectively
write [pin number] [digi\anal] [value]	Write a value to a pin (digital or PWM).
SetPwmFreq [pin number] [divider]	Change the PWM frequency of a pin.
softSerConnect [rx pin] [tx pin] [baudrate] [port number]	Initiates a software serial port using a tx pin and an rx pin that enables external interrupts.
hardSerConnect [baudrate] [port]	Initiates a hardware serial connection.
serSend [hard\soft] [port number]	Send a NULL (0x00) terminated string to a serial port.
serReceive [hard\soft] [port number]	Read the RX buffer of a serial port.
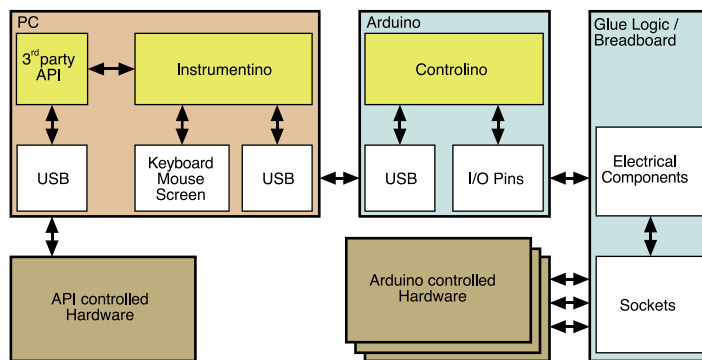
Fig. 1. Data flow in a purpose-made experimental system, using Instrumentino.
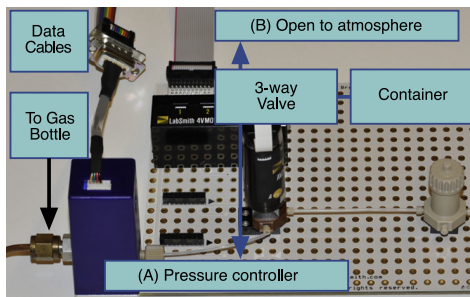

Fig. 2. The hardware components used in the example instrument, overlaid by a corresponding schematic representation.

3.1. The Controlino commands list

The list of available commands implemented in the *Controlino* sketch is shown in Table 1.

Changing the PWM frequency should be done with caution, as it may interfere with other timing related Arduino functions. The number of hardware serial ports is board dependent and up to 4 software serial ports are supported. The *Controlino* sketch is board dependent and different binary files are needed for each type of Arduino board. For now, Arduino boards based on the ATmega328 are supported, as well as the Arduino Mega. Addition of other

boards will require adding board specific settings to the sketch (controlino.ino).

4. The *Instrumentino* package

The *Instrumentino* package provides the front-end for communication with the *Controlino* sketch and acts as the master of the aforementioned communication protocol. It allows the user to directly control the desired experimental parameters (such as pressure, and temperature) without the need to be aware of physical control mechanisms (Arduino pins, voltage levels, etc.). The *Instrumentino* framework enables experimenters and system builders to issue user defined commands and complex running sequences to their system, visually monitor system parameters and automatically acquire experimental data for later analysis, all while requiring minimal programming effort. Moreover, *Instrumentino* is built in such a way that allows the concurrent interaction with several hardware controllers, not necessarily only from the Arduino family. This is very useful when some parts of an experimental system are not readily interfaced to an Arduino. Often manufacturers provide devices, which are designed to be connected directly to a PC (*e.g.* via USB) and communicate via an API. In such cases it is much more straightforward to make use of existing code, rather than to attempt to rewrite it for the Arduino platform. Furthermore the hardware and software details of commercial devices may be proprietary and not available. The *Instrumentino* framework is designed to cope with such situations by using available APIs to address pieces of hardware, thus creating a single control program for the entire system.
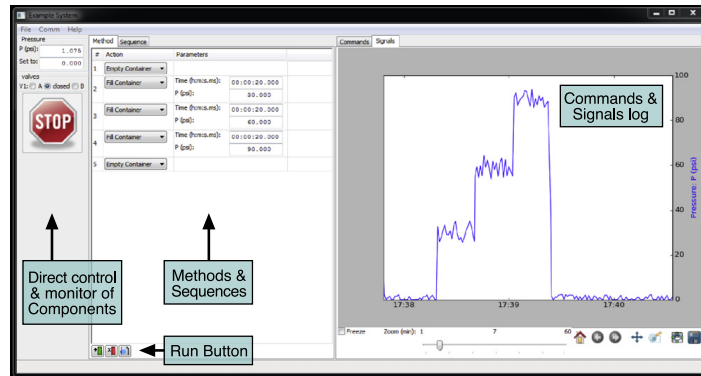
Fig. 3. Screenshot of the Instrumentino application created for container.py. The pressure controller and the valve of the example system can be seen in the components panel. The signal log panel shows how the pressure changed while running the list of actions in the run-control panel.

Python was chosen as programming language for *Instrumentino* because of its ease of use, variety of existing code packages and because it is open source and available for the three operating systems for which the Arduino platform is available. The user interface toolkit chosen for *Instrumentino* was *wxPython*, which is based on the popular cross-platform *wxWidgets* library. It is easy to use and gives a native look on each machine (hence the name wx: Windows & OS X).

To work with *Instrumentino*, the user only needs to provide a system description file (written in Python), which lists the system components and their connections to the Arduino (*e.g.* the Parker pressure controller, connected to the Arduino PWM pin 6 for setting the pressure). It also lets the user define meaningful actions for the system, which can be later executed via the GUI (*e.g.* set the pressure to X psi, wait Y seconds and then turn it off, X & Y being parameters). By listing the components and the actions of a system, *Instrumentino* is provided with all information required to create the specific GUI.

4.1. The system description file structure

The description file is logically divided into the following sections (an example is given in the supplementary material (see Appendix A), container.py):

- **Imports**
  As in any Python module, import statements declare classes and objects defined in other source files. By importing them, it is possible to reference them in the module.
- **Constants**
  It is good coding practice to assign meaningful names to constants relevant to the system, such as Arduino pin assignments.
- **Components**
  The instantiation of objects for each component in the experimental system. Each system component is described in the code by a Python class, which exists in the *Instrumentino* package. Hardware components currently supported include high voltage power supplies, pressure and mass flow controllers, syringe pumps, two-, three- and multi-position valves, and data recording systems.
- **Actions**
  The declaration of basic actions to be performed by the system. Each action is defined as a class, which inherits from the Python class *Instrumentino.action.SysAction*, and needs to implement a method named *Command()*. This method will be called when the action is to be executed.

- **System definition**
  Wrapping up all of the above and some more information (such as the system name and description) in a class, which inherits from the *Instrumentino.Instrument* class.
- **Program run**
  The commands to be executed when this Python file runs. To run the application one needs simply to instantiate the System class defined in the last section. Typing "python container.py" in a terminal will start the application.

4.2. The graphical user interface

The GUI, described by container.py, can be seen in Fig. 3. It features three panels: *components*, *run-control* and *log*, appearing from left to right. The components panel allows the user to directly control and monitor the system components. Each component is represented by a sub-panel and is created according to the components list in the system description file. A component panel is composed of its associated digital and analog variables. A digital variable in a system might be the different positions of a valve (e.g. *A*, *B* or *closed* for the LabSmith valve in the example) or a trigger signal (*on* or *off*). A digital variable is represented by a set of radio buttons with the possible options. An analog variable might be a measurement of some physical quantity (*e.g.* pressure) and is represented by a text box for reading the value and an optional text box for setting it, within the allowed range. The components panel also features a large stop button, to be used in case an experiment needs to be shut off abruptly.

The run-control panel has two modes. The first operates with methods. A method is a successive list of actions, from the actions pool defined in the description file. It conceptually describes a way to achieve a specific experimental goal. The action in each line in the list is picked using a combo-box, and its relevant parameters can be set. The user can then run the method using the run button or save the newly defined method as a *.mtd* file using the *File* menu. The second mode manages sequences, in which the user can create a sequence, composed of previously saved methods. Each method can be run a number of consecutive times, so a whole day of experiments or a long-term monitoring experiment can be planned and run automatically. A defined sequence can also be saved, as a *.seq* file, using the *File* menu.

The *log* panel to the right has two modes as well. One is the *command-log*, which logs each run of a method or a sequence. The

contents of this list are automatically saved as a *.txt* file using the date and time as the file name. It acts as a lab journal and can be referenced later to report on the exact experimental conditions. Another mode is the *signal-log*, an interactive timeline graph, which shows the physical parameters measured by the system. Each parameter has its own *y* axis and a different color on the graph. This data is automatically saved as well as a *.csv* file (comma separated values) using the same file name as the *command log*. The file can be later opened in spreadsheet programs such as Excel (Microsoft Office) or the open source Calc (LibreOffice) for further data analysis.

4.3. Program workflow

When the application starts, the panels are disabled. It is only possible to create methods and sequences until all the required controllers are connected, using the *Comm* menu. Once communication is established, system variables (pressure and valve position in the example) are periodically read and displayed in the left panel, and in the signal log panel. The user can then run a method and observe the signal log. The screenshot in Fig. 3 was taken after a method had been created and run (see center panel). It set the valve to port A to fill the container with gas and set the pressure inside to 30, 60 and 90 psi in steps of 20 s. Afterwards it opened the container by setting the valve to port B. The resulting pressure readings can be seen in the log panel.

The *Instrumentino* code package is available as a Python egg which encapsulates both the Python code and the resource files needed for operation. It can be downloaded from the Computer Physics Communications Program Library (http://cpc.cs.qub.ac.uk/summaries/AETJ_v1_0.html), PyPI repository (https://pypi.python.org/pypi/instrumentino) or Github (https://github.com/yoelk/Instrumentino). Users of *Instrumentino* will need to install the egg file on their computer, create a Python module to describe their experimental set-up and run it (similar to container.py). It is released under the GPLv3 license, to ensure its open-source nature in the future.

5. Conclusions

In research, the construction of purpose made experimental systems is frequently necessary. The introduction of open source electronics, in particular the Arduino platform, is an enabling factor, in providing researchers a tool to build relatively complex systems, which were previously only possible with significantly more effort or were beyond reach. The *Instrumentino/Controlino* software package was developed to streamline the development of the control software for such systems and to allow full automation in order to improve performance or to enable unattended operation. It was built in such a way that only a minimal programming effort is required, greatly simplifying the task of instrument control and making it accessible for less experienced programmers. Since its development, *Instrumentino* has been used extensively in our research groups, saving a significant amount of time and effort, and we believe it can assist other researchers as well in achieving their goals. As a free open source project, users are welcome to contribute and extend *Instrumentino* to support more kinds of controllers and hardware components or to add features they find useful. There is much potential to grow and the use of *Instrumentino* is, of course, not limited to scientific purposes.

Acknowledgment

Conflicts of interest

The authors have declared no conflict of interest.

Appendix A. Supplementary material

Supplementary material related to this article can be found online at http://dx.doi.org/10.1016/j.cpc.2014.06.007.

References

[1] J.M. Pearce, Building research equipment with free, open-source hardware, Science 337 (2012) 1303.
[2] A. D'Ausilio, Arduino: a low-cost multipurpose lab equipment, Behav. Res. Methods 44 (2012) 305.
[3] Brandon121233, Wall avoiding Robot, http://www.instructables.com/id/Make-a-wall-avoiding-Robot!/. Retrieved April 2014.
[4] APM, Ardupilot—official website, http://ardupilot.com/. Retrieved April 2014.
[5] A. Bowyer, RepRap—official website, http://reprap.org/wiki/RepRap. Retrieved April 2014.
[6] J.H. Owen Vallis, Arduinome—official website, http://flipmu.com/work/arduinome/. Retrieved.
[7] Kylemcdonald, Arduino based guitar pedal, http://www.instructables.com/id/Lo-fi-Arduino-Guitar-Pedal/. Retrieved April 2014.
[8] Xiaobo, ArduinoPhone, http://www.instructables.com/id/ArduinoPhone/. Retrieved April 2014.
[9] Aguaviva, Xoscillo, http://code.google.com/p/xoscillo/. Retrieved April 2014.
[10] J.A. Fracassi da Silva, C.L. do Lago, An oscillometric detector for capillary electrophoresis, Anal. Chem. 70 (1998) 4339 (1998/10/01).
[11] K.J.M.F. Claudimir Lucio do Lago, OpenC4D—official website, https://sites.google.com/site/openc4d/home. Retrieved April 2014.
[12] G.C. Anzalone, A.G. Glover, J.M. Pearce, Open-source colorimeter, Sensors 13 (2013) 5338.
[13] M.Y. Kamogawa, J.C. Miranda, Use of "arduino" open source hardware for solenoid device actuation in flow analysis systems, Química Nova 36 (2013) 1232.
[14] T.D. Mai, et al., Portable capillary electrophoresis instrument with automated injector and contactless conductivity detection, Anal. Chem. 85 (2013) 2333. 2013/02/19.
[15] J. Sáiz, T.D. Mai, P.C. Hauser, C. García-Ruiz, Determination of nitrogen mustard degradation products in water samples using a portable capillary electrophoresis instrument, Electrophoresis 34 (2013) 2078.
[16] J. Sáiz, et al., Rapid determination of scopolamine in evidence of recreational and predatory use, Science & Justice 53 (2013) 409.
[17] G. Gasparesc, Development of a low-cost system for temperature monitoring, in: 2013 36th International Conference on Telecommunications and Signal Processing, TSP, 2013, p. 340.
[18] N. Barroca, et al., Wireless sensor networks for temperature and humidity monitoring within concrete structures, Constr. Build. Mater. 40 (2013) 1156.
[19] M.R. Dehmlow, Asme, Affordable universal solar tracker, in: Proceedings of the Asme 5th International Conference on Energy Sustainability 2011, Pts a-C, 2012, pp. 653–661.
[20] A. Abdullah, et al. Development of wireless sensor network for monitoring global warming, in: 2012 International Conference on Advanced Computer Science and Information Systems, 2012, pp. 107–111.
[21] S.-h. Sun, Y.-s. Jin, W.-j. Zhang, Asme, Design and simulation of remote temperature monitor and control system based on embedded web server, in: 2011 International Conference on Instrumentation, Measurement, Circuits and Systems, 2011, pp. 297–300.
[22] M.G. Rodriguez, et al. Wireless sensor network for data-center environmental monitoring, in: 2011 Fifth International Conference on Sensing Technology, ICST 2011, 2011, p. 533.
[23] A.H. Kioumars, T. Liqiong, Wireless network for health monitoring: heart rate and temperature sensor, in: 2011 Fifth International Conference on Sensing Technology, ICST 2011, 2011, p. 362.
[24] J.M. Gomes, P.M. Ferreira, A.E. Ruano, Implementation of an intelligent sensor for measurement and prediction of solar radiation and atmospheric temperature, in: 2011 IEEE 7th International Symposium on Intelligent Signal Processing, WISP 2011, 2011, 6 pp.
[25] F.J. Garcia-Diego, J.J. Pascual, F. Marco-Jimenez, Technical note: design of a large variable temperature chamber for heat stress studies in rabbits, World Rabbit Sci. 19 (2011) 225.
[26] R. Gomaa, I. Adly, K. Sharshar, A. Safwat, H. Ragai, ZigBee wireless sensor network for radiation monitoring at nuclear facilities, in: Proceedings of 2013 6th Joint IFIP Wireless and Mobile Networking Conference, WMNC 2013, 2013, 4 pp.
[27] M. Stalin, C.L. Bennett, in: R. Jung, A.J. McGoron, J. Riera (Eds.), 29th Southern Biomedical Engineering Conference, 2013, pp. 137–138.
[28] F. Grenez, M. Viqueira Villarejo, B. Garcia Zapirain, A. Mendez Zorrilla, Wireless prototype based on pressure and bending sensors for measuring gate quality, Sensors (Basel, Switzerland) 13 (2013) 9679.

[29] L. Russell, A.L. Steele, R. Goubran, Ieee, in: 2012 Ieee International Instrumentation and Measurement Technology Conference, 2012, pp. 2695–2699.

[30] R.P. Rush, Acm, sensation augmentation to relieve pressure sore formation in wheelchair users, in: Assets'09: Proceedings of the 11th International Acm Sigaccess Conference on Computers and Accessibility, 2009, pp. 275–276.

[31] Rmagtibay, Arduino I/O-Matlab basic tutorial, http://www.instructables.com/id/Arduino-IO-Matlab-basic-tutorial/. Retrieved April 2014.

[32] National Instruments, NI LabVIEW Interface for Arduino Toolkit http://sine.ni.com/nips/cds/view/p/lang/en/nid/209835. Retrieved April 2014.

[33] Cowasaki, DueGUI, http://www.cowasaki.co.uk/DueGUI/DueGUI_0_13.pdf. Retrieved April 2014.

[34] Madshobye, Guino: Dashboard for your Arduino, http://www.instructables.com/id/Guino-Dashboard-for-your-Arduino/. Retrieved April 2014.

[35] Arduino, Arduino and Python, http://playground.arduino.cc/interfacing/python-.UxY0Tl7hO2y. Retrieved April 2014.

[36] Intructable, Control your arduino from your PC with the Qt Gui, http://www.instructables.com/id/Control-your-arduino-from-your-PC-with-the-Qt-Gui/. Retrieved April 2014.

Publication #4:

Instrumentino: An Open-Source Software for Scientific Instruments

Instrumentino: An Open-Source Software for Scientific Instruments

Israel Joel Koenka[§*a], Jorge Sáiz[b], and Peter C. Hauser[a]

[§]SCS-Metrohm Award for best oral presentation

Abstract: Scientists often need to build dedicated computer-controlled experimental systems. For this purpose, it is becoming common to employ open-source microcontroller platforms, such as the *Arduino*. These boards and associated integrated software development environments provide affordable yet powerful solutions for the implementation of hardware control of transducers and acquisition of signals from detectors and sensors. It is, however, a challenge to write programs that allow interactive use of such arrangements from a personal computer. This task is particularly complex if some of the included hardware components are connected directly to the computer and not *via* the microcontroller. A graphical user interface framework, *Instrumentino*, was therefore developed to allow the creation of control programs for complex systems with minimal programming effort. By writing a single code file, a powerful custom user interface is generated, which enables the automatic running of elaborate operation sequences and observation of acquired experimental data in real time. The framework, which is written in *Python*, allows extension by users, and is made available as an open source project.

Keywords: *Arduino* · Computer-control of experiments · Data acquisition · Graphical user interface · Purpose-made instruments · *Python*

1. Introduction

Experimental scientists are often confronted with the need to build purpose-made instruments and experimental systems for investigating new scientific phenomena. Building such systems however, requires a range of technical skills, such as machining, electronics and computer programming, in which many scientists are not proficient. For this reason universities employ technical staff to assist in the building process. But while a mechanical workshop is common, and an electronics engineer is often available, the required programming efforts are usually left to the scientists themselves to fulfill. This has been realized by industry, and visual programming environments (such as LabVIEW) have been made available to alleviate some of the difficulties of programming electronically controlled hardware. Unfortunately, these tools are often very expensive and not always sufficiently easy to use.

In the past few years, a new trend has emerged among experimental scientists.[1–13] More and more research groups are inspired by the open-source hardware world, incorporating open-source microcontroller platforms in their systems, *Arduino*[14] being the best known of these.

Arduinos are small electronic printed circuit boards, carrying a programmable microcontroller that allows users to easily operate attached electronic devices by setting and reading voltage levels on its output and input pins. The *Arduino* programming environment provides all that is necessary to set the voltage levels in a predetermined sequence, but very little to interactively control the system or allow the user to monitor the acquired data in real time. This is usually essential for an experimental system. Moreover, experimental set-ups often require hardware units that are connected directly to the computer (*e.g.* through a USB port) and cannot be interfaced through an Arduino. The need for an easy way to create graphical user interface (GUI) programs for custom experimental set-ups was identified in our group, which led us to develop *Instrumentino*.

Instrumentino is an open-source framework for developing custom GUI programs to control experimental systems and instruments, while requiring only a minimal programming effort. The user only needs to provide a single system configuration file in which details about the set-up are given. The outcome is a fully functional and user-friendly graphical control program for that system which is comparable to commercial products. It allows the user to graphically control each individual component in the system, and to orchestrate their operation to create elaborate and automatic running sequences. Moreover, it graphically presents real-time acquired data, and automatically saves it for later analysis. Importantly, *Instrumentino* enables the simultaneous operation of several hardware controllers, which do not necessarily have to be *Arduino* boards.

Instrumentino was written in *Python*, a popular high-level programming language that is easier to learn and understand than most traditional languages (such as C). *Python* has also the advantage of being platform-independent. Free online courses to introduce non-programmers to the world of *Python* are available.[15]

Initially, *Instrumentino* was developed to answer the system control needs of our research group, in particular to operate purpose-made capillary electrophoresis instruments. Soon it became the standard for system control in our group, and more than a dozen projects have been realized in a relatively short time. A publication on *Instrumentino* has appeared in *Computer Science Communications*.[16] The source code is available at the GitHub repository hosting service,[17] and user-contributed additions may be deposited there as well.

Correspondence: I. J. Koenka[a]
Tel.: +41 61 267 1061
E-mail: yoelk@tx.technion.ac.il
[a]Department of Chemistry
University of Basel
Spitalstrasse 51, CH-4056 Basel
[b]Department of Analytical Chemistry,
Physical Chemistry and Chemical Engineering
University of Alcalá
Ctra. Madrid-Barcelona Km 33.6
Alcalá de Henares 28871, Madrid, Spain

2. Controlling/Monitoring Physical Properties

To clarify how *Instrumentino* is used, a simple example system in which an *Arduino* is employed is given in Fig. 1. The dashed parts of the figure represent optional hardware connected *via* a USB interface to the computer. A more complicated example including third-party controllers is given elsewhere.[16] The example instrument is a small box, in which the temperature and pressure need to be controlled. These physical properties can be set in a closed system, by using a thermostat and a pressure controller respectively, both of which can be electronically controlled *via* an *Arduino*.

The way to electronically control a physical property is to combine a sensor and an actuator in a closed feedback loop. A proportional-integral-derivative (PID) thermostat, for example, is composed of a thermometer (sensor) and a heating element (actuator), which in this example are operated directly by the *Arduino*. The temperature is read using an analog input pin (pin A1) and the heating element is periodically turned on and off to reach the desired value using a digital pin (pin D2). The PID control feedback loop for the thermostat is closed in the *Arduino* itself, *i.e.* the actuator is controlled by the software running on the *Arduino* according to the measured sensor signal.

Another example is the control of pressure with a dedicated electronic pressure controller (*e.g.* OEM-EP, Parker–Hannifin, Cleveland OH, USA). The desired pressure can be set *via* the *Arduino* by supplying a voltage between 0 and 5 V proportional to the pressure within the possible range (1000 and 2000 mbar in the example), so 0, 2.5 and 5 volts will result in 1000, 1500 and 2000 mbar pressure respectively. Since most *Arduino* boards do not have analog output pins, an external digital to analog converter (D/A) converts a PWM (Pulse Width Modulation) digital signal from pin D3 to an analog voltage for the pressure controller. The actual pressure can be read from the pressure controller, similar to the temperature, as an analog signal (input pin A0).

3. PC-Arduino Interaction

The physical properties in the example are controlled and monitored by the *Arduino* I/O pins. In order to let the user issue commands to the *Arduino*, a program (called a *Sketch* in the *Arduino* environment) was written to run on the *Arduino* which constantly listens to incoming textual commands from the USB port of the computer and acts upon them. The *Sketch*
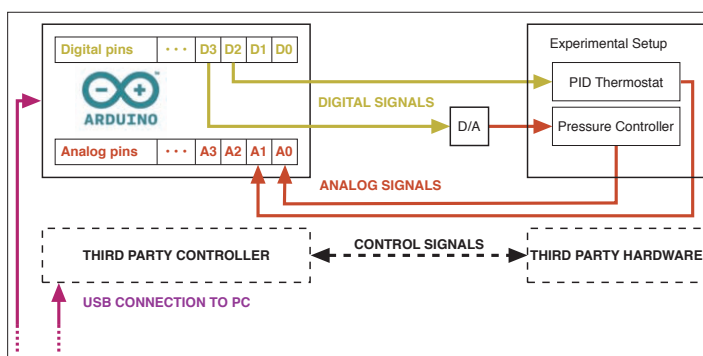

Fig. 1. A simple experimental system, composed of a thermostat and a pressure controller, which are controlled *via* an *Arduino*.

was called *Controlino* to imply that it lets the user control an *Arduino* from the PC. For example, when the user types in 'Read A0' or 'Write D3 0', *Controlino* reads the voltage level on analog pin A0 and sends it back *via* the same serial connection, or sets pin D3 to 0 volts respectively. In the example, this would have the effect of reading the pressure, or setting it to its minimal value of 1000 mbar. On the PC side, the interaction is automated with *Instrumentino*.

4. How *Instrumentino* Works

Instrumentino is a software platform, written in *Python*, for developing custom GUI programs to control scientific instruments. It releases the user from dealing with low-level technical details such as pin numbers and voltage levels.

4.1 *The Python Description File*

An experimental system may involve numerous components of different kinds, and each component in turn may control one or more experimental variables. The thermostat and pressure controller in the example (Fig. 1) are quite simple, having only one variable each (temperature and pressure respectively). Each of these variables are characterized by their operating range and their physical units (*e.g.* 1000–2000 mbar or 0–100 °C), and the required electrical connections for each parameter consist of two pins (an input pin and an output pin). This information is all that is necessary for translating high-level user commands such as 'set the pressure to 2000 mbar' to the low-level operation of setting pin D3 to output 5 volts. This information is provided to *Instrumentino* through a text file, which is written in *Python* and called the *System Configuration File*.

The system configuration is displayed on the left in Fig. 2. As can be seen, the system configuration data is composed of two parts. The first is a list of system com-

ponents, accompanied by the information required for their operation. Appropriate *Python* classes describe the components and are provided with the essential information such as pin numbers, voltage ranges *etc*. If an appropriate class is not already present, it has to be added to *Instrumentino*. Once a new class has been added to the *Instrumentino* source code repository, everyone can use it, which is one of the benefits of being an open-source project.

The second list contains meaningful basic actions that the system is required to perform. These are short pieces of *Python* code (functions) that achieve basic tasks. For example, running the action 'Pressurize' (see Fig. 2) tells the system to set a certain pressure for a given amount of time, after which the pressure is released. Both the pressure and the time to wait are given as arguments to the action function. The user may define many actions with different levels of complexity to account for all of the functionalities of the set-up.

These two lists contain the core information on the system and represent all the required programming effort. The exact technical details on how to correctly define these lists can be found in documents and examples in the *Instrumentino* directory on GitHub.[17] The outcome is an executable *Python* file, which when run, starts a customized GUI program for the set-up defined.

4.2 *The Graphical User Interface*

Instrumentino was designed to provide a system-dependent GUI in a uniform format, using the information given in the system configuration file. The main window is divided into three sub-windows (views) as shown in Fig. 2: the component view, the automation view and the log view.

4.2.1 *The Component View*

The first view from the left is the component view, which provides the most basic way to access the components of the
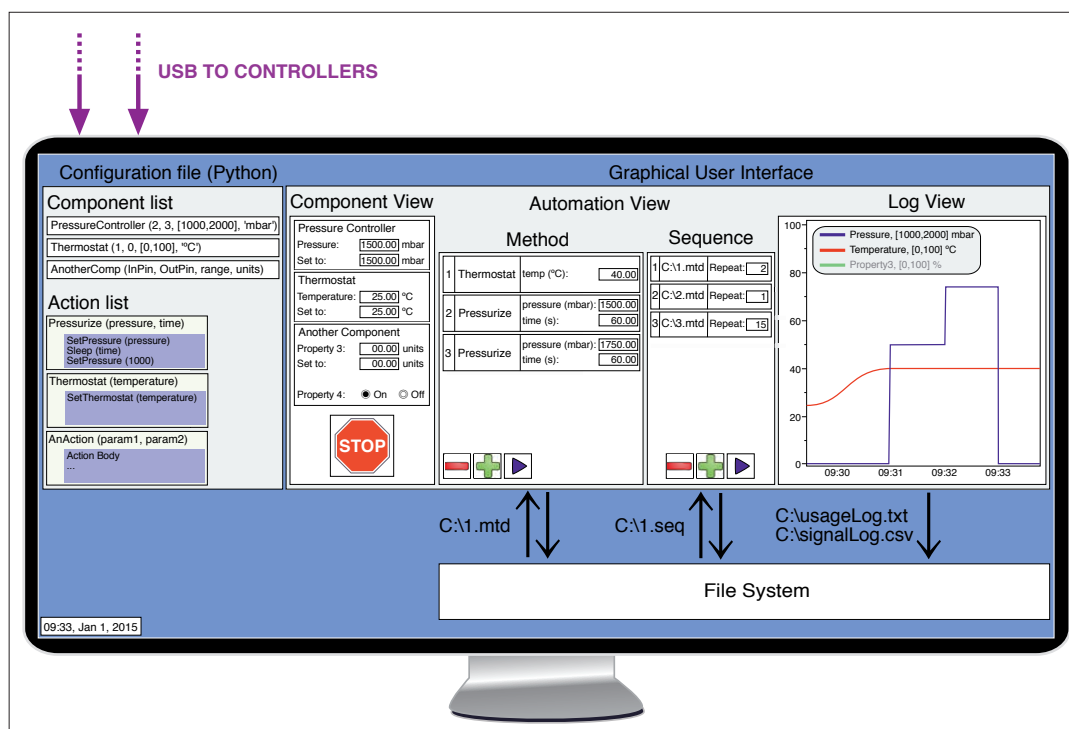
Fig. 2. Schematic diagram of how *Instrumentino* is used to control the example system in Fig. 1.

system. Each component is given a tile in which all of its controllable variables are shown with their current values (*e.g.* as read through the *Arduino*). The values of analog variables such as pressure and temperature can also be set in text boxes within the ranges defined in the system configuration file. Digital on/off-signals are shown as radio buttons and can also be set. It is also possible that a single component of the system may have several variables of different kinds.

4.2.2 The Automation View

The next view from the left is the automation view, in which *Methods* and *Sequences* can be defined and run. *Methods* and *Sequences* present two levels of automation. A *Method* is an extendable list of the actions defined in the system configuration file. The arguments given to the action functions (*e.g.* pressure and time) can be set by the user in matching text boxes, shown alongside the name of the action. In this way, an elaborate method can be defined to achieve a desired experimental goal. Once defined, a *Method* can be saved as a *.mtd* file for later use. This allows the user to define a library of *Methods* in order to save time and effort.

The next level of automation is the *Sequence* mode. A *Sequence* is simply a list of *Methods* from the user's *Method* library. Each item in the list can be defined to be repeated several times if necessary in order to build long operational runs that may last days or even months. This is particularly useful when certain experimental parameters need to be optimized. A series of *Methods* can be made to cover the relevant parameter space and automatically run without user intervention. Once finished, the overall results can be analyzed by inspecting the log view.

4.2.3 The Log View

The rightmost view is used to present the user with graphical and textual records of the usage of the experimental system. As long as the software is running, experimental data of system variables (*e.g.* pressure, temperature) is recorded on the computer and plotted in an overlaid manner as a time series. The log view in Fig. 2 shows the temperature and pressure traces after the example *Method* was started at 09:30. The temperature, which had been set to 40 °C in the first entry, increased over time from 25 °C and was followed by two pressure steps of 1500 and 1750 mbar (50 and 75% respectively).

Each trace is given a different combination of color and line thickness for distinction. As a highly complicated system may have many overlaid traces, it was made possible to turn their visibility on or off by clicking on the matching entry in the graph legend (in the example, the trace of 'Property3' is toggled off). All traces are plotted on a common vertical axis, reflecting the current values as a percentage of the relevant variable range. In case of bipolar variables (*e.g.* –50 to +100), positive results are plotted as solid lines and negative results as dashed lines (for the ranges 0 to +100 and 0 to –50 respectively). This allows to maintain a common zero point on the percentage scale for all variables, as otherwise the display can be very confusing. A set of graph orientation controls (not shown in Fig. 2) allows the user to freeze the timeline and zoom on different areas of interest in the graph.

Like the automation view, the log view can host either a graphical signal log or a textual operation log (not shown) which records the user's operations (*e.g.* 'run method 1.mtd @ 09:30, 1/1/2015'). The outputs of both logs are automatically saved as *.csv* and *.txt* files respectively, using the current date and time as the file name. The signal log can later be opened in any spreadsheet program to view the raw data. For the sake of simplicity digital signals are not shown on the screen but their values are saved in the signal log file.

5. Current Systems Employing *Instrumentino*

As mentioned earlier in the text, most of the projects using *Instrumentino* so far have concerned capillary electrophoresis instruments, built for different purposes. This includes dual-channel portable instruments for the analysis of fireworks[7] (Fig. 3) and for the environmental analysis of surface water near an old mine, a stationary system for unmanned automatic wastewater monitoring, a system for investigating electrophoresis dynamics by using an array of detectors, a system for handling sub-microliter sample volumes, and systems for on-line pre-concentration of diluted samples. *Instrumentino* has also been chosen to be used in projects outside our lab, such as for an automated coulometric micro-titrator, a low-cost apparatus for measuring thermo-mechanical rock properties, and even for teaching students in physics teaching labs.

Fig. 3. Photograph of the dual-channel portable CE system.[7]

Besides simplifying the construction and operation of purpose-made experimental arrangements, another possible benefit of using *Instrumentino* is cost savings. Instruments which are commonly used in laboratories and are usually bought from commercial suppliers may be built in-house at significantly lower cost. For example, an electronic control box for four mass flow controllers (MFC) was built in our group for as little as 50 CHF, while a similar commercial product would have cost about 1,000 CHF. MFCs are used in many laboratories for the exact setting of gas flows towards a reaction or measurement chamber. Each MFC (*e.g.* from MKS Instruments, Andover MA, USA) has a connector with analog input and output pins for setting the desired mass flow and reporting the current flow value respectively. These devices can be controlled by an *Arduino* as easily as the pressure controller of Fig. 1. Therefore, an *Arduino*-based

interface was constructed in our group to control up to four MFCs simultaneously as seen in Fig. 4 and this has been used for different purposes. The design can easily be extended to more MFCs (*e.g.* up to 16 different MFCs when using an *Arduino Mega*[18]). In combination with *Instrumentino* this control box enables the user to control the gas flows in software to conduct experiments automatically.

6. Conclusions

Open-source hardware and software enables researchers with limited expertise in electronics and programming to construct complex apparatus, offering opportunities for substantial cost savings to research labs.[6] *Instrumentino* is one of many such tools to assist in the building of custom-made and routinely used appliances for conducting research. Since its development it has been incorporated in many projects, enabling their quick realization, and it has drawn the attention of peers elsewhere. As a free open-source project, *Instrumentino* has the potential to grow. The authors invite fellow experimental scientists to join the open source development of *Instrumentino*, for a greater mutual benefit.

Conflicts of interest

The authors have declared no conflict of interest.

[1] G. C. Anzalone, A. G. Glover, J. M. Pearce, *Sensors* **2013**, *13*, 5338.
[2] E. T. da Costa, M. F. Mora, P. A. Willis, C. L. do Lago, H. Jiao, C. D. Garcia, *Electrophoresis* **2014**, *35*, 2370.
[3] C. Galeriu, *The Physics Teacher* **2013**, *51*, 156.
[4] G. Gasparesc, '36th International Conference on Telecommunications and Signal Processing (TSP)', **2013**, p. 340, DOI:10.1109/tsp.2013.6613948,
[5] J. A. Kornuta, M. E. Nipper, J. B. Dixon, *J. Biomech.* **2013**, *46*, 183.
[6] J. M. Pearce, *Science* **2012**, *337*, 1303.
[7] J. Sáiz, M. T. Duc, I. J. Koenka, C. Martín-Alberca, P. C. Hauser, C. García-Ruiz, *J. Chromatogr. A* **2014**, *1372*, 245.
[8] J. Sáiz, M. Thanh Duc, P. C. Hauser, C. Garcia-Ruiz, *Electrophoresis* **2013**, *34*, 2078.
[9] A. H. Shajahan, A. Anand, 'International Conference on Energy Efficient Technologies for Sustainability (ICEETS)', **2013**, p. 241.
[10] M. Thanh Duc, P. Thi Thanh Thuy, P. Hung Viet, J. Sáiz, C. Garcia Ruiz, P.C. Hauser, *Anal. Chem.* **2013**, *85*, 2333.
[11] V. Velusamy, K. Arshak, O. Korostynska, A. Al-Shamma'a, *Key Eng. Mat.* **2013**, *543*, 47.
[12] G. S. Zahn, C. Domienikan, R. P. M. Carvalhaes, F. A. Genezini, 'XXXV Brazilian Workshop On Nuclear Physics', **2013**, p. 141.
[13] M. Zolkapli, S. A. M. Al-Junid, Z. Othman, A. Manut, M. A. Mohd Zulkifli, 'International Conference on Technology, Informatics, Management, Engineering and Environment (TIME-E 2013)', **2013**, p. 43.
[14] *Arduino*, http://www.arduino.cc, retrieved Jan. 2015.
[15] B. Klein, online Python course, http://www.python-course.eu/, retrieved Jan. 2015.
[16] I. J. Koenka, J. Sáiz, P. C. Hauser, *Comput. Phys. Commun.* **2014**, *185*, 2724.
[17] I. J. Koenka, Instrumentino repository, https://github.com/yoelk/Instrumentino, retrieved Jan. 2015.
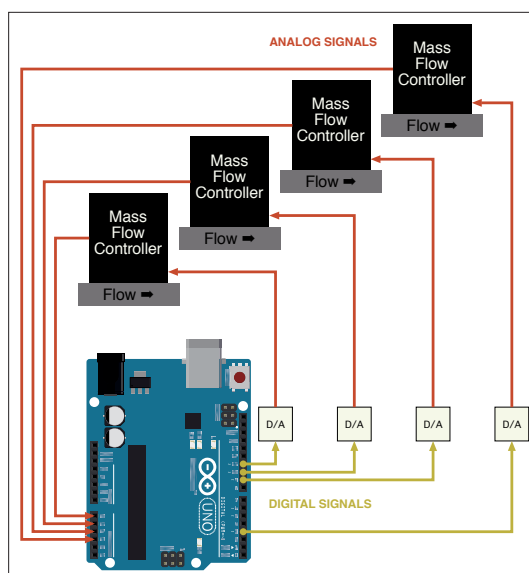[18] *Arduino Mega*, http://arduino.cc/en/Main/arduinoBoardMega, retrieved Jan. 2015.

Fig. 4. Schematic diagram of the electrical connections for an MFC control box.

Publication #5:

Thermostatted dual-channel portable capillary electrophoresis instrument

Israel Joel Koenka[1]
Nina Küng[2,3]
Pavel Kubáň[4]
Thomas Chwalek[2]
Gerhard Furrer[3]
Bernhard Wehrli[2]
Beat Müller[2]
Peter C. Hauser[1]

[1]Department of Chemistry,
University of Basel, Basel,
Switzerland
[2]Eawag, Swiss Federal Institute
of Aquatic Science and
Technology, Kastanienbaum,
Switzerland
[3]Institute of Biogeochemistry
and Pollutant Dynamics,
Department of Environmental
Systems Science, ETH Zurich,
Zurich, Switzerland
[4]Institute of Analytical Chemistry
of the Czech Academy of
Sciences, Brno, Czech Republic

Research Article

Thermostatted dual-channel portable capillary electrophoresis instrument

A new portable CE instrument is presented. The instrument features the concurrent separation of anions and cations in parallel channels. Each channel has a separate buffer container to allow independent optimization of separation conditions. The microfluidics circuit is based on off-the-shelf parts, and can be easily replicated; only four valves are present in the design. The system employs a miniature automated syringe pump, which can apply both positive and negative pressures (-100 to 800 kPa). The application of negative pressure allows a semi-automatic mode of operation for introducing volume-limited samples. The separations are performed in a thermostatted compartment for improved reproducibility in field conditions. The instrument has a compact design, with all components, save for batteries and power supplies, arranged in a briefcase with dimensions of $52 \times 34 \times 18$ cm and a weight of less than 15 kg. The system runs automatically and is controlled by a purpose-made graphical user interface on a connected computer. For demonstration, the system was successfully employed for the concurrent separation and analysis of inorganic cations and anions in sediment porewater samples from Lake Baldegg in Switzerland and of metal ions in a sample from the tailing pond of an abandoned mine in Argentina.

1 Introduction

On-site analysis is important when the results are required for time-critical decisions or if the samples are not stable. The logistics of an analytical campaign can also be significantly streamlined by field analysis. CE is well suited to mobile analysis tasks due to its inherent simplicity compared to other separation methods such as HPLC and ion-chromatography as well as its high versatility for different classes of ionic species. Portable CE instruments have therefore gained in interest in the last few years. Successful examples include many diverse applications such as the determination of residues of improvised explosive devices [1–3], chemical warfare agent detection [4, 5], the detection of amphetamines in street drugs and urine of suspected users [6], the analysis of food samples [7–9], the detection of hydrazines in environmental samples [10], the determination of beta-agonists in pig feed [11], the analysis of volatiles in air samples

(after absorption) with a mobile robotic system [12], organic acids including herbicides in environmental samples [13], DNA fragments [14], inorganic ions in urine, blood serum samples, or exhaled breath condensate [15, 16], as well as in environmental samples [17–22]. Portable CE has also been combined with portable PCR for the detection of viral infections [23], the identification of cattle breeds [24], and forensic purposes [25]. The topic of portable CE has been reviewed by Macka and coworkers in 2010 [26], in 2013 by Lewis *et al.* [27] and very recently by Van Schepdael [28].

A critical challenge for portable CE instruments is the injection. For benchtop instruments the most common approach is direct pressurization of the sample vial after having moved it to the capillary inlet. For a time, a commercial portable instrument was available, which incorporated a conventional sampling tray and hydrodynamic injection [13, 14]. However, it appears that the company is no longer in business. For purpose-made portable CE instruments which have been reported in the scientific literature other approaches have been adapted. The earliest such instruments relied on electrokinetic injection. This is the simplest approach [20–22], as the hardware for applying voltage is inherently available. It is not ideal however, as electrokinetic injection depends on the conductivity of the sample and therefore the results will be biased for varying sample matrices. Improvised siphoning injection by manually lifting the capillary, which is temporarily placed in the sample vial, has also often been used [17–19]. This does not require special hardware either, but the delicate procedure is difficult to carry out in the field.

Correspondence: Professor Peter Hauser, Department of Chemistry, University of Basel, Spitalstrasse 51, 4056 Basel, Switzerland
E-mail: Peter.Hauser@unibas.ch

Abbreviations: C⁴D, capacitively coupled contactless conductivity detection; **HPLC**, high performance liquid chromatography; **HV**, high voltage; **PACE**, pressure-assisted CE; **PID**, proportional-integral-derivative; **PMMA**, polymethylmethacrylate; **SIA**, sequential injection analysis

As the timing is manual the performance is highly dependent on the operator skill. Different approaches to improve sample injection for portable CE instruments have therefore been investigated. Kaljurand and coworkers investigated a syringe-based system, which employed a metering valve in the flow path to restrict and thereby control the flow of sample injected into the capillary [1, 5]. Automated siphoning was recently introduced by Greguš *et al.* [15]. This system has the capillary end connected to an auxiliary tubing leading to a buffer container positioned about 10 cm lower than the inlet; the connection is opened and closed with a tube pinch valve for aspirating the sample at the other end. Hauser and coworkers have reported portable instruments based on pressurization of a buffer reservoir with compressed air and a valving system to achieve hydrodynamic injection [8, 29, 30]. However, these instruments required a relatively large sample volume, giving up one of the advantages of CE, namely its suitability for volume-limited samples.

Frequently, the determination of both, cations and anions, is desired in single samples. While there are several approaches for the concurrent determination of both kinds of ions, including dual-opposite end injection, the only one that allows an independent buffer selection for each channel is dual-channel CE. This has also been implemented in portable systems [8, 29, 30].

For a portable CE instrument to work well under field conditions, care should be taken with regard to the effect of ambient temperature. CE results are temperature sensitive as all transport phenomena in liquid media depend on viscosity (hydrodynamic plug injection, electrophoretic migration, etc.), and even the detector signal itself varies with temperature. Shading from sunlight has therefore been recommended [19], e.g. by enclosing the separation section in an opaque box [15].

In this report, a new portable CE instrument employing a microfluidic breadboard approach based on miniature off-the-shelf parts [31] is presented, which addresses several of the points discussed above: (i) Injection is achieved using a miniature syringe pump, offering full automation when using positive pressure and semi-automation when using negative pressure for aspiration of volume-limited samples, (ii) the CE separations are carried out inside an actively thermostatted compartment, (iii) cations and anions are separated simultaneously in two distinct channels using individual BGEs. The performance of the new system was tested by the analysis of porewater samples extracted from lake sediment cores directly at the sampling site at Lake Baldegg in Switzerland, as well as from a tailing pond of an abandoned mine in Argentina.

2 Materials and methods

2.1 Instrumentation

The briefcase containing the system was sourced from Farnell (Duratool, TC-1, Farnell, Zug, Switzerland). The rechargeable lithium battery packs (Turnigy nano-tech 5000 mAh 4S) and battery charger (IMAX B6-AC Charger/Discharger 1–6 Cells) were obtained from Hobby King (Hong Kong). The foldable solar panel (Solarset Ampera 17V/78W SCR) was purchased from SIStech (Zurich, Switzerland). The high voltage modules (UM30*4) were products from Spellman (Pulborough, UK). The contactless conductivity detectors (ER225B, EA120 amplifier and two capillary head stages ET120) were obtained from eDAQ (Denistone East, NSW, Australia). Note, that this was a special set-up, which had been modified for battery operation and the accommodation of two detector cells. The electropherograms were acquired with the Chart software package from eDAQ. The fluid handling manifold was assembled from parts obtained from LabSmith (Livermore, CA, USA). This included a microfluidic breadboard (uPB-05), a 100 µL syringe pump (SPS01), three-way valves (AV201), a pressure sensor (uPS0800-T116), interconnects (T116-203), and reservoirs (T116-BBRES). Connections were made with 1/16" OD and 0.01" ID PEEK tubing. Fused silica capillaries of 363 µm od of 10 and 25 µm id were obtained from Polymicro Technologies (Phoenix, AZ, USA). Heating films (Minco, HK913-H, Distrelec, Nänikon, Switzerland), a fan (Sunon GM1203PHV2-8.GN, Farnell) and an electronic temperature sensor (Analog Devices, AD22103KTZ, Farnell) was used for thermostatting. The system was controlled via the *Python* based open-source software package *Instrumentino* [32, 33], running on a portable personal computer under *Windows*. The syringe pump and valves were connected to the personal computer via an electronic interface controller (EIB-200) from LabSmith, and the high voltage power supplies, the heating films and the temperature sensor via a purpose-made interface based on an Arduino microcontroller (Arduino Nano 3.0, Distrelec). Communication between *Instrumentino* and the LabSmith parts was enabled by an application programming interface (API) from LabSmith running on the computer, and between Instrumentino and the parts connected to the Arduino board by a purpose written program running on the latter.

2.2 Reagents

All chemicals were of analytical grade and solutions were prepared with ultrapure water, purified using a Milli-Q system from Millipore (Bedford, MA, USA). Sodium chloride, potassium nitrate, potassium sulphate, potassium chloride, magnesium chloride, iron(II) sulphate, zinc sulphate, and copper(II) chloride were purchased from Merck (Darmstadt, Germany). Manganese(II) sulphate, calcium chloride, lactic acid (Lac), citric acid, 18-crown-6, and ammonium chloride were purchased from Fluka (Buchs, Switzerland). L-Histidine (His) and ultrapure nitric acid (HNO_3) were purchased from Sigma–Aldrich (Buchs, Switzerland) and acetic acid (HAc) was purchased from VWR (Dietikon, Switzerland).
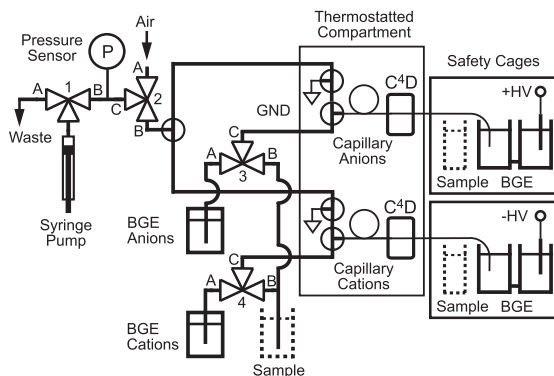
Figure 1. Schematic drawing of the overall configuration of the portable dual channel instrument indicating the two sample injection options.

2.3 On-site sediment porewater measurements at Lake Baldegg

Sediment cores were collected from the deepest part of Lake Baldegg (66 m) with a Uwitec gravity corer (Mondsee, Austria) equipped with a PVC tube (6.5 cm id, 120 cm length). The PVC tube had predrilled holes (Ø 2 mm) with 5 mm vertical spacing. The holes were sealed with adhesive tape prior to sampling. The sediment porewater was sampled directly after core retrieval with MicroRhizon filter tubes (1 mm diameter and 0.20 μm pore size) (Rhizosphere Research Products, Wageningen, Netherlands). A 10 to 100 μl of porewater were extracted by horizontally inserting the MicroRhizon tubes through the taped holes.

3 Results and discussion

3.1 System design

The overall design of the instrument is illustrated in Fig. 1 and a photograph is shown in Fig. 2. It features two separation channels fitted with negative and positive high-voltage power supplies for the concurrent separation of cations and anions in the same sample or two separate samples. Separate background electrolytes can be employed for the cations and anions to allow fully independent optimization of the separation conditions. Fluid handling is automated and based on a single miniature syringe pump and several valves to control aspiration and internal dispensing of BGEs and sample. Two modes of injection were implemented. Samples not limited in volume were aspirated fully automatically into the T-pieces in front of the capillaries from the sample container. This was achieved by opening all four valves to position B (as indicated in Fig. 1) and withdrawing the piston of the syringe pump (step I). However, the volume resolution of the syringe pump is not adequate for subsequent direct metering of the small samples volumes in the low nanoliter to picoliter

Figure 2. Photograph of the instrument. The syringe pump and valves are in the front, the thermostatted compartment in the center and the high voltage compartments are to the right. All compartments have been opened.

range which need to be injected into the capillaries in the second step. Hydrodynamic injection in CE is best handled by applying a controlled pressure for a controlled length of time. The conditions required for a desired injected volume for a given capillary diameter and length can then be calculated with the Hagen-Poiseuille equation. Previously for SIA-CE systems based on syringe pumps injection was achieved by pumping against a flow splitting manifold which created a desired backpressure [34–38]. Here, a different approach was adopted. For the second step of the sample injection the syringe pump was first partly filled with air by opening valve 2 to position A and further withdrawal of the syringe pump. The enclosed air was then compressed while keeping valve 2 in position C (closed)(step II). The desired pressure was achieved with the help of the electronic pressure sensor attached to the manifold and a control loop which is part of the software provided by the supplier of the parts. Once the pressure level was reached, valve 2 was turned to position B for the predetermined length of time while valves 3 and

4 were closed for the injection proper (step III). In step IV, valve 2 was closed and then valves 3 and 4 were opened to position B to release the pressure in the injection areas. Valve 1 was set to position A and the syringe was emptied to waste. After injection of the sample plugs BGE was aspirated to flush the manifold in front of the injection ends of the capillaries by opening valves 3 and 4 to position A and withdrawing the syringe pump, before the high voltage was turned on. Following the separation a final rinsing step was carried out to prepare for the next separation, which consisted of aspirating the BGEs and then flushing the capillaries for a sufficient amount of time.

Samples only available in small volume were aspirated directly into the opposite ends of the capillaries after placing these into the sample containers. The pressure sensor has a range from -100 to 800 kPa relative pressure and thus by withdrawing the piston of the syringe pump it was also possible to precisely create the negative pressure relative to air required for sample injection from the far end of the capillaries. This step was carried out without air in the pump.

Separation and detection took place in an insulated and thermostatted compartment. Temperature directly affects the viscosity of liquids and thus several parameters in capillary zone electrophoresis with conductivity detection. The amount injected, as governed by the Hagen-Poiseuille equation, is thus dependent on temperature as is the electrophoretic mobility. Mobility not only has bearing on the migration times, but also on the peak areas as it affects the residence time in the detector cell. Furthermore, the conductivity, which also originates from the ionic mobility, has a temperature coefficient. While the ambient temperature in a laboratory is often fairly stable, this cannot be expected when working outdoors. In order to keep the volume and the thermal mass to be thermostatted small, temperature control was limited to the separation capillaries and the detectors. These were therefore contained in a separate compartment insulated with a 5 mm thick layer of cork. As it is easier to implement heating rather than cooling this was achieved with resistive heating and the temperature maintained with the help of an electronic temperature sensor and a software control loop (PID, proportional-integral-derivative) running on the Arduino microcontroller board.

The high voltage part of the system, namely the buffer vials with the high voltage electrodes, was contained in two compartments made of poly-methylmethacrylate (PMMA) with the dimensions of 18 × 16 × 16 cm to provide sufficient space to preclude high-voltage discharges through the air. These are covered with a single lid which can be opened easily for small sample volume injection and other manipulations. It was fitted with a safety switch to prevent accidental exposure of the operator to the high voltage. Two separate buffer containers, which are connected with a short length of tubing, are used for each capillary to hold the capillary end and the high-voltage electrode. This approach prevents interference from electrolysis products and was first reported by de Jesus *et al.* [39].

The system was assembled in a briefcase with outer dimensions of 52 × 34 × 18 cm, allowing easy transportation by a single person and the possibility to carry it as hand luggage on aircraft. Power is provided by rechargeable batteries or, where available, mains power can be used via adaptors. The batteries may also be recharged from the mains supply, but in order to allow work at remote locations a portable solar power panel was included in the system. This provides a maximum of 4.3 A at 17 V and has the dimensions of 137 × 48 cm when expanded, but a compact 31 × 48 cm when folded for transport (weight = 2.25 kg).

3.2 Performance

The effect of ambient temperature on the measurements and its alleviation by thermostatting was studied by performing electrophoresis experiments in the lab at temperatures of about 25°C and in a cooled room at a temperature of 10°C. Three sets of determinations of K^+ were carried out: without thermostatting in a cold room and with thermostatting in both, the cold room and the laboratory. The resulting average migration times and peak areas for K^+ are shown in Fig. 3. As expected, the migration times obtained in the cold-room without thermostatting were about 40% longer than those recorded for the two thermostatted experiments. These gave very similar results (with the temperature control set to 27°C in both cases). A reduction of approximately 12% was obtained for the peak areas at the lower ambient temperature when thermostatting was not employed, while very similar
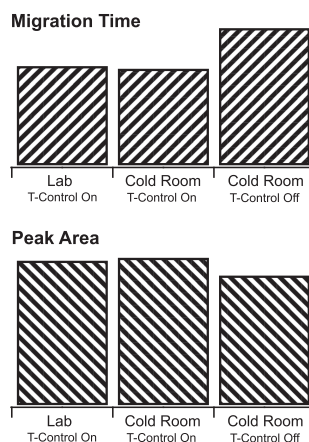
Figure 3. The effect of thermostatting on migration times and peak areas. Experiments were done in the laboratory and in a cold-room (T = 10°C), with and without thermostatting to 27°C. Sample: KCl 100 μM, BGE: HAc 500 mM. Capillary: 10 μm id, 45/60 cm L_{eff}/L_{tot}. Injection: 200 kPa, 10 s. Separation voltage: −30 kV.
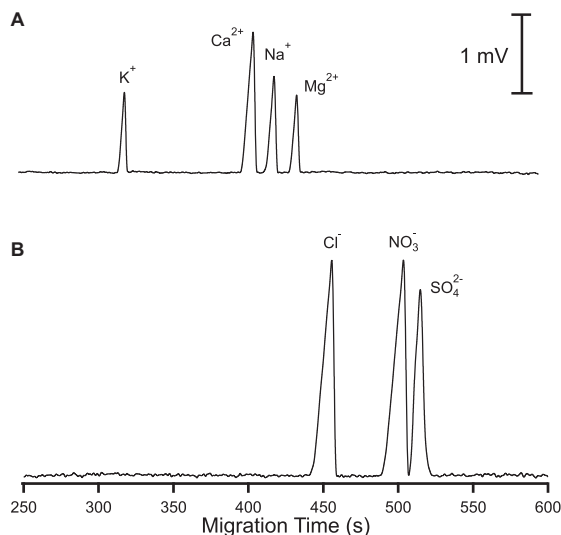
Figure 4. Dual separation of (A) cations and (B) anions in a well-water sample. Capillaries: 25 μm id, 80/90 cm L_{eff}/L_{tot}. Injection: 20 kPa, 10 s. Separation voltage: ± 25 kV. The thermostat was set to 30°C. BGE for cations: 9 mM His, 4.6 mM Lac, 25 mM HAc, and 1 mM 18-crown-6. BGE for anions: 7.5 mM His and 40 mM HAc.

results were obtained for the thermostatted experiments in the two environments. The prolonged migration time at the reduced temperature is expected to lead to an increase in peak area due to an extended residence time of the analyte plug in the detector. The fact that actually a decrease is observed must be caused by opposite temperature effects on the injection volume and the measurement of the conductivity signal. Thermostatting was thus found to be effective and it is expected to also work outdoors. Under hot ambient conditions the temperature control can also be set to a value above 27°C.

In Fig. 4 the electropherograms for cations and anions for a typical sample consisting of water from a drinking well are shown. These were acquired concurrently by making use of the dual channel facility of the instrument. Two different BGE solutions were employed for the separations of cations and anions. The BGE for the separation of the cations consisted of 9 mM His, 4.6 mM Lac, 25 mM HAc, and 1 mM 18-crown-6 (appr. pH 4.3), which had previously been shown to be suitable for simultaneous baseline separation of alkali, alkaline earth and transition metal cations through weak complexation [40]. For the anions a BGE consisting of 7.5 mM His and 40 mM HAc was adopted from a previous publication [19]. Electropherograms for a sample taken from the tailing pond of a mining operation are shown in Fig. 5. As the peak for the copper ion was found to be considerably delayed compared to the other analytes, the possibility of implementing pressure-assisted CE (PACE) in order to shorten the analysis time is demonstrated. The well water and the specimen from the tailing pond were collected during a sampling campaign carried out at the abandoned mining site *Pan de Azúcar* located in

a remote area of the north western part of Argentina. The calibration data to allow quantification of the ions in these samples is given in Table 1.

3.3 Case study: sediment pore-water at Lake Baldegg

Lake Baldegg is a 66 m deep eutrophic lake on the Swiss Plateau. Due to its relatively small hypolimnion volume and wind shielded geographic location the oxygen (O_2) concentration of the lake is critically sensitive to nutrient loads from the agriculturally dominated catchment. Deep-water anoxia has prevailed from the late 19th century until today, and the lake is artificially aerated with molecular oxygen (O_2) during the stratification period [41]. Settling organic and inorganic particulate matter constitute the sediments of lakes. Fresh deposits are mineralized by microorganisms consuming organic matter thereby releasing a variety of reduced substances such as NH_4^+, Fe(II), Mn(II), S(-II), and methane. Oxygen, which is critical for all higher life forms in the deep water of lakes, is consumed at or near the sediment-water interface [42]. The determination of concentration profiles of the dissolved reduced components in the porewater of the top 10–20 cm of the sediment is of great interest to lake bio-geochemists to estimate areal flux rates, and hence consumption rates of O_2 and the trophic state of lakes. Only small porewater volumes can be retrieved from the sediment in order to allow high spatial resolution and avoid bias of the local concentration gradients. Hence, a wide range of
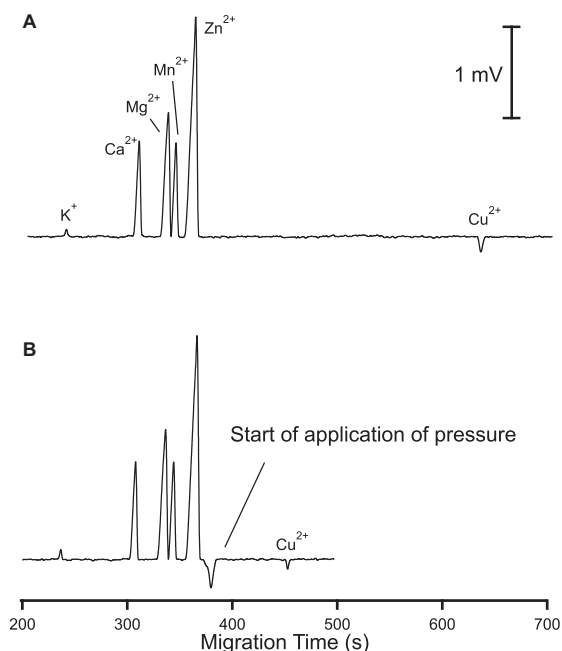
Figure 5. Cations in a sample from a mining pond (1:100 dilution), measured (A) without and (B) with pressure assistance. Capillaries: 25 μm id, 65/80 cm L_{eff}/L_{tot}. Injection: 50 kPa, 9 s. Separation voltage: −25 kV. Co-flow: 70 kPa applied after 375 s. BGE for cations: 9 mM His, 4.6 mM Lac, 25 mM HAc and 1 mM 18-crown-6. BGE for anions: 7.5 mM His and 40 mM HAc.

Table 1. Calibration data

Ion	Calibration range (μM)	Reproducibility of peak area (% RSD)*	Correlation coefficient, r	LOD (μM)
NH_4^+	5–150	9.4	0.9988	4.8
K^+	5–400	10.5	1.0000	4.7
Ca^{2+}	5–200	8.2	0.9999	3.4
Na^+	5–200	11.6	0.9996	4.6
Mg^{2+}	5–100	10.0	0.9980	2.8
Mn^{2+}	5–100	9.1	0.9992	3.0
Zn^{2+}	5–200	6.4	0.9997	4.2
Cu^{2+}	50–1000	6.5	0.9840	18
Cl^-	20–1000	7.3	0.9998	11
NO_3^-	20–1000	7.1	1.0000	12
SO_4^{2-}	20–1000	6.3	0.9998	10

*$n = 4$, determined at 100 μM for the cations, 500 μM for the anions.

chemical parameters has to be analyzed in small volumes (10–50 μL). This should be carried out immediately as sample conservation and transport often introduces a bias and bears the risk of contaminations.

Concentration profiles of cations and anions determined with the instrument in the field are shown in Fig. 6. Concentration gradients of dissolved substances which are consumed (such as the electron acceptors NO_3^- and SO_4^{2-}) or produced (such as NH_4^+, Mn(II) and Fe(II)) in the top 10 cm of the sediment are well pronounced. The electron acceptors NO_3^- and SO_4^{2-} are consumed in the anoxic sediment and delivered from the lake bottom water with rates corresponding to their concentration gradients. Similarly, Fe(III) and Mn(IV) are used as electron acceptors for the mineralization of organic matter thereby releasing Fe(II) and Mn(II). NH_4^+ is a degradation product of organic amines and transported by molecular diffusion toward the sediment surface where it is eventually oxidized. Its production rate is directly proportional to the mineralization rate of organic matter in lake sediments. It is remarkable how well Fe(II) can be analyzed with the CE instrument since it is extremely sensitive to oxidation and reliable measurements in porewaters are otherwise very laborious (e.g. sediment extrusion in N_2-filled glove bags and conservation). Ca^{2+} and Mg^{2+} are products of the dissolution of calcite and dolomite in the sediment as a consequence of decreasing pH due to the CO_2 released during the mineralization of organic matter. Their concentration in lake water, however, is already high and thus no pronounced concentration differences develop between sediment porewater and lake bottom water. Chloride is an example of a conservative parameter that does not play a role in diagenetic processes. Fluxes of individual compounds and areal rates of their formation or consumption were determined by fitting the concentration profiles with a one-dimensional model that
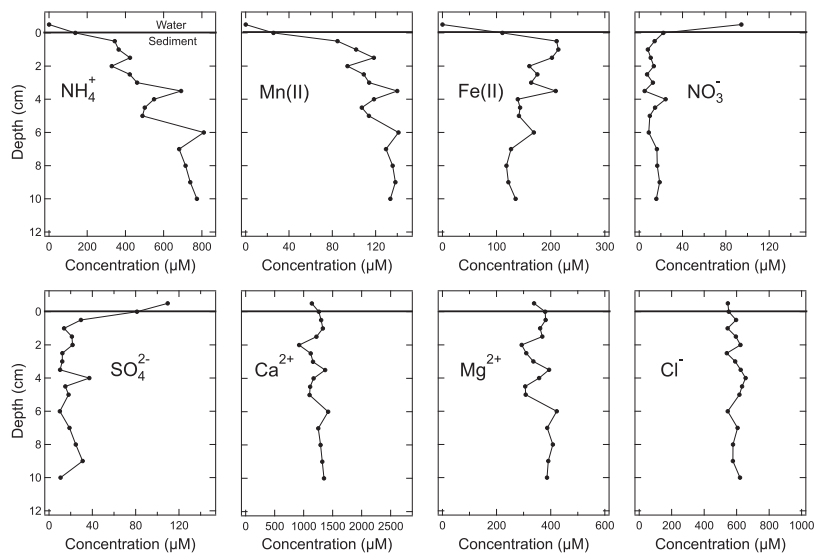
Figure 6. Depth profiles of major cations and anions in pore-water samples from a sediment core taken at Lake Baldegg. BGE: 11 mM His, 50 mM HAc, 1.5 mM 18-crown-6, and 0.1 mM citric acid. Capillaries: 25 μm id, 75/80 cm L_{eff}/L_{tot}. Injection: −30 kPa, 11 s. Separation voltage: ± 30 kV.

Table 2. Reaction-diffusion model fittings for datasets acquired with the CE instrument

Parameter	Areal fluxes (mmol m^{-2} d^{-1})
NH$_4^+$	−3.0
Mn(II)	−0.22
Fe(II)	−0.67
NO$_3^-$	0.45
SO$_4^{2-}$	0.59

Areal fluxes of dissolved compounds from (negative values) and to (positive values) the sediment determined with a diagenetic reaction-diffusion model for the datasets.

considered reaction and transport [43] and are presented in Table 2. Reduced compounds diffusing from the sediment to the overlying water consume O$_2$ in proportion (NH$_4^+$ consumes two equivalents of O$_2$, Mn(II) and Fe(II) consume 0.5 and 0.25 equivalents, respectively) and thus areal fluxes as given in Table 2 help quantifying the sinks of O$_2$ in lakes.

4   Concluding remarks

A dual-channel CE instrument with separate BGEs and a thermostatted compartment was constructed and demonstrated for the monitoring of inorganic ions in environmental water samples. The use of automated sample aspiration allowed

the semiautomatic handling of small volumes of pore-water samples. The fact that the fluidic section was based on commercially available microfluidic parts allowed the easy construction of the system without sophisticated workshop facilities. The system is compact and can be carried by hand. It can be powered either from the grid or from batteries, which in turn can be recharged by solar cells, enabling the operation of the system in remote locations. For samples with low background conductivity it should be possible to implement sample stacking schemes (such as simple large volume injection) in order to achieve lower limits of detection. The broad applicability of CE-C^{4}D for ionic species makes this instrument also potentially useful outside environmental studies, such as for clinical or forensic tests, or for food analysis.

The authors have declared no conflict of interest.

5   References

[1] Kobrin, E.-G., Lees, H., Fomitsenko, M., Kubáň, P., Kaljurand, M., *Electrophoresis* 2014, *35*, 1165-1172.

[2] Hutchinson, J. P., Johns, C., Breadmore, M. C., Hilder, E. F., Guijt, R. M., Lennard, C., Dicinoski, G., Haddad, P. R., *Electrophoresis* 2008, *29*, 4593-4602.

[3] Hutchinson, J. P., Evenhuis, C. J., Johns, C., Kazarian, A. A., Breadmore, M. C., Macka, M., Hilder, E. F., Guijt, R. M., Dicinoski, G. W., Haddad, P. R., *Anal. Chem.* 2007, *79*, 7005-7013.

[4] Sáiz, J., Mai, T. D., Hauser, P. C., Garcia-Ruiz, C., *Electrophoresis* 2013, *34*, 2078-2084.

[5] Kubáň, P., Seiman, A., Makarotseva, N., Vaher, M., Kaljurand, M., *J. Chromatogr. A* 2011, *1218*, 2618-2625.

[6] Nguyen, H. T. A., Pham, T. N. M., Ta, T. T., Nguyen, X. T., Nguyen, T. L., Le, T. H. H., Koenka, I. J., Sáiz, J., Hauser, P. C., Mai, T. D., *Sci. Justice* 2015, *55*, 481-486.

[7] Mark, J. J. P., Kumar, A., Demattio, H., Hoffmann, W., Malik, A., Matysik, F. M., *Electroanalysis* 2011, *23*, 161-168.

[8] Mai, T. D., Le, M. D., Sáiz, J., Duong, H. A., Koenka, I. J., Pham, H. V., Hauser, P. C., *Anal. Chim. Acta* 2016, *911*, 121-128.

[9] Jayarajah, C. N., Skelley, A. M., Fortner, A. D., Mathies, R. A., *Anal. Chem.* 2007, *79*, 8162-8169.

[10] Kumar, A., Burns, J., Hoffmann, W., Demattio, H., Malik, A. K., Matysik, F. M., *Electrophoresis* 2011, *32*, 920-925.

[11] Nguyen, H. T. A., Pham, T. N. M., Doan, T. T., Ta, T. T., Sáiz, J., Nguyen, T. Q. H., Hauser, P. C., Mai, T. D., *J. Chromatogr. A* 2014, *1360*, 305-311.

[12] da Costa, E. T., Neves, C. A., Hotta, G. M., Vidal, D. T. R., Barros, M. F., Ayon, A. A., Garcia, C. D., do Lago, C. L., *Electrophoresis* 2012, *33*, 2650-2659.

[13] Xu, Y., Wang, W., Li, S. F. Y., *Electrophoresis* 2007, *28*, 1530-1539.

[14] Xu, Y., Li, S. F. Y., *Electrophoresis* 2006, *27*, 4025-4028.

[15] Greguš, M., Foret, F., Kubáň, P., *J. Chromatogr. A* 2016, *1427*, 177-185.

[16] Ansari, K., Ying, J. Y. S., Hauser, P. C., de Rooij, N. F., Rodriguez, I., *Electrophoresis* 2013, *34*, 1390-1399.

[17] Torres, N. T., Och, L. M., Hauser, P. C., Furrer, G., Brandl, H., Vologina, E., Sturm, M., Bürgmann, H., Müller, B., *Environ. Sci.: Processes Impacts* 2014, *16*, 879-889.

[18] Torres, N. T., Hauser, P. C., Furrer, G., Brandl, H., Müller, B., *Environ. Sci.: Processes Impacts* 2013, *15*, 715-720.

[19] Kubáň, P., Nguyen, H. T. A., Macka, M., Haddad, P. R., Hauser, P. C., *Electroanalysis* 2007, *19*, 2059-2065.

[20] Kappes, T., Galliker, B., Schwarz, M. A., Hauser, P. C., *TrAC, Trends Anal. Chem.* 2001, *20*, 133-139.

[21] Kappes, T., Hauser, P. C., *Anal. Commun.* 1998, *35*, 325-329.

[22] Kappes, T., Schnierle, P., Hauser, P. C., *Anal. Chim. Acta* 1999, *393*, 77-82.

[23] Lim, S., Nan, H., Lee, M.-J., Kang, S. H., *J. Chromatogr. B* 2014, *963*, 134-139.

[24] Lee, M., Cho, K., Yoon, D., Yoe, D. J., Kang, S. H., *Electrophoresis* 2010, *31*, 2787-2795.

[25] Liu, P., Seo, T. S., Beyor, N., Shin, K.-J., Scherer, J. R., Mathies, R. A., *Anal. Chem.* 2007, *79*, 1881-1889.

[26] Ryvolova, M., Preisler, J., Brabazon, D., Macka, M., *TrAC, Trends Anal. Chem.* 2010, *29*, 339-353.

[27] Lewis, A. P., Cranny, A., Harris, N. R., Green, N. G., Wharton, J. A., Wood, R. J. K., Stokes, K. R., *Meas. Sci. Technol.* 2013, *24*, 042001 (20pp).

[28] Van Schepdael, A., *Separations* 2016, *3*, 12.

[29] Sáiz, J., Mai, T. D., Koenka, I. J., Martin-Alberca, C., Hauser, P. C., Garcia-Ruiz, C., *J. Chromatogr. A* 2014, *1372*, 245-252.

[30] Mai, T. D., Pham, T. T. T., Pham, H. V., Sáiz, J., Garcia Ruiz, C., Hauser, P. C., *Anal. Chem.* 2013, *85*, 2333-2339.

[31] Koenka, I. J., Sáiz, J., Rempel, P., Hauser, P. C., *Anal. Chem.* 2016, *88*, 3761-3767.

[32] Koenka, I. J., Sáiz, J., Hauser, P. C., *Comput. Phys. Commun.* 2014, *185*, 2724-2729.

[33] Koenka, I. J., Sáiz, J., Hauser, P. C., *Chimia* 2015, *69*, 172-175.

[34] Mai, T. D., Hauser, P. C., *Talanta* 2011, *84*, 1228-1233.

[35] Mai, T. D., Hauser, P. C., *Electrophoresis* 2011, *32*, 3000-3007.

[36] Mai, T. D., Hauser, P. C., *J. Chromatogr. A* 2012, *1267*, 266-272.

[37] Mai, T. D., Schmid, S., Müller, B., Hauser, P. C., *Anal. Chim. Acta* 2010, *665*, 1-6.

[38] Wu, C.-H., Scampavia, L., Růžička, J., *Analyst* 2002, *127*, 898-905.

[39] de Jesus, D. P., Brito-Neto, J. G. A., Richter, E. M., Angnes, L., Gutz, I. G. R., do Lago, C. L., *Anal. Chem.* 2005, *77*, 607-614.

[40] Kubáň, P., Kubáň, P., Kubáň, V., *Electrophoresis* 2002, *23*, 3725-3734.

[41] Wehrli, B., Lotter, A. F., Schaller, T., Sturm, M., *Aquat. Sci.*, *59*, 285-294.

[42] Müller, B., Bryant, L. D., Matzinger, A., Wüest, A., *Environ. Sci. Technol.* 2012, *46*, 9964-9971.

[43] Müller, B., Wang, Y., Dittrich, M., Wehrli, B., *Water Res.* 2003, *37*, 4524-4532.

Publication #6:

Micro-injector for capillary electrophoresis

Electrophoresis (2015), 36(16), 1941-1944

Jorge Sáiz[1,2,3]
Israel Joel Koenka[3]
Carmen García-Ruiz[1,2]
Beat Müller[4]
Thomas Chwalek[4]
Peter C. Hauser[3]

[1]Department of Analytical
 Chemistry, Physical Chemistry
 and Chemical Engineering,
 University of Alcalá, Alcalá de
 Henares, Madrid, Spain
[2]University Institute of Research
 in Police Sciences (IUICP),
 University of Alcalá, Alcalá de
 Henares, Madrid, Spain
[3]Department of Chemistry,
 University of Basel, Basel,
 Switzerland
[4]EAWAG, Swiss Federal Institute
 of Aquatic Science and
 Technology, Kastanienbaum,
 Switzerland

Short Communication

Micro-injector for capillary electrophoresis

A novel micro-injector for capillary electrophoresis for the handling of samples with volumes down to as little as 300 nL was designed and built in our laboratory for analyses in which the available volume is a limitation. The sample is placed into a small cavity located directly in front of the separation capillary, and the injection is then carried out automatically by controlled pressurization of the chamber with compressed air. The system also allows automated flushing of the injection chamber as well as of the capillary. In a trial with a capillary electrophoresis system with contactless conductivity detector, employing a capillary of 25 μm diameter, the results showed good stability of migration times and peak areas. To illustrate the technique, the fast separation of five inorganic cations (Na^+, K^+, NH_4^+, Ca^{2+}, and Mg^{2+}) was set up. This could be achieved in less than 3 min, with good limits of detection (10 μM) and linear ranges (between about 10 and 1000 μM). The system was demonstrated for the determination of the inorganic cations in porewater samples of a lake sediment core.

CE is well known for being a separation technique that requires only very small samples volumes. The internal diameters of the capillaries employed are in the range from 75 μm (for detection by optical absorption measurement) down to 10 μm (for detection by contactless conductivity measurement or MS). Typically a sample plug of about 1 cm length is injected, therefore the sample volumes consumed for a single separation run are between about 1 and 50 nL in dependence on the capillary diameter. However, in practice the volumes of samples needed are significantly higher. The commercial benchtop instruments employ automated injectors based on sampling trays fitted with vials into which the capillary ends are temporarily dipped and injection is carried out by pressurization of the container or applying a vacuum at the other end of the capillary. The minimum sample volume that can be handled with these instruments is perhaps about 50 μL. For purpose built CE instruments built in laboratories around the world (see [1–22]) different approaches have been employed. The most simple instruments are based on manual hydrodynamic injection by syphoning in which the end of the capillary is placed into a vial containing the sample and lifting this to a defined height for a defined period

Correspondence: Professor Peter C. Hauser, Department of Chemistry, University of Basel, Spitalstrasse 51, 4056 Basel, Switzerland
E-mail: Peter.Hauser@unibas.ch
**Fax**: +41-61-267-10-13

Abbreviation: HV, high voltage; **PMMA**, poly(methyl methacrylate)

of time. This allows working with sample volumes down to about 10 μL [23, 24]. However, it is difficult to carry this out with high precision, and it is tedious in particular when working with field portable instruments out of doors. Purpose built CE-instruments that have employed automated injection have usually been based on either passing a sample plug to an injection cell with a sequential-injection manifold [9, 16, 18, 25] or on a flow-through arrangement employing a sample loop [13, 15, 19, 20, 26]. However, the sample volumes to be inserted into the capillary are too small to be manipulated directly with standard fluid handling apparatus based on rotary injection valves or standard stepper motor driven syringe pumps. Therefore these systems work with larger volumes and employ split injection methods as introduced by Kubáň et al. [26]. Such automated split injector systems have also been incorporated into field portable instruments [11, 13, 14, 16, 19], but require relatively large sample volumes of at least 500 μL.

On the other hand, for certain applications only very limited sample volumes are available. An example encountered in our laboratories is the analysis of porewater in lake sediments. The extraction from the sediment core brought to the surface only provides a few tens of microliters of sample [23, 24] and the amount of liquid that can be withdrawn from the sediment decreases strongly with depth. If the volume that needs to be extracted for analysis from the core can be reduced, it is also possible to obtain a higher resolution in the depth profile, thus the ability to work with the

www.electrophoresis-journal.com

smallest possible volumes is highly desirable. A further study in progress based on highly limited sample volumes is the determination of leachable nutrients on rock surfaces. While these projects would not have been possible without CE, manual siphoning injection has been mandatory in order to handle the small sample volumes. Also clinical analysis, such as the CE-C[4]D methods developed in our laboratory for the determination of the only weakly UV-absorbing creatine [27], valproic acid [28, 29], carnitines [30], lactic acid [31], or uric acid [32], can benefit from a possible reduction in sample size. In recognition that the capability of CE for the analysis of very low sample volumes has not been fully realized, recently Grundmann and Matysik developed a new sampler based on the technique of capillary batch injection [33]. Their injection system employed a separate capillary connected to a ultra-high precision syringe pump to pick up the sample. In the second step, the end of this sampling capillary was then moved with computer controlled micromanipulators and butted directly to the end of the separation capillary. The sample previously picked up was then dispensed into the latter for injection proper. This allowed very precise injections into the separation capillary with efficiencies of up to 100% [33].

The injector presented here is based on a small cell into which the sample is placed manually, but the actual injection into the capillary and flushing operations are then carried out automatically under computer control. Mechanical movements of any parts are not necessary. A schematic drawing of the injection cell can be seen in Fig. 1A. It consists of a small block of poly(methyl methacrylate) (PMMA) with dimensions of a 30 × 25 × 20 mm (H × W × D). The vertical channel has a diameter of 5 mm on top but narrows to a width of 0.66 mm at the bottom. The separation capillary meets this narrow section in a 90° angle. Additional ports serve for connection of the electrophoretic ground electrode, as entry points for air and BGE, and as a fluid drain. A removable lid fitted to the top with an o-ring provides an air-tight seal. The fluidic connections were made with 1/16″ od and 0.01″ id tubings using standard 1/4″-28 flangeless fittings and the electrode was mounted likewise.

The complete assembly is shown in Fig. 1B. Compressed air is employed for propulsion of fluids and the pressure is regulated with miniature electronic pressure controllers (OEM-EP, Parker Hannifin Corporation, Cleveland, OH) with pressure ranges from 0 to 15 psi. Three switching valves (AV201-T116, LabSmith Inc., Livermore CA, USA), labeled V1, V2, and V3, were used in combination with the pressure regulators to control all the fluidic steps. The electrophoretic separation was carried out with a high voltage (HV) power supply from Spellman (CZE2000, Pulborough, UK). A purpose made detector with high voltage excitation and a measuring cell based on a previous design [34, 35] was used in combination with an e-corder 401 and the software Chart (eDAQ, Denistone East NSW, Australia) for data acquisition. Silica capillaries (Polymicro, Phoenix AZ, USA) of 25 μm id and 375 μm od were used. For safety, the HV electrode and the BGE vial were placed inside a cage made of PMMA. The pressure controllers and the high voltage module were controlled with a personal computer
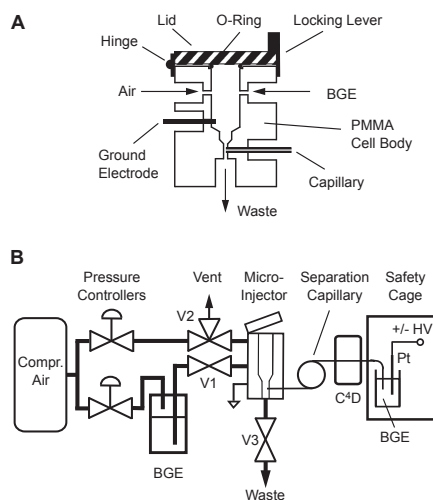
Figure 1. Schematic drawings of the injector cell (A) and the complete CE-C[4]D system with automated microinjector (B). The system was supplied with compressed air, which was regulated by two pressure controllers. This, in combination with three valves (V1, V2, and V3), allowed to carry out all the steps for the analysis of samples.

via an Arduino microcontroller board (www.arduino.cc) and the valves via a proprietary interface from LabSmith. The sequencing of steps was programmed with the graphical user interface *Instrumentino* [36]. This is a versatile software package, based on the programming language *Python*, which was recently developed in our laboratory and simplifies the control of experimental assemblies of different hardware components. It was primarily designed for parts interfaced via an Arduino board, but also allows the integration of other components that are connected directly to the personal computer. This software is available for download under an open source licence for general use (http://www.chemie.unibas.ch/~hauser/open-source-lab/instrumentino/index.html).
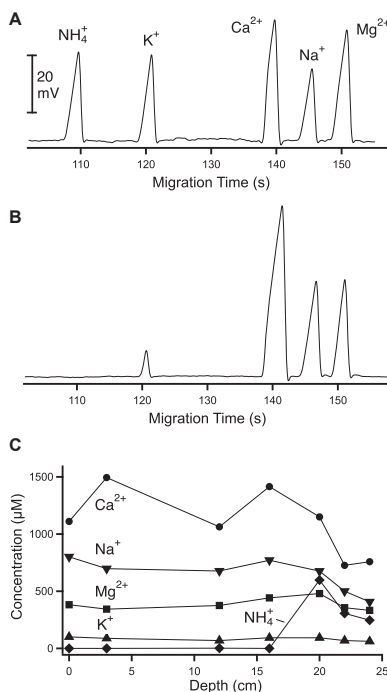
The sequence of operations is illustrated in Fig. 2. First, BGE is delivered to the micro-injector by opening valve V1 (Step 1) while the lid remains closed. Then, the injector is pressurized to flush the capillary with BGE by opening V2 (Step 2). Next, the BGE is removed from the nano-injector by gravity flow following the opening of V3 to waste and V2 to air (Step 3). The lid of the micro-injector is then manually opened and a drop of sample placed in the sample receptacle with a micro-syringe (Step 4). The lid is closed again and part of the sample plug is injected into the capillary by applying air pressure (Step 5). The amount of sample injected is optimized for the task at hand by setting the pressure and the duration of its application. Following this, the injector chamber is flushed with BGE in order to remove excess sample and to fill the
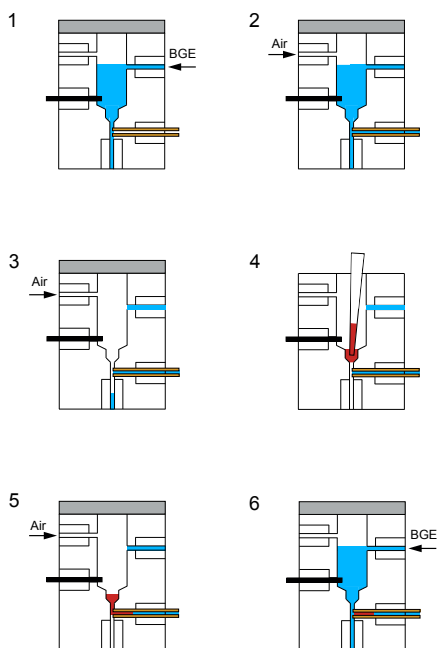
Figure 2. Steps for the analysis of a single sample (drawings not to scale). (1) Buffer delivery to the micro-injector; (2) Capillary flushing; (3) Draining of the injector; (4) Sample placement; (5) Sample injection; (6) Flushing of the injector and buffer delivery prior to the electrophoretic separation.

Figure 3. Determination of five inorganic cations. (A) Electropherogram for an aqueous solution of standards: 500 μM NH_4^+, K^+, Ca^{2+}, Na^+, and Mg^{2+}. (B) Determination of NH_4^+, K^+, Ca^{2+}, Na^+, and Mg^{2+} in a porewater sample of a lake sediment. (C) Depth profiles for the five cations. Details on the sampling procedure can be found in a previous publication [24]. Conditions for the CE-C^{4}D analysis are given in the text.

injector with BGE (Step 6). The high voltage is then turned on and the separation is carried out.

Due to the design of the micro-injector, in which the bottom of the sample receptacle is immediately adjacent to the capillary inlet and consists of a narrow channel, it was possible to employ sample volumes down to as little as 300 nL. But note that it is possible to work with larger volumes as well (up to 100 μL) if so desired, as the channel above the intersection with the capillary widens. CE is a versatile technique, which can be optimized in different ways in order to meet different objectives, i.e. high resolution, low detection limits, or fast analysis times. Relatively high resolutions and wide linear ranges can be obtained in short separations when the parameters are well optimized. In Fig. 3A, the separation of five inorganic cations within less than 3 min is shown. A fused silica capillary of 25 μm id was used to achieve good peak resolution [16]. A BGE consisting of 30 mM MES and histidine at pH 6.0 with 2 mM 18-crown-6 was used because it allowed the separation on NH_4^+ and K^+ while Ca^{2+} and Na^+ were still baseline resolved. The capillary had a total length of 60 cm and an effective length of 49 cm. Injection was performed at 2 psi for 2 s and the separation was carried out at –30 kV. The sample volume placed in the micro-injector

was 300 nL. The LODs for the cations were 10 μM. The stability of migration times was studied over ten separations, obtaining good RSD values of around 0.3%. The peak areas could be reproduced with RSD values between 7 and 10%. The linear ranges for the cations extended from 10 to 1500 μM in the case of NH_4^+, K^+, and Ca^{2+} and from 10 to 1000 μM for Na^+ and Mg^{2+}. These results show a good stability of the system and the electrophoretic procedure, which is comparable to that of other automated systems produced in our laboratories, even though the sample volume is much reduced.

The system was then used with the same electrophoretic conditions for the analysis of porewater samples withdrawn from a sediment core of Lake Baldegg in Switzerland [24]. The electropherogram obtained for one of the samples is shown in Fig. 3B. In Fig. 3C a depth profile for the cations is shown. Notable is the absence of ammonium until a certain depth, which presumably is due to more pronounced reducing conditions a lower levels.

In conclusion, it has been found possible to create an automated CE-injector suitable for sample volumes down to 300 nL with acceptable reproducibilities. It is expected, that, besides the demonstrated porewater analysis, the method will be useful for other applications in environmental studies. The overall system is fairly compact and the techniques employed are not more complex than those previously implemented in automated portable CE-instruments reported by our group. Therefore the system is suitable for ready implementation in such instruments as well and expected to be sufficiently robust for field applications. It may also prove useful for clinical applications such as the analysis of biopsy samples or blood samples from small infants. Note, that it may be possible to refine the injection approach to further reduce the required sample volume, perhaps by constructing an injector using microlithographic techniques. However, it has to be borne in mind that ultimately the sample needs to be transferred from somewhere, even if directly from the sampling site into the instrument, and that the handling becomes increasingly more difficult as the volume is reduced.

The authors have declared no conflict of interest.

References

[1] Gaudry, A. J., Nai, Y. H., Guij, R. M., Breadmore, M. C., *Anal. Chem.* 2014, *86*, 3380–3388.

[2] Alhusban, A. A., Gaudry, A. J., Breadmore, M. C., Gueven, N., Guijt, R. M., *J. Chromatogr. A* 2014, *1323*, 157–162.

[3] Gaudry, A. J., Guijt, R. M., Macka, M., Hutchinson, J. P., Johns, C., Hilder, E. F., Dicinoski, G. W., Nesterenko, P. N., Haddad, P. R., Breadmore, M. C., *Anal. Chim. Acta* 2013, *781*, 80–87.

[4] Kobrin, E. G., Lees, H., Fomitsenko, M., Kuban, P., Kaljurand, M., *Electrophoresis* 2014, *35*, 1165–1172.

[5] Ryvolova, M., Preisler, J., Brabazon, D., Macka, M., *Trac-Trends Anal. Chem.* 2010, *29*, 339–353.

[6] Kubáň, P., Seiman, A., Makarotseva, N., Vaher, M., Kaljurand, M., *J. Chromatogr. A* 2011, *1218*, 2618–2625.

[7] da Costa, E. T., Neves, C. A., Hotta, G. M., Vidal, D. T. R., Barros, M. F., Ayon, A. A., Garcia, C. D., do Lago, C. L., *Electrophoresis* 2012, *33*, 2650–2659.

[8] Seiman, A., Jaanus, M., Vaher, M., Kaljurand, M., *Electrophoresis* 2009, *30*, 507–514.

[9] Wu, C.-H., Scampavia, L., Ruzicka, J., *Analyst* 2002, *127*, 898–905.

[10] Wu, C. H., Scampavia, L., Ruzicka, J., *Analyst* 2003, *128*, 1123–1130.

[11] Sáiz, J., Mai, T. D., Koenka, I. J., Martín-Alberca, C., Hauser, P. C., García Ruiz, C., *J. Chromatogr. A* 2014, *1372*, 245–252.

[12] Nguyen, T. A. H., Pham, T. N. M., Doan, T. T., Ta, T. T., Saiz, J., Nguyen, T. Q. H., Hauser, P. C., Mai, T. D., *J. Chromatogr. A* 2014, *1360*, 305–311.

[13] Pham, T. T. T., Mai, T. D., Nguyen, T. D., Sáiz, J., Pham, H. V., Hauser, P. C., *Anal. Chim. Acta* 2014, *841*, 77–83.

[14] Sáiz, J., Mai, T. D., Hauser, P. C., Garcia-Ruíz, C., *Electrophoresis* 2013, *34*, 2078–2084.

[15] Mai, T. D., Pham, T. T. T., Pham, H. V., Saiz, J., Ruiz, C. G., Hauser, P. C., *Anal. Chem.* 2013, *85*, 2333–2339.

[16] Mai, T. D., Hauser, P. C., *Talanta* 2011, *84*, 1228–1233.

[17] Kubáň, P., Nguyen, H. T. A., Macka, M., Haddad, P. R., Hauser, P. C., *Electroanalysis* 2007, *19*, 2059–2065.

[18] Mai, T. D., Schmid, S., Müller, B., Hauser, P. C., *Anal. Chim. Acta* 2010, *665*, 1–6.

[19] Kubáň, P., Reinhardt, M., Müller, B., Hauser, P. C., *J. Environ. Monit.* 2004, *6*, 169–174.

[20] Kubáň, P., Kubáň, P., Hauser, P. C., Kubáň, V., *Electrophoresis* 2004, *25*, 35–42.

[21] Kappes, T., Galliker, B., Schwarz, M. A., Hauser, P. C., *Trends Anal. Chem.* 2001, *20*, 133–139.

[22] Kappes, T., Schnierle, P., Hauser, P. C., *Anal. Chim. Acta* 1999, *393*, 77–82.

[23] Torres, N. T., Och, L. M., Hauser, P. C., Furrer, G., Brandl, H., Vologina, E., Sturm, M., Bürgmann, H., Müller, B., *Environ. Sci.-Process Impacts* 2014, *16*, 879–889.

[24] Torres, N. T., Hauser, P. C., Furrer, G., Brandl, H., Müller, B., *Environ. Sci.-Process Impacts* 2013, *15*, 715–720.

[25] Wuersig, A., Kubáň, P., Khaloo, S. S., Hauser, P. C., *Analyst* 2006, *131*, 944–949.

[26] Kubáň, P., Engström, A., Olsson, J. C., Thorsén, G., Tryzell, R., Karlberg, B., *Anal. Chim. Acta* 1997, *337*, 117–124.

[27] See, H. H., Schmidt-Marzinkowski, J., Pormsila, W., Morand, R., Krahenbühl, S., Hauser, P. C., *Anal. Chim. Acta* 2012, *727*, 78–82.

[28] Pham, T. T. T., See, H. H., Morand, R., Krahenbühl, S., Hauser, P. C., *J. Chromatogr. B* 2012, *907*, 74–78.

[29] Belin, G. K., Krähenbühl, S., Hauser, P. C., *J. Chomatogr. B* 2007, *847*, 205–209.

[30] Pormsila, W., Morand, R., Krähenbühl, S., Hauser, P. C., *J. Chromatogr. B* 2011, *879*, 921–926.

[31] Pormsila, W., Morand, R., Krähenbühl, S., Hauser, P. C., *Electrophoresis* 2011, *32*, 884–889.

[32] Pormsila, W., Krahenbühl, S., Hauser, P. C., *Anal. Chim. Acta* 2009, *636*, 224–228.

[33] Grundmann, M., Matysik, F.-M., *Anal. Bioanal. Chem.* 2012, *404*, 1713–1721.

[34] Zhang, L., Khaloo, S. S., Kubáň, P., Hauser, P. C., *Meas. Sci. Technol.* 2006, *17*, 3317–3322.

[35] Tanyanyiwa, J., Galliker, B., Schwarz, M. A., Hauser, P. C., *Analyst* 2002, *127*, 214–218.

[36] Koenka, I. J., Sáiz, J., Hauser, P. C., *Comput. Phys. Commun.* 2014, *185*, 2724–2729.

Publication #7:

Microfluidic breadboard approach to capillary electrophoresis

Analytical Chemistry (2016), 88(7), 3761-3767

Microfluidic Breadboard Approach to Capillary Electrophoresis

Israel Joel Koenka,[†] Jorge Sáiz,[†,‡,§] Paul Rempel,[†] and Peter C. Hauser*[,†]

[†]Department of Chemistry, University of Basel, Spitalstrasse 51, 4056 Basel, Switzerland

[‡]Department of Analytical Chemistry, Physical Chemistry and Chemical Engineering, University of Alcalá, Ctra. Madrid-Barcelona Km 33.6, Alcalá de Henares, 28871, Madrid, Spain

[§]University Institute of Research in Police Sciences (IUICP), University of Alcalá, Ctra. Madrid-Barcelona Km 33.6, 28871 Alcalá de Henares, Madrid, Spain

ABSTRACT: A breadboard approach for electrophoretic separations with contactless conductivity detection is presented. This is based on miniature off-the-shelf components such as syringe pumps, valves, and pressure controllers which could be set up in a very compact overall arrangement. It has a high flexibility for different tasks at hand, and the common operations of hydrodynamic injection and capillary flushing are automated. For demonstration of the versatility of the proposition, several very diverse configurations and modes of electrophoresis were successfully implemented, namely, standard capillary zone electrophoresis, pressure assisted zone electrophoresis, the simultaneous separation of cations and anions by dual-capillary zone electrophoresis, the separation of cationic amino acids by isotachophoresis, as well as the separation of small carboxylic acids by gradient elution moving boundary electrophoresis. The system also allows fast separations, as demonstrated by the analysis of six inorganic cations within 35 s. The approach addresses respective limitations of either conventional capillary electrophoresis instruments as well as electrophoretic lab-on-chip devices, while maintaining a performance in terms of detection limits and reproducibility comparable to standard instrumentation.
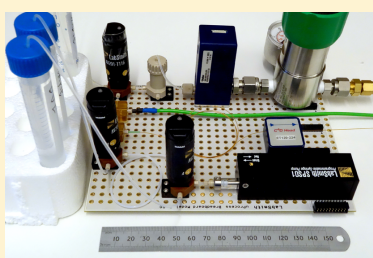
C apillary electrophoresis (CE) is a very flexible method. Not only is it suitable for the determination of essentially any ionic species but also different modes of separation, such as isotachophoresis (ITP), are possible besides the most commonly employed capillary zone electrophoresis (CZE). Generally, compromise operating conditions have to be established with regard to the analytical goals. Low limits of detection are achieved by injecting relatively large amounts of sample, which then require long separation times. Large dynamic ranges require modest injected amounts. Fast separations are only possible with small sample plugs in short separation channels and fast injection procedures, but this will impart a loss of sensitivity. It is important to realize that optimization with regard to these parameters therefore requires full flexibility in the amount injected, the applied voltage, and crucially, in the length of the separation channel. For an illustration of this seldom dicussed aspect see, for example, Mai et al.[1]

Besides the length of the separation channel, also its diameter has a strong bearing on the separation efficiency as the Joule heat produced on application of the separation voltage creates a temperature gradient which leads to differences in migration velocity. It is therefore highly desirable to employ the narrowest possible capillaries. On the other hand, the standard UV-absorbance detection is not readily feasible with internal diameters of less than 50 μm because of the shortening of the optical path length and the required reduction in the size of the aperture. An alternative detection method is contactless conductivity detection, which is universal and simpler in configuration than optical detection. As had been demonstrated by Mayrhofer et al. in 1999, capacitively coupled contactless conductivity detection (C[4]D) can be used with narrower separation channels of 25 or 10 μm diameter.[2] This is possible with negligible effect on the limit of detection.[3] Besides improved resolution, a further important benefit of the use of such narrow capillaries is the possibility of employing hydrodynamic pumping, which in capillaries of larger diameters incurs significant bandbroadening[3] as the laminarity of the flow is limited in narrow channels. When C[4]D is employed in CZE, concurrent pumping may therefore be used for optimization of the residence time of the analytes in the electric field in order to obtain best analysis times or best resolution[3] or for the compensation of the electroosmotic flow (EOF) in the determination of anions.[4] Pumping also allows the placement of one or more samples plugs at desired positions along the capillary length prior to optimized separations.[5] Han et al. have also employed pressure driven CE to overcome variations in the electroosmotic flow.[6] In comparison to UV-detection, C4D therefore is not only simpler and less expensive but also enables the two benefits of narrower capillaries, i.e., improved resolution

3761

and the ability to employ hydrodynamic pumping for further optimization.

A common goal in CE is the determination of cations and anions in the same sample (for a review see Sáiz et al.[7]), which not only requires different applied polarities, but often different buffers are needed as well as a surface modification of the capillary in order to reverse the electroosmotic flow. The concurrent use of two separation channels is the best approach as the operating conditions can be optimized independently.

In practice, capillary electrophoresis is usually carried out in conventional capillaries with commercial instruments available from several manufacturers, which were either designed for zone electrophoresis or for isotachophoresis. These instruments feature a high degree of automation, but on the other hand are not well suited for full optimization with regard to capillary diameter, capillary length, fast injections, the use of hydrodynamic manipulations or the employment of multiple capillaries. C[4]D, while becoming a regular option for some newer commercial instruments, can only be retrofitted as a third party module to instruments of the industry leaders which feature fixed built-in UV-detectors. Alternatively, electrophoretic separations may also be implemented on lab-on-chip devices which contain a separation channel embedded in a planar substrate made of glass or a polymer. A large number of publications has appeared on the evaluation of such systems (for a recent review see, for example, Castro and Manz[8]). However, this arrangement also has certain practical problems, such as the presence of siphoning effects if the chips are not placed perfectly horizontal, difficulties in flushing of the manifold, geometric constraints for setting up efficient detection, and a lack of flexibility in particular with regard to the length of the separation channel. Several workers have thus proposed the use of interlocking microfluidic building blocks for the flexible construction of devices, but electrophoretic separations have not been demonstrated.[9−11] In a different approach to alleviate design and construction constraints, Garcia and co-workers proposed the use of standard capillaries and off-the-shelf connectors to emulate the standard elongated cross configuration of electrophoretic lab-on-chip devices[12] and demonstrated the separation of inorganic cations. It also should be borne in mind, that for efficient use electrophoresis in conventional capillaries and on lab-on-chip devices has to be automated and also the latter require a periphery with pumps and valves for flushing and sample introduction. A further discussion of some of the aspects of capillary electrophoresis on either platform and a comparison with liquid chromatography can be found in a review by Breadmore.[13]

The miniature microfluidic breadboard approach to electrophoretic separations and the adoption of contactless conductivity detection proposed here has evolved from our work with both conventional capillaries and lab-on-chip devices, conducted over a number of years, in which we sought to develop cost-effective instruments from components of standard size and methods for such applications as field analysis, automated monitoring, and the concurrent determination of cations and anions (see, for example, refs 1,5,7,14−19). The term *breadboard* is borrowed from the electronics laboratory where electronic circuits are arranged by plugging components into a support with a grid of holes. It is demonstrated that it is possible to set up very flexible CE systems, which can be rearranged for different needs as they may arise, from standard capillaries, miniature fluidic interconnects, miniature syringe pumps, and miniature pressure controllers as components which are all reusable in different

configurations. The approach alleviates the respective limitations of conventional CE instrumentation as well as of lab-on-chip devices with regard to full flexibility of separation channel length and internal cross-section, fast and precise injections, best detection geometry, the use of hydrodynamic pumping, the use of multiple separation channels, etc. without incurring compromises in performance compared to those platforms.

■ EXPERIMENTAL SECTION

Instrumentation. The miniature syringe pump (SPS01), valves (AV201), airtight liquid reservoirs (T116-BBRES), interconnects (T116-203, T116-204), and connecting tubing were obtained from LabSmith (Livermore, CA). The fused silica capillaries were sourced from Polymicro (Phoenix, AZ) except for the coated low-EOF capillary (Guarant from Alcor Bioseparations, Palo Alto, CA). Separation voltages were applied by using ±30 kV high voltage modules (CZE2000) from Spellman (Pulborough, UK) and pressurization was achieved with pneumatic pressure controllers (OEM-EP) from Parker Hannifin (Etoy, Switzerland). The LabSmith parts were connected to a LabSmith electrical interface board. The pressure regulator and high voltage units were controlled with a purpose built electronic interface based on an Arduino microcontroller board (www.arduino.cc) and attached solid state relays for power switching and digital-to-analog convertors for setting voltages. Each system was connected to a personal computer via a separate universal serial bus (USB) connection and controlled with a single program running on the computer, which is based on the open source and Python based Instrumentino package.[20,21] The program interacts with the LabSmith components by making use of an application programming interface (API) from the device manufacturer installed on the personal computer and with the Arduino attached components via a purpose written software package running on the microcontroller board. Detection was carried out either with an in-house built conductivity detector (C[4]D)[22,23] or a commercially available version from eDAQ (Denistone East, NSW, Australia). An e-corder 401 and the Chart software (both from eDAQ) were used for data acquisition.

Reagents and Samples. All chemicals used were of analytical grade. Sodium hydroxide, L-histidine (His), 2-(*N*-morpholino)ethanesulfonic acid (MES), 18-crown-6, sodium nitrite, propionic acid, lithium chloride, DL-lactic acid (Lac), and L-lysine (Lys) were obtained from Fluka (Buchs, Switzerland). Potassium perchlorate, calcium nitrate, ammonium fluoride, potassium acetate, and magnesium sulfate were purchased from Merck (Darmstadt, Germany). Formic acid, acetic acid, and butyric acid were obtained from Sigma-Aldrich (Buchs, Switzerland), and arginine (Arg) was obtained from Acros (Geel, Belgium). The sample of Himalayan rock salt was bought at a local supermarket. All solutions were prepared using ultrapure water, purified using a Milli-Q system (Millipore, Bedford, MA).

■ RESULTS AND DISCUSSION

Components. The essential components required in setting up a capillary electrophoresis system are depicted in schematic form in Figure 1. Pumps are required for fluid handling if the system is to be automated. Several hydrodynamic operations are required, i.e., flushing of capillaries and manifold as well as sample uptake and hydrodynamic sample injection into the capillary. Different pumping options are possible. Small peristaltic or membrane pumps are available. These are not suited for precise
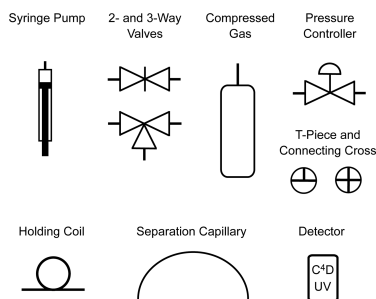
Figure 1. Components for building microfluidic CE systems.

operations and only produce limited pressures but may still be useful for such tasks as aspiration of a sample into a manifold. Stepper motor driven syringe pumps allow the precise movement of solutions, including withdrawal, and are suitable for high pressures. However, the volume resolution of syringe pumps is generally not adequate for direct metering of the small volumes in the low nanoliter to picoliter range to be injected into the separation capillaries. Stepper motor driven pumps are also not ideal when a smooth, pulse free hydrodynamic flow is required concurrent with a separation run. For these tasks it is preferable to employ controlled pressurization, which alleviates the aforementioned shortcomings and was therefore adopted for our work. A hydrodynamic flow can be achieved by using a solution container pressurized with a compressed gas in the headspace and a valve for flow control. Electronic pressure controllers are available which allow the electronic setting of the desired gas pressure. This approach is also useful if pumping from the high voltage side is desired. Conventional pumps and valves are not designed to be exposed to a liquid at a high voltage, but pressurization with a compressed gas provides inherent electrical isolation. Small valves are available from different suppliers; important parameters are low internal volumes and a low displacement volume of solutions on actuation. It is also desirable that the valve is of the latching type, i.e., it consumes power only on switching, which is critical if the setup is to be battery operated.

The capillaries usually employed for separation are made of fused silica have an outer diameter of 365 μm and are available with a wide range of internal diameters. For optical detection, 75 or 50 μm i.d.s have to employed, but as discussed in the introduction, narrower capillaries of 25 or even 10 μm i.d. in combination with C^{4}D are often preferable as better separation efficiencies are obtained and hydrodynamic pumping is possible. The available channel cross sections of a standard capillary are therefore comparable to those of separation channels on the chip platform. The use of C^{4}D also has the advantage of allowing easy adjustment of the effective separation length to the detector as it is not necessary to remove the protective polyimide coating in order to create a UV transparent window. Commercially available low dead volume interconnects (T-pieces and crosses) for these standard capillaries may be used for making up a manifold.

If the standard UV-absorption detection is desired, commercial detectors may be integrated, but these are expensive and bulky. It is, however, also feasible to construct relatively compact UV-detectors based on newly available deep-UV light-emitting

diodes.[24−28] Conctactless conductivity detection has the advantages discussed in the introduction. Furthermore, also the detection cells can be very small enabling precise positioning on short capillaries. These detectors are commercially available, but with some attention to detail well performing units can also be built in-house.[16,22,29,30]

A large range of high voltage modules with different maximum voltage levels and current as well as a range of secondary features are available from different suppliers. For precise control of the voltage the simplest models should be avoided in favor of devices which include a feedback mechanism for regulating the output. Many modules also provide monitor signals which allow one to keep track of the actual output voltage and sometimes also of the current, which are both very useful features. A reversible polarity is highly desirable, as this allows to change between cation and anion separation via electronic control, but this is a rare feature. Discussions of small high voltage modules can be found in Lewis et al.[31] and Blanes et al.[32] Attention has to be paid to the potential hazard of the electrophoretic separation voltage. This is best addressed by enclosing the high voltage bearing parts in an insulated case which is fitted with a microswitch to interrupt the high voltage on opening. To avoid the exposure of a fluid handling manifold based on pumps and valves at the inlet end of a capillary to the separation voltage, it always has to be applied at the detection end of the capillary, which is the reverse of the usual arrangement. This is not a problem with optical detectors and C^{4}D but would not allow the use of end-capillary detection schemes.

Standard Zone Electrophoresis. The setup for a standard zone electrophoretic separation with hydrodynamic injection is shown in Figure 2A and consists of a sequential injection analysis (SIA)-CE arrangement. Such a setup was first described by Ruzicka and co-workers[33] and has previously been employed successfully on a conventional scale in our group.[19,30,34−37] The manifold consists of a miniature syringe pump and 3-way valves instead of the selection valve more commonly employed in SIA and an electronically controlled pressurization section. The syringe pump serves for delivery of the background electrolyte, sample uptake, and sample transport to the injection point. Standard T-pieces were employed for connection of the capillary and the ground electrode to the fluidic manifold. Injection of sample into the capillary and capillary flushing is achieved by pressurization using the electronic pressure controller. Setting the time and pressure allows precise control of the desired length of the sample plug injected into the capillary. The entire manifold can fit into a space of approximately 20 cm by 20 cm (not including the power supplies and cylinder of pressurized gas).

The separation of a standard solution of six common inorganic cations (NH$_4^+$, K$^+$, Na$^+$, Ca^{2+}, Mg^{2+}, Li$^+$) is shown in Figure 2B. A BGE optimized for best separation of these ions consisting of 30 mM lactic acid and histidine (Lac/His) (pH 4.9) and 4 mM 18-crown-6 was employed. The crown ether allows the separation of ammonium from potassium, while lactate modifies the mobilities of Ca^{2+} and Mg^{2+} through complexation. The performance in terms of linear ranges, correlation coefficients, LODs, and reproducibilities is illustrated by the data of Table 1. These are generally comparable with the parameters obtained for conventional CE-C^{4}D, but it is noteworthy that the Lac/His buffer allows one to work with larger linear ranges for these cations than the more commonly employed MES/His buffer.[14] This BGE is therefore suitable for the analysis of samples in which the analytes are present at very different concentrations. For such samples, dilution is not an option as that will lower the concentrations of

A

B

C
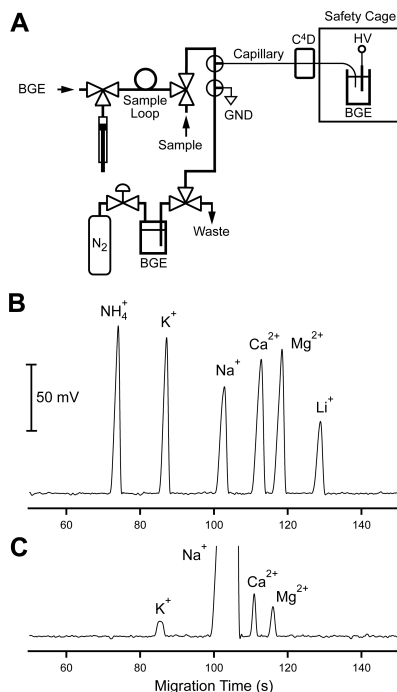
Figure 2. (A) Schematic drawing of a microfluidic system for zone electrophoresis with automated hydrodynamic injection and capillary flushing employing the SIA approach. (B) Separation of cations at 200 μM. BGE: 30 mM Lac/His pH 4.9 and 4 mM 18-crown-6. Capillary: 25 μm i.d., 365 μm o.d., 35 cm effective length, 50 cm total length. Injection: 22 s at 1.6 psi, occupying 10 mm of the capillary length as calculated by the Hagen–Poiseuille equation. Separation voltage at detection end, −30 kV. (C) Separation of a sample of Himalayan rock salt in water at 0.175 mg/mL. Note that the large peak for Na$^+$ is measurable but truncated in the figure.

certain analytes below their LODs. An example for such an application is the analysis of Himalayan rock salt, usually sold in health stores. Unlike normal table salt, rock salts are taken directly from the mines and therefore contain impurities. The electropherogram for a solution of 0.175 mg/mL of a rock salt sample is shown in Figure 2C. Using the Lac/His buffer it was

possible to determine K$^+$ at 17.5 μM, Ca^{2+} at 18.5 μM and Mg^{2+} at 14.3 μM alongside Na$^+$ at a concentration 1950 μM.

Fast Separation. Impressively fast separations have been reported for electrophoretic separations on lab-on-chip devices, and this is usually considered to be one of the main selling points if not a unique feature of the approach. It appears that it is commonly perceived that this is largely due to the special injection mode based on the cross formed between injection and separation channels. However, it has repeatedly been demonstrated over the years that very fast separations are also possible in short conventional capillaries when used in arrangements that allow fast and precise injection operations.[38−46]

The analysis time for the separation presented in the previous section with 2 min is relatively short for capillary electrophoresis, but an even faster separation is possible using the same setup of Figure 2A simply by reducing the effective capillary length to 10 cm and the injection time to 0.5 s in order to place only a short sample plug into the capillary and thus maintain the resolution. The separation of the 6 cations within 35 s is illustrated in Figure 3. However, as discussed in the introduction, this is achieved at
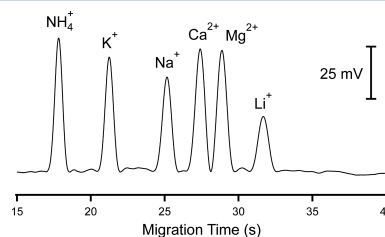
Figure 3. Fast separation of 200 μM NH$_4^+$, K$^+$, Na$^+$, Ca^{2+}, Mg^{2+}, and Li$^+$ in water. Capillary: 25 μm i.d., 365 μm o.d., 10 cm effective length, 50 cm total length. Injection: 0.5 s at 1.6 psi, occupying 0.2 mm of the capillary length as calculated by the Hagen–Poiseuille equation. Other conditions as for Figure 2.

the cost of a loss of sensitivity and under these conditions the LODs for NH$_4^+$, K$^+$, Na$^+$, Ca^{2+}, Mg^{2+}, and Li$^+$ were determined as 9.6, 11, 14, 11, 12, and 27 μM, respectively, which are about 4 times higher than those for the separation reported in the previous section.

Pressure Assisted Capillary Electrophoresis (PACE). As discussed in the introduction, when using narrow capillaries of 25 or 10 μm i.d. it is possible to employ hydrodynamic pumping in CE without penalty in laminar flow induced bandbroadening. One possible application of PACE, i.e., for speeding up the analysis, as implemented with the manifold shown in Figure 2A is illustrated in Figure 4. As can be seen in Figure 4A, under

Table 1. Validation Data for the Determination of Cations

ion	linear range (μM)	correlation coefficient r^2	limit of detection[a] (μM)	reproducibility of migration time (% RSD)[b]	reproducibility of peak area (% RSD)[b]
NH$_4^+$	5−4000	0.998	2	0.7	3.4
K$^+$	5−4000	0.998	3	0.7	4.0
Na$^+$	5−3000	0.999	3.5	0.7	3.7
Ca^{2+}	5−750	0.996	2.5	0.8	4.0
Mg^{2+}	5−750	0.996	2.5	0.8	4.6
Li$^+$	10−4000	0.997	7	1.0	4.0

[a]Peak heights corresponding to 3 times the baseline noise. [b]Determined for 200 μM NH$_4^+$, K$^+$, Na$^+$, Ca^{2+}, Mg^{2+}, and Li$^+$. $n = 9$.
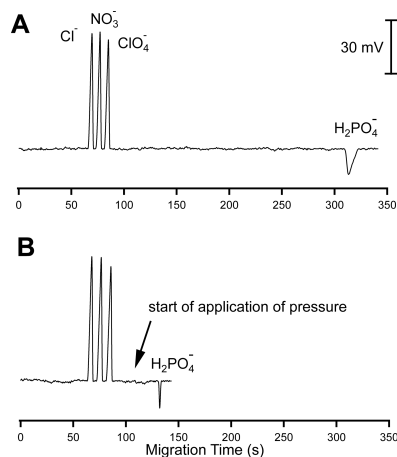
Figure 4. Separation of anions with pressure assistance. (A) Normal zone electrophoretic separation of anions. BGE: 30 mM Lac/His pH 4.9. Capillary: 10 μm i.d., 365 μm o.d., 20 cm effective length, 50 cm total length. Injection: 20 psi, 10 s. Separation voltage at detection end: +30 kV. Cl$^-$, 300 μM; NO$_3^-$, 300 μM; ClO$_4^-$, 300 μM; H$_2$PO$_4^-$, 600 μM. (B) Separation of the anions with superimposed hydrodynamic flow to speed up the migration of the phosphate. A pressure of 50 psi was continuously applied from t = 100 s.

conditions necessary for the separation of a group of anions, phosphate will arrive only much later at the detector. Note that the negative going peak for phosphate is nothing unusual for C^{4}D. The time saving that can be achieved by introducing a hydrodynamic flow is illustrated in Figure 4B. Pressurization was turned on following the passage of the last peak of the early analytes. The introduction of pressure was found not to have an adverse effect on the repeatability of the migration time for the phosphate peak as the relative standard deviation was found to be even better for pressurization than without (0.6% vs 0.9% RSD for migration time, respectively, n = 9). Similarly, also the reproducibility for the area of the phosphate peak was found to be improved (12% vs 6.5% RSD with and without hydrodynamic flow, respectively). It was also found that the migration times and peak areas for phosphate obtained with pressurization were also not adversely affected when the system was disassembled and then reassembled between measurements (0.4% and 6.5% RSD for migration time and peak area for 9 measurements in 3 sets with disassembly between the sets).

Dual Capillary Zone Electrophoresis. The use of two separation channels is not readily possible with conventional commercial CE instrumentation, but in principle not a significant complication as the required components are significantly less costly than for other quantitative analytical methods, such as HPLC. dual channel electrophoresis as previously reported for conventional scale fluidic setups[14,16] could therefore relatively easily be implemented in the here proposed microfluidic breadboard approach as shown in Figure 5A. It is possible to achieve this using a single syringe pump and pressurization section. Using this configuration, inorganic cations (NH$_4^+$, K$^+$, Na$^+$, Ca^{2+}, Mg^{2+}, Li$^+$) and anions (Cl$^-$, NO$_2^-$, NO$_3^-$, SO$_4^{2-}$, ClO$_4^-$) were simultaneously analyzed, as can be seen in Figure
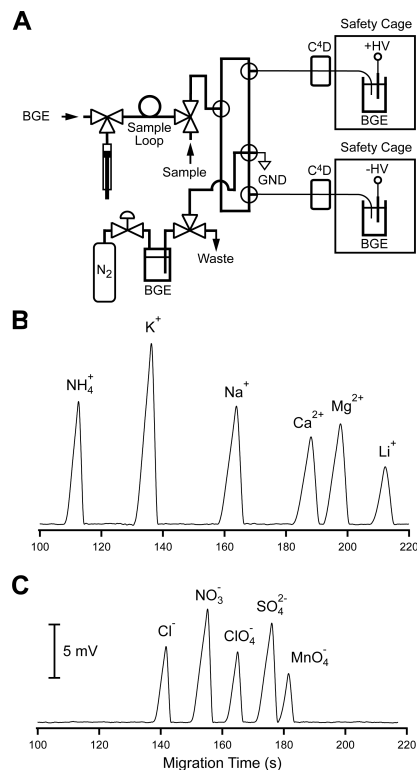

Figure 5. Concurrent electrophoretic separation of cations and anions. (A) Extended manifold for two separation capillaries. (B) Cations. BGE: 30 mM Lac/His pH 4.9. Capillary: 25 μm i.d., 365 μm o.d., 35 cm effective length, 60 cm total length. Injection: 6 psi, 7 s. Separation voltage at detection end: $-$30 kV. NH$_4^+$ 200 μM, K$^+$ 400 μM, Na$^+$ 400 μM, Ca^{2+} 200 μM, Mg^{2+} 200 μM, Li$^+$ 200 μM. (C) Anions. BGE: 30 mM Lac/His pH 4.9. Capillary: 25 μm i.d., 365 μm o.d., 50 cm effective length, 60 cm total length. Injection: 6 psi, 7 s. Separation voltage at detection end: $-$30 kV. Cl$^-$, 200 μM; NO$_3^-$, 400 μM; ClO$_4^-$, 200 μM; SO$_4^2$, 200 μM; MnO$_4^-$, 400 μM.

5B. The same BGE was used for both types of ions and the effective lengths of the capillaries and separation voltages were adjusted so both cations and anions were baseline separated and appear within the same time frame. If it is desired to use different BGEs for the cations and anions as well as inject individually optimized amounts, this will also be possible with an extended system.

Isotachophoresis (ITP). In ITP, a sample plug is introduced between a leading electrolyte (LE), which has a higher mobility than the analyte ions, and a terminating electrolyte, with a lower mobility. The only change in the instrumentation necessary for performing ITP is the ability to manipulate three solution (LE, TE, sample) rather than only two (BGE, sample) as in CZE. This could be implemented by employing an additional three-way valve as shown in Figure 6A. In order to demonstrate its use, an

ITP separation of cationic amino acids[47] was performed, as can be seen in Figure 6B.
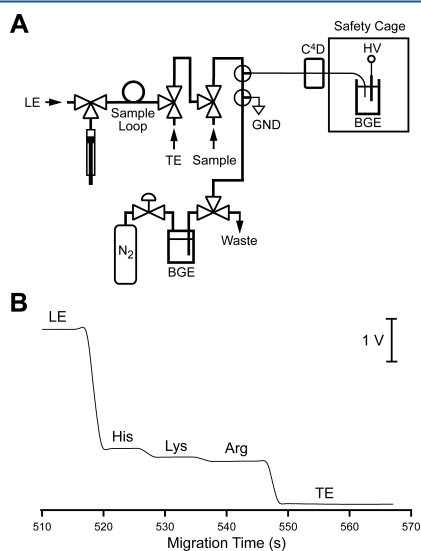
Figure 6. Isotachophoretic separation of amino acids. (A) Manifold for the injection of two separate electrolytes. (B) Isotachopherogram for a standard solution of 2 mM His, Lys, and Arg in water. LE: 10 mM potassium acetate and 52.3 mM acetic acid (pH 4.0). TE: 10 mM Ala. Low EOF-capillary: 25 μm i.d., 365 μM o.d., 60 cm effective length, 75 cm total length. Injection for 10 s at 6 psi. Separation voltage at detection end: −30 kV.

Gradient Elution Moving Boundary Electrophoresis (GEMBE). GEMBE is an electrophoretic separation method relying on the simultaneous application of a hydrodynamic flow and an electric field which was introduced by Ross and co-workers in 2007.[48−52] This generates two opposing forces on each ion, and at first a relatively high counter-pressure is applied to prevent any analyte ion from entering the capillary. The pressure is then linearly decreased (while keeping the voltage constant), which reduces the opposing force, allowing the different analytes to enter the capillary in turn, from fastest to slowest. This creates a set of boundaries moving against the applied pressure, toward the detector. Each new segment includes all of the ions from the earlier segments, so the measured conductivity is increased stepwise. The implementation of this less commonly employed mode of electrophoresis on the microfluidic platform is illustrated in Figure 7A. The length of the capillary from the injection point to the detector was as short as 3.5 cm and a controlled counter-pressure was applied again by pressurization with compressed nitrogen using the electronic pressure controller. Pumping from the high voltage end of the capillary does not present a problem when using this approach as the only contact with the solution at the elevated voltage is via the compressed nitrogen. The analysis of a mixture of four carboxylic acids in 160 s is illustrated in Figure 7B. The counter pressure was slowly reduced from 100 to 50 psi in steps of 0.5 psi,
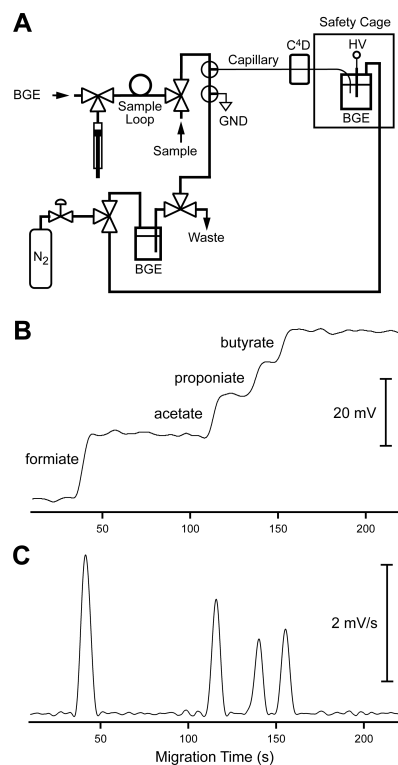
Figure 7. GEMBE separation. (A) Manifold for pressure application from the detection end of the capillary. (B) GEMBE-electropherogram of 200 μM formic, acetic, propionic and butyric acids (all 200 μM). Capillary: 10 μm i.d., 365 μM o.d., 3.5 cm effective length, 30 cm total length. Separation voltage at detection end: −30 kV. Pressure gradient: 100 to 50 psi over 400 steps of 0.5 psi. (C) Derivative of the raw electropherogram given in part B.

demonstrating the fine level of pressure control available in this system. The rate of the reduction of the pressure affects the analysis time but also the separation. It is also possible to evaluate the GEMBE data in peak mode, simply by forming the first derivative of the electropherogram, as illustrated in Figure 7C.

■ CONCLUSION

It was found possible to assemble very compact electrophoresis instrumentation from off-the-shelf miniature components. This alleviates the limitations of commercial electrophoresis instruments in terms of implementing different electrophoretic modes. The standard building blocks needed for hydrodynamic injection, capillary flushing, and detection can quickly be rearranged for different purposes, and the Instrumentino package allows easy adaptation of the software control. The contactless conductivity detector can be placed anywhere on the capillary without the need to produce a detection window which allows one to easily adjust compromise conditions between the degree

-100-

of separation and analysis time. The performance of the microfluidic breadboard approach was found to be similar to commercial CE systems. Furthermore, fast separations are possible, but the approach has none of the limitations of lab-on-chip electrophoretic devices with regard to the inflexibility of the separation length and the geometrical constraints for detection. It also should be borne in mind that lab-on-chip electrophoresis devices require a periphery with pumps and valves for flushing and sample introduction, and the chip is only part of a larger fluidic manifold. The breadboard approach thus provides high flexibility in a small space at moderate cost without penalty in performance.

■ **AUTHOR INFORMATION**

Corresponding Author
*E-mail: Peter.Hauser@unibas.ch. Phone: +41 61-267-1003. Fax: +41 61-267-1013.

Notes
The authors declare no competing financial interest.

■ **REFERENCES**

(1) Mai, T. D.; Pham, T. T. T.; Pham, H. V.; Saiz, J.; Ruiz, C. G.; Hauser, P. C. *Anal. Chem.* **2013**, *85*, 2333−2339.
(2) Mayrhofer, K.; Zemann, A. J.; Schnell, E.; Bonn, G. K. *Anal. Chem.* **1999**, *71*, 3828−3833.
(3) Mai, T. D.; Hauser, P. C. *Talanta* **2011**, *84*, 1228−1233.
(4) Mai, T. D.; Hauser, P. C. *Electrophoresis* **2011**, *32*, 3000−3007.
(5) Mai, T. D.; Hauser, P. C. *J. Chromatogr. A* **2012**, *1267*, 266−272.
(6) Han, C.; Sun, J.; Liu, J.; Cheng, H.; Wang, Y. *Analyst* **2015**, *140*, 162−173.
(7) Sáiz, J.; Koenka, I. J.; Mai, T. D.; Hauser, P. C.; García-Ruiz, C. *TrAC, Trends Anal. Chem.* **2014**, *62*, 162−172.
(8) Castro, E. R.; Manz, A. *J. Chromatogr. A* **2015**, *1382*, 66−85.
(9) Lim, J.; Maes, F.; Taly, V.; Baret, J. C. *Lab Chip* **2014**, *14*, 1669−1672.
(10) Yuen, P. K. *Lab Chip* **2008**, *8*, 1374−1378.
(11) Bhargava, K. C.; Thompson, B.; Malmstadt, N. *Proc. Natl. Acad. Sci. U.S.A.* **2014**, *111*, 15013−15018.
(12) Segato, T. P.; Bhakta, S. A.; Gordon, M. T.; Carrilho, E.; Willis, P. A.; Jiao, H.; Garcia, C. D. *Anal. Methods* **2013**, *5*, 1652−1657.
(13) Breadmore, M. C. *J. Chromatogr. A* **2012**, *1221*, 42−55.
(14) Sáiz, J.; Duc, M. T.; Koenka, I. J.; Martín-Alberca, C.; Hauser, P. C.; García-Ruiz, C. *J. Chromatogr. A* **2014**, *1372*, 245−252.
(15) Nguyen, T. A. H.; Pham, T. N. M.; Doan, T. T.; Ta, T. T.; Saiz, J.; Nguyen, T. Q. H.; Hauser, P. C.; Mai, T. D. *J. Chromatogr. A* **2014**, *1360*, 305−11.
(16) Pham, T. T. T.; Mai, T. D.; Nguyen, T. D.; Sáiz, J.; Pham, H. V.; Hauser, P. C. *Anal. Chim. Acta* **2014**, *841*, 77−83.
(17) Ansari, K.; Ying, J. Y. S.; Hauser, P. C.; de Rooij, N. F.; Rodriguez, I. *Electrophoresis* **2013**, *34*, 1390−1399.
(18) Mahabadi, K. A.; Rodriguez, I.; Lim, C. Y.; Maurya, D. K.; Hauser, P. C.; de Rooij, N. F. *Electrophoresis* **2010**, *31*, 1063−1070.
(19) Mai, T. D.; Schmid, S.; Muller, B.; Hauser, P. C. *Anal. Chim. Acta* **2010**, *665*, 1−6.
(20) Koenka, I. J.; Sáiz, J.; Hauser, P. C. *Comput. Phys. Commun.* **2014**, *185*, 2724−2729.
(21) Koenka, I. J.; Sáiz, J.; Hauser, P. C. *Chimia* **2015**, *69*, 172−175.
(22) Tanyanyiwa, J.; Galliker, B.; Schwarz, M. A.; Hauser, P. C. *Analyst* **2002**, *127*, 214−218.
(23) Zhang, L.; Khaloo, S. S.; Kubáň, P.; Hauser, P. C. *Meas. Sci. Technol.* **2006**, *17*, 3317−3322.
(24) Bui, D. A.; Hauser, P. C. *J. Chromatogr. A* **2015**, *1421*, 203−208.
(25) Kraiczek, K. G.; Bonjour, R.; Salvadé, Y.; Zengerle, R. *Anal. Chem.* **2014**, *86*, 1146−1152.
(26) Marini, R. D.; Rozet, E.; Montes, M. L. A.; Rohrbasser, C.; Roht, S.; Rheme, D.; Bonnabry, P.; Schappler, J.; Veuthey, J. L.; Hubert, P.; Rudaz, S. *J. Pharm. Biomed. Anal.* **2010**, *53*, 1278−1287.
(27) Rohrbasser, C.; Rheme, D.; Decastel, S.; Roth, S.; Montes, M. D. A.; Veuthey, J. L.; Rudaz, S. *Chimia* **2009**, *63*, 890−891.
(28) Krcmova, L.; Stjernlof, A.; Mehlen, S.; Hauser, P. C.; Abele, S.; Paull, B.; Macka, M. *Analyst* **2009**, *134*, 2394−2396.
(29) Francisco, K. J. M.; do Lago, C. L. *Electrophoresis* **2009**, *30*, 3458−3464.
(30) Stojkovic, M.; Koenka, I. J.; Thormann, W.; Hauser, P. C. *Electrophoresis* **2014**, *35*, 482−486.
(31) Lewis, A. P.; Cranny, A.; Harris, N. R.; Green, N. G.; Wharton, J. A.; Wood, R. J. K.; Stokes, K. R. *Meas. Sci. Technol.* **2013**, *24*, 042001.
(32) Blanes, L.; Tomazelli Coltro, W. K.; Saito, R. M.; Van Gramberg, A.; do Lago, C. L.; Doble, P. *Electrophoresis* **2012**, *33*, 893−898.
(33) Wu, C.-H.; Scampavia, L.; Ruzicka, J. *Analyst* **2002**, *127*, 898−905.
(34) Stojkovic, M.; Mai, T. D.; Hauser, P. C. *Anal. Chim. Acta* **2013**, *787*, 254−259.
(35) Mai, T. D.; Hauser, P. C. *J. Chromatogr. A* **2012**, *1267*, 266−272.
(36) Mai, T. D.; Hauser, P. C. *Talanta* **2011**, *84*, 1228−1233.
(37) Mai, T. D.; Hauser, P. C. *Electrophoresis* **2011**, *32*, 3000−3007.
(38) Zemann, A. J. *J. Chromatogr. A* **1997**, *787*, 243−251.
(39) Chan, K. C.; Muschik, G. M.; Issaq, J. H. *J. Chromatogr., Biomed. Appl.* **1997**, *695*, 113−115.
(40) Bjørnsdottir, I.; Hansen, S. H. *J. Biochem. Biophys. Methods* **1999**, *38*, 155−161.
(41) Yang, W.; Zhang, Z. *Anal. Lett.* **2003**, *36*, 465−477.
(42) Yang, W.; Zhang, Z. *Int. J. Environ. Anal. Chem.* **2002**, *82*, 353−360.
(43) Yang, W.-P.; O'Flaherty, B.; Cholli, A. L. *J. Environ. Sci. Health, Part A: Toxic/Hazard. Subst. Environ. Eng.* **2001**, *36*, 1271−1285.
(44) Rainelli, A.; Hauser, P. C. *Anal. Bioanal. Chem.* **2005**, *382*, 789−794.
(45) Wuersig, A.; Kubáň, P.; Khaloo, S. S.; Hauser, P. C. *Analyst* **2006**, *131*, 944−949.
(46) Mark, J. J. P.; Piccinelli, P.; Matysik, F. M. *Anal. Bioanal. Chem.* **2014**, *406*, 6069−6073.
(47) Kubacak, P.; Mikui, P.; Valaikova, I.; Havranek, E. *Arch. Pharm.* **2006**, *339*, 96−99.
(48) Flanigan, P. M.; Ross, D.; Shackman, J. G. *Electrophoresis* **2010**, *31*, 3466−3474.
(49) Ross, D. *Electrophoresis* **2010**, *31*, 3658−3664.
(50) Ross, D. *Electrophoresis* **2010**, *31*, 3650−3657.
(51) Strychalski, E. A.; Henry, A. C.; Ross, D. *Anal. Chem.* **2009**, *81*, 10201−10207.
(52) Shackman, J. G.; Munson, M. S.; Ross, D. *Anal. Chem.* **2007**, *79*, 565−571.

-101-

Publication #8:

Simultaneous separation of cations and anions in capillary electrophoresis

Trends in Analytical Chemistry (2014), 62, 162–172

Simultaneous separation of cations and anions in capillary electrophoresis

CrossMark

Jorge Sáiz [a,b], Israel Joel Koenka [c], Thanh Duc Mai [c,d], Peter C. Hauser [c,*], Carmen García-Ruiz [a,b]

[a] Department of Analytical Chemistry, Physical Chemistry and Chemical Engineering, University of Alcalá, Ctra. Madrid-Barcelona Km 33.6, 28871 Alcalá de Henares (Madrid), Spain
[b] University Institute of Research in Police Sciences (IUICP), University of Alcalá, Ctra. Madrid-Barcelona Km 33.6, 28871 Alcalá de Henares (Madrid), Spain
[c] Department of Chemistry, University of Basel, Spitalstrasse 51, 4056 Basel, Switzerland
[d] Centre for Environmental Technology and Sustainable Development (CETASD), Hanoi University of Science, Nguyen Trai Street 334, Hanoi, Viet Nam

ARTICLE INFO

ABSTRACT

With capillary electrophoresis, it is desirable to have simultaneous determination of cations and anions, which avoids costs and time spent on separate analyses, so concurrent approaches to separation gained popularity in recent years. We review the different strategies employed for the simultaneous separation and determination of cations and anions, including the use of complexing agents, micelles, two injectors, dual detectors, or two capillaries. We give an overview of the methods reported to date, and their benefits and drawbacks, and we evaluate the instrumental requirements of the different approaches.

© 2014 Elsevier B.V. All rights reserved.

Contents

1. Introduction

Capillary electrophoresis (CE) is an electrokinetic analytical technique for the separation of ionic species by their relative electrophoretic mobilities. The capillaries, with sub-millimeter inner diameter and a length of typically 50 cm, are filled with a background electrolyte (BGE) and a high voltage (HV) of up to 30 kV

is applied. Samples are injected into one end of the capillary and a detector is normally placed at the other end. Usually, only cations or anions can be determined, depending on the polarity of the applied electric field. The capillaries commonly used in CE are made of fused silica, for which an electroosmotic flow (EOF) in the direction of the cathode occurs. The EOF will cause loss of cation resolution due to accelerated migration (co-EOF migration). In contrast, the EOF equally slows down all anions as they move towards the anode (counter-EOF migration) and anions with low mobility may be carried towards the cathode by the EOF.

If cations and anions have to be determined in the same sample, two separate analysis runs with changed polarity are usually required. If different separation buffers are needed for the two groups of ions, then the capillary also needs to be rinsed and re-conditioned when changing over.

Concurrent determination of cations and anions in CE is therefore a very desirable feature as it saves both time and the expense of separate analyses. For this reason, a considerable effort has been devoted by research groups over the past three decades to the development of such methods. A number of very different strategies have been proposed. Some methods involve modification of the sample or the BGE with additional reagents; others change the magnitude and the direction of the EOF. Certain strategies require modification of conventional commercial CE systems, while some require purpose-made instruments.

We survey the state-of-the-art of simultaneous separations of anions and cations in this review. We discuss the principles of operation, types of injection, specific options and the technology required for each method. We critically compare different approaches and note their advantages and disadvantages. Table 1 shows the advantages, the disadvantages and the system requirements for each of the methods compared in this review. Our aim is to provide a contemporary guide reviewing all the approaches used to date for the simultaneous separation of differently charged analytes.

2. Complexing agents

The employment of complexing agents for simultaneous separation of cations and anions is well known from ion chromatography. The procedure consists of a reaction between a metal cation and a ligand or complexing agent to form an anionic complex, which can be separated together with the native anions in the sample. The resulting complexes must be stable, soluble and have good detectability. Cation complexation is a relatively simple technique, which does not require special instrumentation. There are two approaches for this procedure: pre-capillary and on-capillary complexation.

2.1. Pre-capillary complexation

In pre-capillary complexation, the complexing agent is added to the sample before injection into the capillary. This process is usually time consuming and often requires heating of the sample, which is not always feasible. Moreover, the addition of a complexing agent in excess will result in an additional peak in the electropherogram, which might overlap with other peaks of interest.

The use of pre-capillary complexations of metal cations in CE was reported several times in the 1990s and several complexing agents have been used. Krokhin et al. [1] simultaneously determined the anionic 4-(2-pyridylazo)resorcinol chelates of Co(II), Ni(II) and Fe(II) alongside Br⁻, Cl⁻, I⁻, NO₂⁻, NO₃⁻, SO₄²⁻, ClO₄⁻, F⁻, HPO₄²⁻, HCO₃⁻ and acetate. Pozdniakova and Padarauskas [2] compared the use of 1,2-cyclohexanediaminetetraacetic acid (CDTA), ethylenediaminetetracetic acid (EDTA) and diethylenetriaminepentaacetic acid (DTPA) as complexing agents for the speciation of Cr(VI/III) and V(V/IV), in different water samples. Cr(VI) is normally present as the CrO₄²⁻ anion, and Cr(III) as the cationic Cr³⁺

ion. Complexation with DTPA allowed the determination of both species as anions, together with other anionic complexed metal cations and native inorganic anions. V(IV) in solution is present as the cationic vanadyl (VO²⁺) ion and V(V) as an anionic vanadate ion. To enable concurrent determination, these were separated as the VOEDTA²⁻ and VO₂EDTA³⁻ complexes. The simultaneous separation of Cr(III) and Cr(VI) alongside other metal cations and anions has also been achieved by treating the sample with CDTA [3,4]. EDTA has been used for the simultaneous determination of Ba²⁺, Ca²⁺, Mg²⁺, Ni²⁺, Cu²⁺, lactate, butyrate, salicylate, propionate, acetate, phosphate, formate and citrate [5].

2.2. On-capillary complexation

The addition of the complexing agent to the BGE is known as on-capillary complexation, since the complexation reaction occurs inside the capillary, while the compounds are being separated. Besides saving time compared to the pre-capillary approach, a further advantage is prevention of in-capillary dissociation of unstable transition-metal complexes.

EDTA has also been used for on-capillary complexation of several metal cations and their simultaneous determination with a variety of anions [6]. However currently, 2,6-pyridinedicarboxylic acid (PDCA) is the most popular complexing agent for creating anionic metal chelates. The main reason for this preference is that it also allows the indirect detection of anions having little or no UV absorbance alongside the direct detection of chelated cations. PDCA was first used by Soga and Ross [7] for the determination of Cu²⁺, Ni²⁺ and Fe²⁺, and several inorganic anions and organic acids. Recently, it was used by Wharton and Stokes [8] for the separation of Cu²⁺, Ni²⁺ and Fe³⁺ in an NaCl solution, by Sarazin et al. [9] for aluminum and other metal cations and anions, and by Wang et al. [10] for the separation of phosphate and calcium in river water.
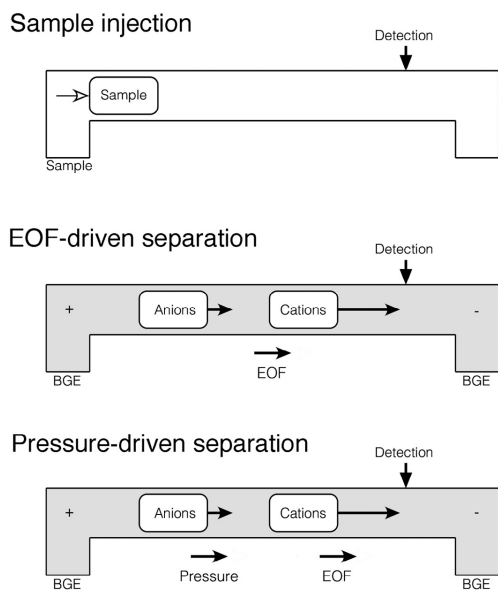
3. Micelles

Wei et al. [11] recently demonstrated the use of micelles for concurrent determination of basic and acidic drugs. The procedure consisted of an injection sequence, in which the acidic drugs were electrokinetically injected first, followed by a hydrodynamic plug of BGE and finally the electrokinetic injection of the basic drugs. The plug of BGE was necessary, probably because the anions were attracted to the inlet end during cationic injection because of the direction of their electrophoretic mobilities. The acidic drugs (in their anionic form in the sample matrix) turned to neutral after their introduction due to the low pH of 3.0 in the BGE. The separation was then carried out via micellar electrokinetic chromatography. The fast-moving anionic micellar phase carried both neutral and cationic analytes toward the detector in a reverse migration mode for cations. In this work, electrokinetic injection was used and the acidic analytes were determined in their neutral form. Although it has not been performed to date, it should also be possible to use hydrodynamic instead of electrokinetic injection. As is the case for complexing agents, this separation method can be implemented on an unmodified conventional CE system.

4. Capillary electrophoresis driven by electroosmotic flow

As can be seen in Fig. 1, this approach uses traditional single-end injection with detection near the opposite end. In conventional capillary-zone electrophoresis (CZE), a cathodic EOF is created when the electric field is established. Anions with electrophoretic mobilities of lower magnitudes than the EOF will be carried toward the cathode, their effective mobilities being opposite to their electrophoretic mobilities. Certainly, an EOF of high magnitude will be

Table 1
General characteristics of the different methods used for the simultaneous separation of cations and anions

Method	Advantages	Disadvantages	Specific system requirements
Pre-capillary complexation	- Does not require specific instrumentation.	- Requires sample pre-treatment. - Appearance of additional peaks. - Only works for some metal cations. - Labile complexes will decay in capillary.	None
In-capillary complexation	- Does not require specific instrumentation. - PDCA can be used for indirect photometric detection of anions.	- Only works for some metal cations. - Requires the modification of the BGE.	None
Micelles	- Does not require specific instrumentation.	- Requires modification of the BGE. - Limited applicability.	None
EOF-driven CE	- Does not require specific instrumentation.	- Requires BGEs at high pH values. - Long migration times for anions. - Loss of resolution for (fast) cations. - Very fast anions cannot be detected. - Formation of insoluble hydroxides of alkaline earth metal ions. - Cationic probes used for indirect photometric detection may not be protonated at high pH values. - Enhanced absorption of CO_2, and baselines instabilities with C^4D. - Gap between anions and cations.	None
Pressure-driven CE	- Faster migration of analytes. - Does not require use of BGEs at high pH values. - Easy to optimize and to control. - Pressure can be changed on demand during the separation.	- Hydrodynamic flow causes peak broadening unless capillaries of less than 50 μm ID are used. - Fast analytes can co-migrate. - Gap between anions and cations, unless pressure is adjusted during run.	- Requires a CE instrument capable of applying well-controlled pressure during separation.
DOEI	- No need to force ions against their electrophoretic mobilities. - Does not require BGE modification.	- The sample can be lost at one end of the capillary if process is not well controlled and optimized. - Peaks of anions and cations may overlap.	- A system able to inject into both ends of the capillary. - A movable detector, preliminary transport or a modified cartridge may be necessary to avoid co-detection.
Dual single-end injection	- Easy placement of the sample plug at the HV end of the capillary. - No need to force ions against their electrophoretic mobilities. - Does not require BGE modification.	- The sample can be lost at one end of the capillary if process is not well controlled and optimized. - Peaks of anions and cations may overlap.	- Requires a CE instrument capable of applying well-controlled pressures. - A movable detector, a preliminary transport or a modified cartridge may be necessary to avoid co-detection.
Single injection with positioning of the sample plug	- No need to force ions against their electrophoretic mobilities. - Does not require BGE modification.	- Cannot be performed in unmodified commercial CE systems.	- Requires a CE instrument capable of applying well-controlled pressures. - Requires two detectors.
Dual-channel CE	- No need to force ions against their electrophoretic mobilities. - Independent optimization.	- Cannot be performed in unmodified commercial CE systems.	- Requires two capillaries and two high-voltage electrodes.

PDCA, 2,6-pyridinedicarboxylic acid; C^4D, Capacitively coupled contactless conductivity detection; DOEI, Dual opposite-end injection.

Sample injection

EOF-driven separation

Pressure-driven separation

Fig. 1. Sample injection followed by simultaneous separation of cations and anions by electroosmotic force (EOF)-driven separation and pressure-driven separation. The first approach uses a strong EOF to carry anions toward the cathode while the second uses pressure for the same purpose.

needed to displace fast anions and the simplest way to increase the magnitude of a cathodic EOF is to increase the pH of the BGE.

In 1981, Jorgenson and Lukacs [12] were, to our knowledge, the first authors to use a high-magnitude EOF to sweep ions with opposite mobilities towards the detector. Their experimental set-up consisted of a +30 kV HV supply connected to the injection end of the capillary and a fluorescence detector placed at the opposite grounded end. Several dansyl derivatives of amino acids, fluorescamine derivatives of dipeptides and fluorescamine derivatives of amines were injected electrokinetically. Using a BGE at pH 7, most of the analyzed substances had a net negative charge and hence they were expected to move toward the anode. However, they were found to move toward the cathode end of the capillary. This work laid the foundations of the EOF-driven simultaneous determination of anions and cations, and the apparent contradiction found by Jorgenson and Lukacs [12] was easily explained by the strong EOF created due to the relatively high pH of the BGE, which was even able to reverse the migration of small triply-charged anions toward the detector. The order of appearance of the anions in the electropherograms was thus: first cations, then neutral compounds and finally anions, all of them separated within 25 min.

EOF-driven separations can be performed on any CE system and do not require special reagents. However, this approach shows several disadvantages: anions have long migration times; there is a loss of resolution for (fast) cations; and, fast anions are not detected if their mobility is higher than the EOF. Moreover, BGEs of high-pH values may lead to the formation of insoluble hydroxides of alkaline earth metal ions. Furthermore, cationic probes used for indirect photometric detection may not be protonated at high pH values. Another

difficulty caused by high-pH BGEs is the enhanced absorption of CO_2 from air, which may lead to baseline instabilities when using certain detectors, such as capacitively coupled contactless conductivity detection (C^4D).

Shamsi and Danielson [13] showed that decreasing the pH value of the BGE, in order to improve the resolution of peaks, from pH 7.5 to an apparent pH 6.0 using methanol, prolonged the analysis time of 18 anionic and cationic surfactants from 6 min to more than 40 min. Moreover, the authors did not show the last four peaks in the electropherogram, as these small anionic surfactants had migration times that were too long. As time saving is the main motivation for concurrent cation-anion separations, this approach might prove counter-productive. If the sample is composed of fast cations and fast anions, there will be a gap between both groups of peaks, as shown in Fig. 2. The faster the cations and the anions are, the larger this gap will be. A peak corresponding to non-charged compounds will also appear in this gap. Foret et al. [15] had a 6-min gap in a separation taking 16 min for fast, inorganic cations and relatively slow, organic anions. Similar gaps were observed by Haumann et al. [14], Gallagher and Danielson [16] and Raguénès et al. [17]. However, very fast concurrent separations have also been achieved. Cunha et al. [18] managed the simultaneous separation of diclofenac and its common counter-ions in less than 1 min. The separation was carried out in a capillary with an effective length of 10 cm. The efficiency of this approach is, of course, highly dependent on the mobility of the anions. The lower their mobility, the faster they appear in the electropherogram. This EOF-driven method is very easy to use, but restricted to relatively slow anions, at least when short analysis times are important.

Combining two or more approaches can be useful. On-capillary complexation was used together with EOF-driven separation for the determination of Fe^{2+} and Fe^{3+}, whose mobilities do not differ sufficiently for direct electrophoretic separation. Fe^{2+} was complexed with o-phenanthroline (resulting in a positively-charged complex) and Fe^{3+} was complexed with EDTA [19] and CDTA [2,20] (resulting in negatively-charged complexes). Then, both complexes were separated in an EOF-driven separation.

EOF-driven separations are normally used with the cathode at the detector end and a high-pH BGE. However, a recent report [21] suggested using didodecyldimethyl-ammonium bromide for EOF reversal for the simultaneous separation of anions and cations. Under these conditions, anions migrate before neutral compounds, which, in turn, migrate before cations. As inorganic cations generally have electrophoretic mobilities of lower magnitude than anions, this approach has the potential to reduce the analysis time, because their low mobilities are easier to overcome by the EOF [21]. This was shown by the authors, with a separation of three inorganic anions and six inorganic cations within 3.5 min, using a capillary of 40-cm length to the detector. Another important advantage is that a reversed EOF allows the use of BGE at low pH values, which overcome the problems of high-pH BGEs mentioned above.

EOF-driven separations have also been used for the separation of inorganic cations, such as NH_4^+, K^+, Na^+, Li^+, alongside inorganic ions [22] and organic anions [23].

Although electrokinetic injection was used by Jorgenson and Lukacs [12] in the first work published about EOF-driven separation of anions and cations, this injection method was never reported again for this mode of separation. Even though the establishment of the EOF inside the capillary may force the introduction of ions into the capillary against their electrophoretic mobilities, the situation is not well defined at the capillary end. Thus, hydrodynamic injection should be more reliable when employing EOF-driven concurrent separations. Furthermore, electrokinetic injection generally tends to suffer from a sampling bias due to variations in conductivity of samples, unless a high concentration of an electrolyte is added to all samples to obtain uniform background conductivity.
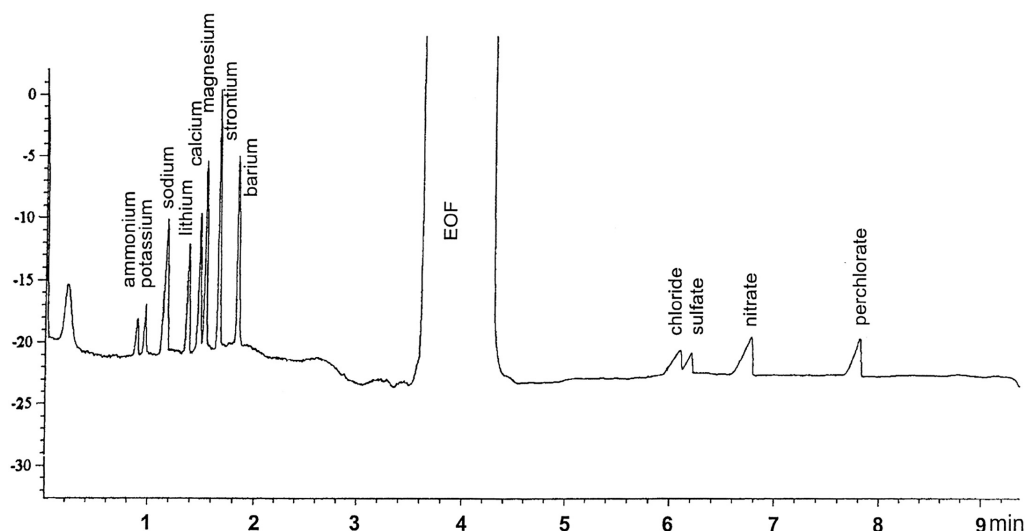
Fig. 2. Concurrent separation of several cations and anions using a strong electroosmotic force (EOF) to carry anions toward the cathode. A gap between cations and anions is created where a big peak corresponding to non-charged compounds appears. {Reprinted from [14] with permission from Elsevier}.

5. Pressure-driven capillary electrophoresis

Pressure-assisted capillary electrophoresis has been used to counterbalance the EOF, to increase the residence time, and hence improve separation, or to push ions towards the detector for faster analysis [12,24,25]. Another possible use of pressure is to carry analytes against their electrophoretic migration towards the detector, achieving concurrent detection of differently charged species. Fig. 1 shows the principle of separation of this approach.

To our knowledge, this was first reported by Haumann et al. [14] in 2010. The authors applied pressure at the anodic end of the capillary to force anions towards the detector, as the EOF was not strong enough to overcome the high mobility of the anions. There are two challenges when performing pressure-assisted separations. First, it requires a CE instrument capable of applying well-controlled pressures during separation. Second, the pressure induces hydrodynamic flow in the capillary, which has a parabolic profile. Such flows are known to broaden peaks and diminish resolution. However, the EOF profile is flat and does not significantly contribute to band broadening. Nevertheless, Mai and Hauser [24] proved that, when employing C⁴D, pressure-assisted separations in narrow capillaries with internal diameters of 10 μm or 25 μm are possible without significant penalty in terms of separation efficiency and sensitivity. Applying pressure during separation needs to be done carefully. The situation is similar to the use of EOF as sweeping force. High pressures, needed to push fast anions to the detector end, may move cations through the detector before separation of the latter is achieved.

Typically, an electropherogram for a pressure-assisted separation of anions and cations is similar to electropherograms obtained with an EOF-driven concurrent separation of both species (Fig. 2), featuring a large peak corresponding to neutral compounds and a gap between anionic and cationic species. In order to reduce separation time, Mai and Hauser [26] conceived a system with two C⁴D detectors. With this approach, they also avoided the appearance of

the neutral compounds in the gap between anions and cations in the electropherogram. The first detector was placed close to the injection end of the capillary and was used for the detection of anions, which moved slowly, carried by the combination of the EOF and the assisting pressure. The second detector was placed at the opposite end and was used for the detection of the fast-moving cations. With this design, the authors obtained two electropherograms, one for anions and the other for cations, and successfully resolved 14 organic cations and anions within 2.5 min. To optimize the separation time, the detectors should be movable along the capillary, as is possible with a C⁴D cell. This approach obviously needs a purpose-made instrument.

A completely different approach was taken by Flanigan et al. [27]. The authors employed a technique termed gradient elution moving boundary electrophoresis and C⁴D detection on a 5-cm capillary with an effective length of 2 cm. This technique uses a continuous injection, while the elution of the analytes from the sample reservoir is controlled by a variable hydrodynamic counter-flow. At the beginning, the hydrodynamic counter-flow is so strong that all analytes remain in the sample reservoir. As the pressure is decreased, the fastest analyte enters the capillary and moves towards the detector. A further decrease in the magnitude of the counter-flow allows the subsequent migration of the rest of the analytes towards the detector. A reversal of the direction of the counter-flow (using a vacuum pump) then allows analytes of opposite charge to enter the capillary and to be detected. The reversal of the direction of flow creates a discontinuity in the detector signal that visually separates the anion and cation fronts. The electropherogram obtained is a series of steps that can be interpreted directly or as peaks following derivation of the signal.

Compared to EOF-driven CE, pressure-driven CE is easier to optimize. The pressure system can be electronically controlled while the EOF needs adjustment of pH and/or ionic strength. Moreover, pressure can be changed during a run for flexible adjustment of the hydrodynamic flow [24].

6. Dual opposite-end injection capillary electrophoresis

A different approach for the simultaneous separation of anionic and cationic species is dual opposite-end injection (DOEI). In DOEI, the sample is introduced into both ends of the capillary and the detector is located somewhere near the middle of the capillary. The cation separation is then carried out in one part of the capillary, while the anion separation is carried out in the other. Unlike the above approaches, in which anions and cations move in the same direction, in DOEI, cationic and anionic species move towards the detector from opposite sides; anions from the cathode and cations from the anode. In order to achieve optimized separation of cations as well as anions the EOF is usually suppressed in these methods by reducing the pH of the BGE, using dynamic capillary coatings or even using capillaries of different material showing lower EOF magnitudes, such as polyether ether ketone [28].

6.1. Types of injection

Priego-Capote and Luque de Castro [29] reviewed in 2004 the works published in which DOEI-CE was used. According to them, sample introduction in DOEI-CE can be classified into three types: simultaneous electrokinetic DOEI, sequential electrokinetic DOEI, and sequential hydrodynamic DOEI.

Fig. 3 illustrates the simplest, fastest and earliest [30] DOEI method, which is based on simultaneous electrokinetic injection. This approach can be performed on a commercial CE instrument and is achieved by simply applying voltage while both capillary ends are placed in sample reservoirs. Anions are injected at the cathodic end and cations at the anodic end of the capillary, simultaneously. Several further reports on this approach have appeared for the determination of inorganic anions and cations [28,30,31] pharmaceutical bases and weakly acidic positional isomers [32], inorganic nitrogen species in rainwater [33], organic and pharmaceutical compounds [34], anionic and cationic homologous surfactants [35] and proteins [36].

Sequential electrokinetic injection [34] is a variant carried out in two steps; the first injection is carried out into one end of the capillary and the second into the opposite end (Fig. 3). The advantage of sequential electrokinetic DOEI, compared to simultaneous electrokinetic DOEI, is that it allows optimization of the injected amounts of anions and cations independently, which is useful when different levels of species of interest must be determined.

Hydrodynamic injection again is also preferable for DOEI in order to avoid sampling bias [34]. Since it is impossible to introduce sample hydrodynamically into both ends of the capillary at the same time, it is necessary to perform hydrodynamic injections sequentially (Fig. 3). There are three ways of achieving hydrodynamic DOEI, regardless of whether the hydrodynamic flow is created by lifting the ends of the capillary or by applying pressure or vacuum at the capillary ends. The first method, illustrated in Fig. 3, is to inject larger volumes of sample in the first injection, as the second injection at the opposite end will displace a similar volume of the sample from the other end. This method is most commonly used because it is easy to perform and it is the only approach that has been used in non-automated purpose-made or modular CE systems with manual injection by lifting the ends of the capillary [16,37–42]. It has also been used with commercial systems [43–45]. A second approach to perform hydrodynamic DOEI is to inject a small volume of BGE following the first sample plug. This volume of BGE is expelled out of the capillary when the second injection is performed. Probably due to the inherent complexity, which could lead to operating errors and the introduction of air bubbles in the capillary when done manually, this latter variation has been used only on automated, commercial CE systems [34,46,47,48]. Although the benefits of
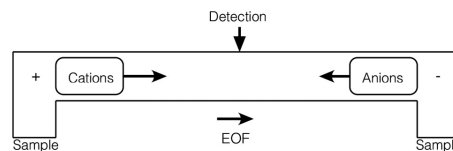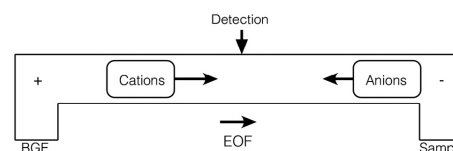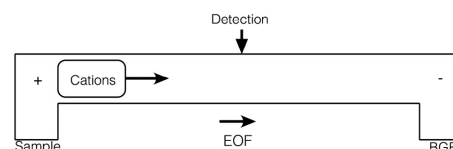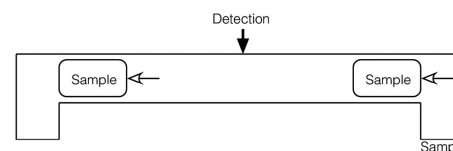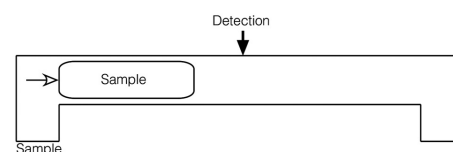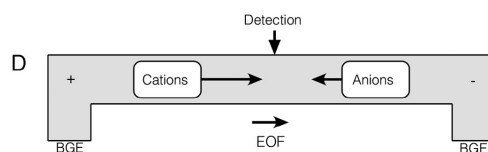
Fig. 3. Different injection modes for dual opposite-end injection (DOEI). The injection of cations and anions occurs at the same time in electrokinetic DOEI while cations are injected first, before anions, for sequential electrokinetic DOEI. For hydrodynamic DOEI, a plug of sample is injected first in one end of the capillary and then a new plug is injected in the opposite end, resulting in the expulsion of a fraction of the first plug. Refer to the text in Section 6 for more options.

introducing a plug of BGE behind the first simple, instead of introducing larger volumes of simple, have not been studied, it has been stated that the plug of BGE prevents the loss of sample when the second sample is injected [34]. The third approach for hydrodynamic DOEI is the brief application of HV after the first injection. In this way, the analytes migrate far enough from the end of the capillary and the expulsion of the sample is avoided during the second injection [49]. This displacement of sample far from the capillary inlet has been termed "preliminary transport" and can also be done hydrodynamically [49].

While hydrodynamic injection is preferable to electrokinetic injection, due to possible sampling bias, electrokinetic injection is easier to implement. It allows the coupling of the technique to flow-injection analysis, which enables automated sequential DOEI injections without the necessity to interrupt the separation voltage. Fig. 4 gives an example, just showing two subsequent injections. The BGE flows around both capillary ends permanently while the HV is on and sample is introduced periodically in the BGE flow. When the sample passes each capillary end, it is introduced into the capillary electrokinetically [47]. This approach is useful for monitoring operations, as demonstrated by Kubáň et al. in the determination of anions and cations in drainage water [50].

6.2. Avoiding co-detection

A point to consider, when using DOEI-CE, is that analytes concurrently move from both ends and might pass the detector at the same time. To avoid co-detection, different approaches have been devised. The detector can be moved along the capillary until a point without co-detection is found. However, this approach can only be taken if the detector is movable, as in purpose-made or modular CE instruments. On commercial systems, this is not easily done, although some authors were successful in modifying commercial instruments for their needs.

Macka et al. [44] designed a miniaturized C⁴D cell, which could be moved along the capillary inside the cartridge of an Agilent CE system. The employment of C⁴D became very popular for DOEI-CE after its introduction. These detectors are normally much smaller and lighter than optical detectors, so they can be moved along the capillary and no optical window is needed. Moreover, BGEs for photometric detection in DOEI-CE are complex and those for indirect UV detection require two chromophores, one cationic and one anionic. Such complications are avoided by using C⁴D.

In another study, the same Agilent cartridge was modified in order to extend the capillary length after the optical detection window. This allowed the detection window to be placed approximately in the middle of the capillary. A different approach to avoid co-detection is to include a preliminary transport of the first injected sample plug. This is useful when detector displacement is not possible. Another strategy is to adjust the EOF to change the apparent mobilities, so that cation and anion peaks do not appear at the same time. Finally, pressure or vacuum can also be used to avoid co-detection. It is also possible to use these means to create small separations between groups of ions or to change their migration order [34].

7. Dual single-end injection capillary electrophoresis

In hydrodynamic DOEI, precision while injecting is crucial, so it is best done using an automated instrument. The only way to perform this injection in non-automated CE systems is by manual siphoning. Nevertheless, almost half the CE systems reported for DOEI were purpose-made and non-automated. The main difficulty lies in implementing an automated injection system at the HV electrode end.
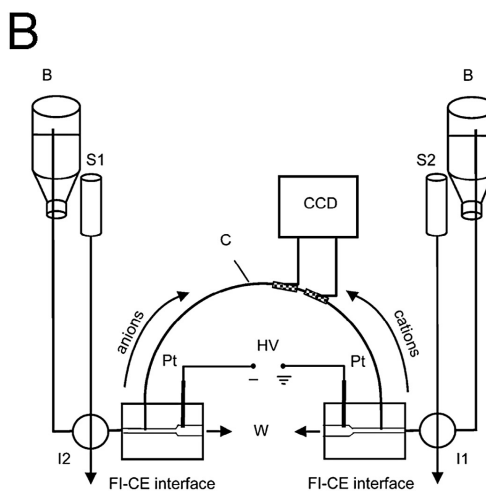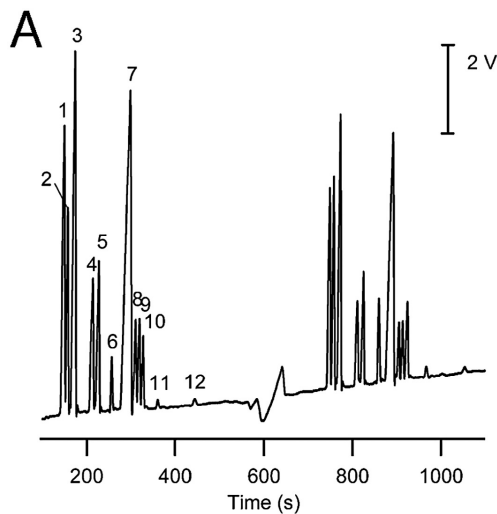

Fig. 4. (A) Simultaneous determination of cations and anions using flow dual opposite-end injection (DOEI). Two consecutive on-site analyses of drainage water samples. (1) Cl⁻, (2) NO₃⁻, (3) SO₄²⁻, (4) NH₄⁺, (5) K⁺, (6) oxalate, (7) Ca²⁺, (8) Na⁺, (9) Mg²⁺, (10) Co²⁺, (11) phosphate, (12) NO₂⁻. (B) Flow-injection capillary electrophoresis used. B, Background electrolyte reservoir; S1 and S2, Sample reservoirs; C, Capillary; I1 and I2, Injection valves; Pt, Electrodes; W, Waste, CCD, Contactless conductivity detector [50]. (Reproduced by permission of The Royal Society of Chemistry).

To overcome this problem, Mai and Hauser [26] conceived a new injection method based on the principle of DOEI, in which only one injector was needed. The approach was called dual single-end injection because both sample plugs were injected from the same end of the capillary (Fig. 5). As the authors stated, this strategy resembles the DOEI approach, but both sample plugs were injected
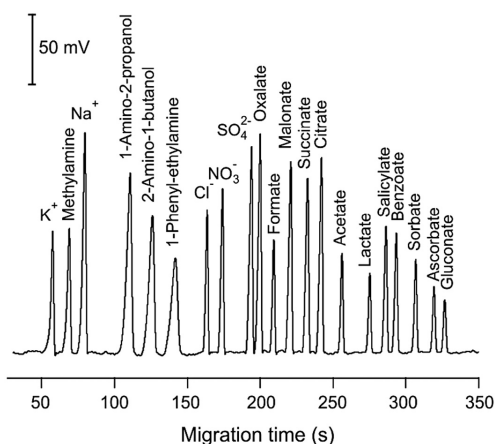
Fig. 5. Concurrent separations of anions and cations with dual single-end injection, single capacitively coupled contactless conductivity detection (C^{4}D) and with pressure-assisted capillary electrophoresis (CE). {Reprinted from [26] with permission from Elsevier).

NO_3^-, Na^+ and K^+ was positioned between detectors 8 and 9, before applying the separation voltage. The outcome was a series of electropherograms, dynamically showing the separation development of both anions and cations [51].

Fig. 6. Dual single-end injection and single injection with sample positioning. For dual single-end injection, the first sample plug is pressure-delivered from the injection end of the capillary close to the opposite end and then a second plug is injected before separation (in grey color). For this approach, a single detector placed between the two injected plugs is needed. Performing a single injection with sample positioning capillary electrophoresis (CE) needs two detectors, placed at each end of the capillary and the sample plug is pressure-delivered between them before separation (in grey color).
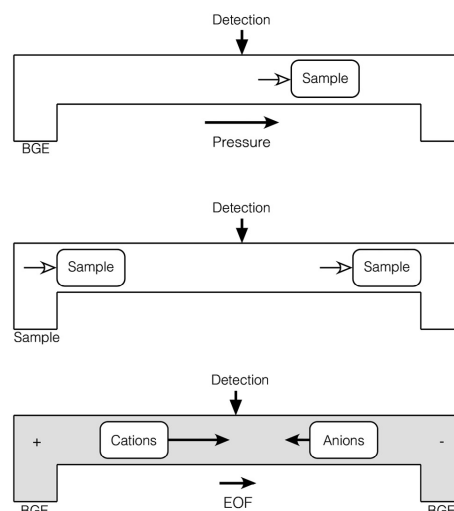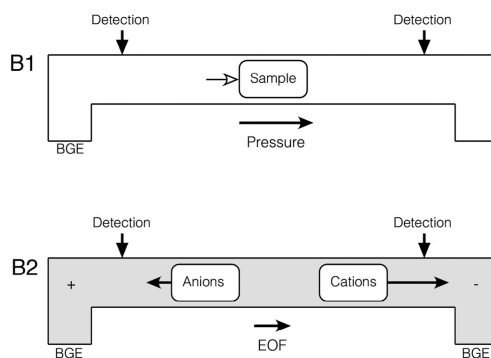
from the same end. In order to place a sample plug at each end of the capillary, the first plug injected is pumped through the capillary until it reaches the opposite end. Then, the second sample plug was injected normally. The first sample plug is pumped almost to the end of the capillary, allowing space downstream to ensure that the second injection will not pump the first plug out. Therefore, a small volume of BGE must remain at this end, to be expelled during the second injection. This is a simpler alternative to DOEI, which is carried out using a purpose-made instrument with narrow capillaries and C^{4}D, but it may also be possible to implement it on a conventional commercial instrument. An example of dual single-end injection CE is shown in Fig. 5.

8. Single injection with positioning of the sample plug

Mai and Hauser [26] also conceived a different approach for the concurrent separation of anions and cations. The strategy was similar to dual single-end injection since the sample plug was also pumped through the capillary. However, in this case, a single sample plug was positioned around the middle of the capillary between two C^{4}D detectors, placed close to the anode and cathode. Single injection with sample positioning was conceived in order to overcome the limitation of assisting pressure for the simultaneous separation of fast-moving anions with cations, which needs large pressures to pump anions toward the cathode, reducing the residence time of the cations in the electric field. With the sample placed between two detectors, when the electric field is established anions move toward one detector and cations toward the other (Fig. 6). Two electropherograms are then obtained, one for cations and another for anions. By using two detectors, the problem of co-detection is eliminated. An example can be seen in Fig. 7. Compared to dual single-end injection, the only instrumental requirement is that two detectors must be placed close to the capillary ends, which is not always the possible for commercial instruments. Single injection with sample delivery CE was recently also used in a purpose built set-up with an array of 16 C^{4}D detectors. A sample plug containing Cl$^-$,

9. Dual-channel capillary electrophoresis

The use of two capillaries for concurrent separation is currently known as dual-channel CE and was first proposed by Bächmann et al. [52] in 1992 for the simultaneous separation of inorganic cations and anions (Fig. 8). In this work, the authors considered both capillaries as single separation channel and they described the injection procedure to be performed in the central part of the capillary, using a single BGE. A modified CE system was used, and injection was carried out via syphoning. Since the capillaries used had the same length, identical volumes were injected. The sample vial was then replaced by a third vial, containing the BGE. The electric field was applied across both capillaries using a single HV supply and the dual separation of ions was recorded by two fluorescence detectors. Dual-channel CE was not reported again until 2013, when Gaudry et al. [53] developed a purpose-made set-up with two capillaries and two C⁴D detectors. The injection ends of the capillaries were both grounded, and the detection ends of the anion and cation separation capillaries were connected to a
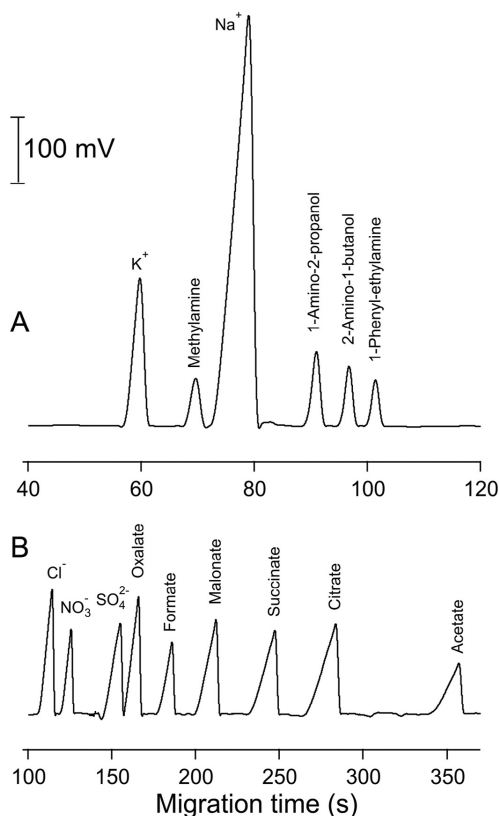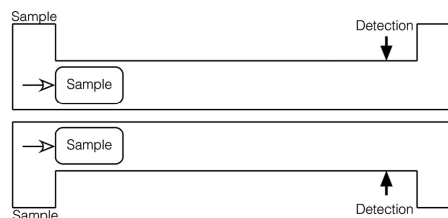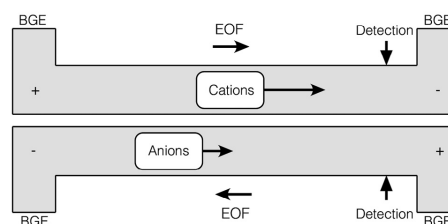

Fig. 8. Dual-channel capillary electrophoresis (CE) with hydrodynamic injection, in which two capillaries and two detectors are needed.

positive and a negative HV supply respectively. Injection was performed electrokinetically into both capillaries with an automatic injector, which was also used to rinse both capillaries with the same BGE. Huang et al. [42] published a new study in the same year in which a purpose-made system was also used for dual-channel CE. The sample was injected hydrodynamically into both capillaries, but different injection methods were applied subsequently for each channel. A flow injector with a manual valve was used for injection for the anion separation capillary while the other capillary was elevated for the injection for the cation separation capillary. In this case also, a single BGE was used for the separation of anions and cations. The authors of this last study used two C⁴D cells, but they were electronically coupled and only a single electropherogram was produced. Pham et al. developed an automated dual-channel CE purpose-made set-up with two C⁴D cells for the determination of cationic NH_4^+ and anionic NO_3^- and NO_2^- in water samples [54]. Two capillaries with two C⁴D cells were used, and were filled with the same buffer. In this case, samples were injected at the same time hydrodynamically with a split injector.

10. Conclusions and future prospects

In this review, we described different approaches for the simultaneous separation of anions and cations in capillary zone electrophoresis. The use of complexing agents, micelles and EOF-driven approaches have the benefit of requiring no special instrument and can be performed on practically any working CE instrument, whether commercial, purpose-made or modular. Their common disadvantage is that they require special chemical conditions, in the form of a specific pH or addition of compounds to the sample and/or to the BGE. These limit the applicability of these approaches to some types of analyte and may have other negative implications, such as sensitivity reduction, and baseline drifts. However, pressure-assisted separations, DOEI, dual single-end injection, single injection

Fig. 7. Simultaneous separation of organic and inorganic cations and anions using a single injection with positioning of the sample plug. {Reprinted from [26] with permission from Elsevier}.

with sample delivery and dual-channel CE often require special instrumentation or instrument modifications. They all rely on mechanical concepts rather than chemical concepts. This is a crucial point, as not all research groups have the technical means to create systems tailored to their needs. Some of these approaches require the use of pressure, which is detrimental to the separation resolution for large inner diameter capillaries (>25 μm).

C^4D detectors are inexpensive and small, compared to most optical detectors, so C^4D allows the use of multiple detectors and shows very little restriction with regard to their position along the capillary, which is important to avoid co-detection in DOEI and dual single-end injection. An important issue is the injection method. We strongly recommend that, if possible, the injection method is automatic, rather than manual. Manual operation of complicated injection schemes is more prone to error and might be difficult to reproduce reliably.

Dual-channel CE may be considered the newest technique for concurrent separation of anions and cations, even though it was first suggested more than two decades ago. The original work of Bächmann et al. [52] with dual-channel CE was considered "experimentally complicated" [37]. However, it is a very promising method, mostly because it only allows altogether different conditions for concurrent separations, such as different capillary lengths, and inner diameters, to optimize each separation independently. However, the systems published to date used a single BGE for both separations, which, as discussed by Gaudry et al. [53], is a limitation. The use of a single BGE for both cations and anions is a compromise, as, for example, different pH values will be optimal for the different classes of ions.

It has been shown that CE instruments with excellent performance can be constructed at relatively low cost [55], so the added complexity of dual-channel systems with individual BGEs is not a significant obstacle. The approach has not yet reached its full potential, and further developments can be expected in this regard.

Acknowledgments

References

[1] O.V. Krokhin, H. Hoshino, O.A. Shpigun, T. Yotsuyanagi, Use of cationic polymers for the simultaneous determination of inorganic anions and metal-4-(2-pyridylazo)resorcinolato chelates in kinetic differentiation-mode capillary electrophoresis, J. Chromatogr. A 776 (1997) 329–336.

[2] S. Pozdniakova, A. Padarauskas, Speciation of metals in different oxidation states by capillary electrophoresis using pre-capillary complexation with complexones, Analyst 123 (1998) 1497–1500.

[3] O.P. Semenova, A.R. Timerbaev, R. Gagstädter, G.K. Bonn, Speciation of chromium ions by capillary zone electrophoresis, J. High Resolut. Chromatogr. 19 (1996) 177–179.

[4] A.R. Timerbaev, O.P. Semenova, W. Buchberger, G.K. Bonn, Speciation studies by capillary electrophoresis – simultaneous determination of chromium(III) and chromium(VI), Fresenius. J. Anal. Chem. 354 (1996) 414–419.

[5] S.J. Chen, M.J. Chen, H.T. Chang, Light-emitting diode-based indirect fluorescence detection for simultaneous determination of anions and cations in capillary electrophoresis, J. Chromatogr. A 1017 (2003) 215–224.

[6] P. Kubáň, P. Kubáň, V. Kubáň, Simultaneous capillary electrophoretic separation of small anions and cations after complexation with ethylenediaminetetraacetic acid, J. Chromatogr. A 836 (1999) 75–80.

[7] T. Soga, G.A. Ross, Simultaneous determination of inorganic anions, organic acids and metal cations by capillary electrophoresis, J. Chromatogr. A 834 (1999) 65–71.

[8] J.A. Wharton, K.R. Stokes, Analysis of nickel–aluminium bronze crevice solution chemistry using capillary electrophoresis, Electrochem. Commun. 9 (2007) 1035–1040.

[9] C. Sarazin, N. Delaunay, A. Varenne, C. Costanza, V. Eudes, P. Gareil, Simultaneous capillary electrophoretic analysis of inorganic anions and cations in post-blast extracts of acid– aluminum mixtures, J. Sep. Sci. 33 (2010) 3177–3183.

[10] Q.P. Wang, Z.L. Chen, G.N. Chena, J.M. Lin, Simultaneous determination of phosphate and calcium in river water samples by capillary zone electrophoresis with UV detection, Int. J. Environ. Anal. Chem. 91 (2011) 255–262.

[11] S.Y. Wei, L.F. Wang, Y.H. Yang, H.H. Yeh, Y.C. Chen, S.H. Chen, Sample stacking by field-amplified sample injection and sweeping for simultaneous analysis of acidic and basic components in clinic application, Electrophoresis 33 (2012) 1571–1581.

[12] J.W. Jorgenson, K.D. Lukacs, Zone electrophoresis in open-tubular glass capillaries, Anal. Chem. 53 (1981) 1298–1302.

[13] S.A. Shamsi, N.D. Danielson, Individual and simultaneous class separations of cationic and anionic surfactants using capillary electrophoresis with indirect photometric detection, Anal. Chem. 67 (1995) 4210–4216.

[14] I. Haumann, J. Boden, A. Mainka, U. Jegle, Simultaneous determination of inorganic anions and cations by capillary electrophoresis with indirect UV detection, J. Chromatogr. A 895 (2000) 269–277.

[15] F. Foret, S. Fanali, L. Ossicini, P. Boček, Indirect photometric detection in capillary zone electrophoresis, J. Chromatogr. A 470 (1989) 299–308.

[16] P.A. Gallagher, N.D. Danielson, Capillary electrophoresis of cationic and anionic surfactants with indirect conductivity detection, J. Chromatogr. A 781 (1997) 533–540.

[17] C. Raguénès, X. Xiong, H.K. Lee, S.F.Y. Li, Single UV-absorbing background electrolyte for simultaneous detection of cations and anions in capillary electrophoresis, J. Liq. Chromatogr. Relat. Technol. 22 (1999) 2353–2365.

[18] R.R. Cunha, D.T. Gimenes, R.A.A. Munoz, C.L. do Lago, E.M. Richter, Simultaneous determination of diclofenac and its common counter-ions in less than 1 minute using capillary electrophoresis with contactless conductivity detection, Electrophoresis 34 (2013) 1423–1428.

[19] S. Schäffer, P. Gared, C. Dezael, D. Richard, Direct determination of iron(II), iron(III) and total iron as UV-absorbing complexes by capillary electrophoresis, J. Chromatogr. A 740 (1996) 151–157.

[20] S. Pozdniakova, A. Padarauskas, G. Schwedt, Simultaneous determination of iron(II) and iron(III) in water by capillary electrophoresis, Anal. Chim. Acta 351 (1997) 41–48.

[21] C. Johns, W. Yang, M. Macka, P.R. Haddad, Simultaneous separation of anions and cations by capillary electrophoresis with high magnitude, reversed electroosmotic flow, J. Chromatogr. A 1050 (2004) 217–222.

[22] X. Xiong, S.F.Y. Li, Dual UV-absorbing background electrolytes for simultaneous separation and detection of small cations and anions by capillary zone electrophoresis, Electrophoresis 19 (1998) 2243–2251.

[23] X. Xiong, S.F.Y. Li, Selection and optimization of background electrolytes for simultaneous detection of small cations and organic acids by capillary electrophoresis with indirect photometry, J. Chromatogr. A 822 (1998) 125–136.

[24] T.D. Mai, P.C. Hauser, Pressure-assisted capillary electrophoresis for cation separations using a sequential injection analysis manifold and contactless conductivity detection, Talanta 84 (2011) 1228–1233.

[25] T.D. Mai, P.C. Hauser, Anion separations with pressure-assisted capillary electrophoresis using a sequential injection analysis manifold and contactless conductivity detection, Electrophoresis 32 (2011) 3000–3007.

[26] T.D. Mai, P.C. Hauser, Simultaneous separations of cations and anions by capillary electrophoresis with contactless conductivity detection employing a sequential injection analysis manifold for flexible manipulation of sample plugs, J. Chromatogr. A 1267 (2012) 266–272.

[27] P.M. Flanigan, D. Ross, J.G. Shackman, Determination of inorganic ions in mineral water by gradient elution moving boundary electrophoresis, Electrophoresis 31 (2010) 3466–3474.

[28] J. Tanyanyiwa, S. Leuthardt, P.C. Hauser, Electrophoretic separations with polyether ether ketone capillaries and capacitively coupled contactless conductivity detection, J. Chromatogr. A 978 (2002) 205–211.

[29] F. Priego-Capote, M.D. Luque de Castro, Dual injection capillary electrophoresis: foundations and applications, Electrophoresis 25 (2004) 4074–4085.

[30] A. Padarauskas, V. Olšauskaitė, G. Schwedt, Simultaneous separation of inorganic anions and cations by capillary zone electrophoresis, J. Chromatogr. A 800 (1998) 369–375.

[31] A. Padarauskas, V. Olšauskaitė, V. Paliulionytė, Simultaneous determination of inorganic anions and cations in waters by capillary electrophoresis, J. Chromatogr. A 829 (1998) 359–365.

[32] D. Durkin, J.P. Foley, Dual-opposite injection electrokinetic chromatography for the unbiased, simultaneous separation of cationic and anionic compounds, Electrophoresis 21 (2000) 1997–2009.

[33] A. Padarauskas, V. Paliulionyte, B. Pranaityte, Single-run capillary electrophoretic determination of inorganic nitrogen species in rainwater, Anal. Chem. 73 (2001) 267–271.

[34] M.X. Zhou, J.P. Foley, Dual opposite injection electrokinetic chromatography: nonionic microemulsion pseudostationary phase and novel approach to electrokinetic sampling bias, Electrophoresis 25 (2004) 653–663.

[35] F. Priego-Capote, M.D. Luque de Castro, Dual-opposite injection capillary electrophoresis for the determination of anionic and cationic homologous surfactants in a single run, Electrophoresis 26 (2005) 2283–2292.

[36] L. Xu, X.Y. Dong, Y. Sun, Novel poly(vinyl alcohol)-based column coating for capillary electrophoresis of proteins, Biochem. Eng. J. 53 (2010) 137–142.

[37] P. Kuban, B. Karlberg, Simultaneous determination of small cations and anions by capillary electrophoresis, Anal. Chem. 70 (1998) 360–365.

[38] P. Kubáň, P. Kubáň, V. Kubáň, Simultaneous determination of inorganic and organic anions, alkali, alkaline earth and transition metal cations by capillary electrophoresis with contactless conductometric detection, Electrophoresis 23 (2002) 3725–3734.

[39] P. Kubáň, B. Karlberg, P. Kubáň, V. Kubáň, Application of a contactless conductometric detector for the simultaneous determination of small anions and cations by capillary electrophoresis with dual-opposite end injection, J. Chromatogr. A 964 (2002) 227–241.

[40] P. Kubáň, P. Kubáň, V. Kubáň, Speciation of chromium (III) and chromium (VI) by capillary electrophoresis with contactless conductometric detection and dual opposite end injection, Electrophoresis 24 (2003) 1397–1403.

[41] P. Kubáň, E.G. Kobrin, M. Kaljurand, Capillary electrophoresis – a new tool for ionic analysis of exhaled breath condensate, J. Chromatogr. A 1267 (2012) 239–245.

[42] T. Huang, Q. Kang, X. Zhu, Z. Zhang, D. Shen, Determination of water-soluble ions in PM2.5 using capillary electrophoresis with resonant contactless conductometric detectors in a differential model, Anal. Methods 5 (2013) 6839–6847.

[43] V. Unterholzner, M. Macka, P.R. Haddad, A. Zemann, Simultaneous separation of inorganic anions and cations using capillary electrophoresis with a movable contactless conductivity detector, Analyst 127 (2002) 715–718.

[44] M. Macka, J. Hutchinson, A. Zemann, Z. Shusheng, P.R. Haddad, Miniaturized movable contactless conductivity detection cell for capillary electrophoresis, Electrophoresis 24 (2003) 2144–2149.

[45] K.G. Hopper, H. LeClair, B.R. McCord, A novel method for analysis of explosives residue by simultaneous detection of anions and cations via capillary zone electrophoresis, Talanta 67 (2005) 304–312.

[46] R. Nehmé, A. Lascaux, R. Delépée, B. Claude, P. Morin, Capillary electrophoresis procedure for the simultaneous analysis and stoichiometry determination of a drug and its counter-ion by using dual-opposite end injection and contactless conductivity detection: application to labetalol hydrochloride, Anal. Chim. Acta 663 (2010) 190–197.

[47] P. Kubáň, P. Kubáň, P.C. Hauser, V. Kubáň, A flow injection-capillary electrophoresis system with high-voltage contactless conductivity detection for automated dual opposite end injection, Electrophoresis 25 (2004) 35–42.

[48] C. Lopez, R. Nehme, B. Claude, P.H. Morin, J.P. Max, R. Pena, et al., A convenient approach to simultaneous analysis of a pharmaceutical drug and its counter-ion by CE using dual-opposite end injection and contactless conductivity detection, Chromatographia 75 (2012) 25–32.

[49] B.S. Weekley, J.P. Foley, Dual-opposite-injection CZE: theoretical aspects and application to organic and pharmaceutical compounds, Electrophoresis 28 (2007) 697–711.

[50] P. Kubáň, M. Reinhardt, B. Müller, P.C. Hauser, On-site simultaneous determination of anions and cations in drainage water using a flow injection-capillary electrophoresis system with contactless conductivity detection, J. Environ. Monit. 6 (2004) 169–174.

[51] M. Stojkovic, I.J. Koenka, W. Thormann, P.C. Hauser, Contactless conductivity detector array for capillary electrophoresis, Electrophoresis 35 (2014) 482–486.

[52] K. Bächmann, I. Haumann, T. Groh, Simultaneous determination of inorganic cations and anions in capillary zone electrophoresis (CZE) with indirect fluorescence detection, Fresenius. J. Anal. Chem. 343 (1992) 901–902.

[53] A.J. Gaudry, R.M. Guijt, M. Macka, J.P. Hutchinson, C. Johns, E.F. Hilder, et al., On-line simultaneous and rapid separation of anions and cations from a single sample using dual-capillary sequential injection-capillary electrophoresis, Anal. Chim. Acta 781 (2013) 80–87.

[54] T.T.T. Pham, T.D. Mai, T.D. Nguyen, J. Sáiz, H.V. Pham, P.C. Hauser, Automated dual capillary electrophoresis system with hydrodynamic injection for the concurrent determination of cations and anions, Anal. Chim. Acta 841 (2014) 77–83, doi:10.1016/j.aca.2014.05.046.

[55] T.D. Mai, T.T.T. Pham, H.V. Pham, J. Sáiz, C. García-Ruiz, P.C. Hauser, Portable capillary electrophoresis instrument with automated injector and contactless conductivity detection, Anal. Chem. 85 (2013) 2333–2339.
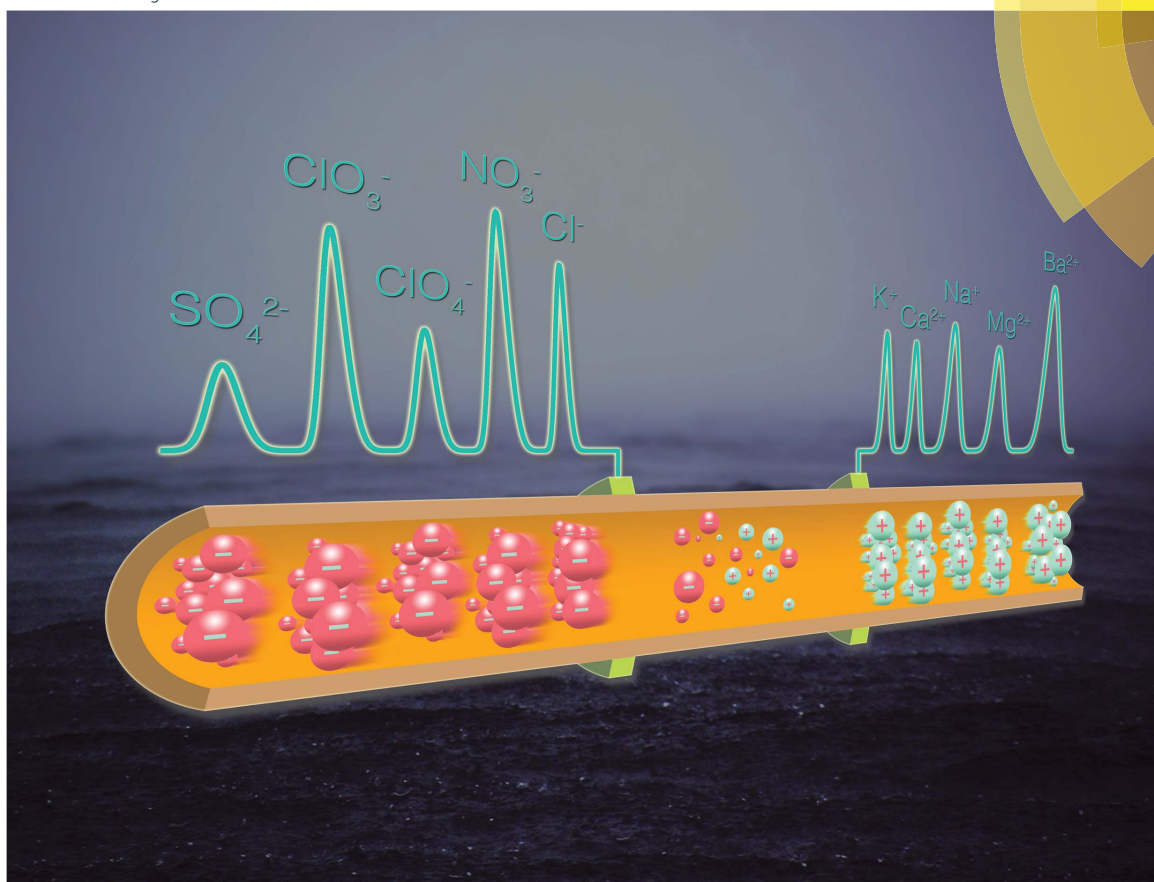
Publication #9:

Simultaneous separation of cations and anions in capillary electrophoresis - Recent applications

Analytical Methods (2016), 8, 1452–1456

Analytical Methods

ROYAL SOCIETY
OF CHEMISTRY

MINIREVIEW
Jorge Sáiz *et al.*
Simultaneous separation of cations and anions in capillary
electrophoresis – recent applications

175 YEARS

-119-

MINIREVIEW

Simultaneous separation of cations and anions in capillary electrophoresis – recent applications

Israel Joel Koenka,[a] Thanh Duc Mai,[ab] Peter C. Hauser[a] and Jorge Sáiz†[*a]

In this review, the simultaneous determination of anionic and cationic species in capillary electrophoresis for different applications such as water quality analysis, medical diagnosis, pharmaceutical analysis, forensic science and food control is discussed. The simplicity and electronic nature of capillary electrophoresis allow the easy modification of custom made set-ups in order to realise various techniques for the simultaneous separation of different ionic analytes. As a continuation of our earlier review, in which the details of the working principles were described, this report is focussed on the applications of the simultaneous electrokinetic separation methods reported during the last five years (2011–2015).

Introduction

Capillary electrophoresis is an analytical technique for the separation and detection of ionic species. Although traditionally only one type of charged species (positive or negative ions) is determined in a single run, simultaneous determination of both cations and anions is often desirable, saving time and cost. The simultaneous determination of anions and cations is useful in many types of applications, as it is common that not all target ions are of the same type. For example, in environmental monitoring applications, potentially hazardous species may be cationic as well as anionic.

As discussed in a recent review,[1] the different approaches to accomplish simultaneous separation of cations and anions can be divided into "chemical approaches" – in which ion mobilities are modified by using some chemical additives – and "instrumental approaches" – which depend on some special instrumental setups. One of the chemical ways to modify ion mobilities is to use complexing agents that can form anionic complexes with transition metal cations, allowing their detection alongside native anions in the sample.[2] Another way is to use cationic micelles to sweep anionic compounds towards the detector end of the capillary.[3] In counter electroosmotic flow (EOF) mode CE, an increase in the pH of the background electrolyte is created, which increases the magnitude of the EOF to such an extent that the migration direction of slow anions is reversed and they can be detected alongside analytes of opposite charge.[4]

[a]Department of Chemistry, University of Basel, Spitalstrasse 51, 4056 Basel, Switzerland. E-mail: jorge.saizg@gmail.com

[b]Centre for Environmental Technology and Sustainable Development (CETASD), Hanoi University of Science, Nguyen Trai Street 334, Hanoi, Viet Nam

† Current address: Department of Instrumental Analysis and Environmental Chemistry, Institute of General Organic Chemistry (CSIC), Juan de la Cierva 3, Madrid 28006, Spain.

It is also possible to achieve this instrumentally by applying an external pressure during the CE separation.[5] Two more common instrumental approaches are dual opposite end injection (DOEI) and dual single end injection (DSEI), in both of which two sample plugs are placed in the two opposite ends of the capillary prior to the separation and a single detector is placed somewhere between them. In the former method[6] each plug is injected from its respective side, and in the latter method[7] both of the plugs are injected from one side, and one of them is hydrodynamically transported to the other side. Alternatively, it is also possible to employ two detectors which are placed at both ends of the capillary and hydrodynamically transport a single sample plug to the centre of the capillary, so that when the HV is turned on anions and cations are simultaneously determined at different detectors.[7] Finally, another approach employing two detectors is dual channel CE or dual CE (DCE). In this approach, which was first reported in 1992,[8] the CE instrument employs two separate capillaries and two detectors for cations and anions, respectively.

More details on the principles of the different approaches can be found in our previous review.[1] In this article, the different analytical questions that were solved by the simultaneous determination of cations and anions in CE, covering the period from 2011 to 2015, are reviewed. Our aim is to provide a guide reviewing the latest applications where simultaneous separation of differently charged analytes was used. These applications are wide in nature and cover such diverse fields as environmental, medical, pharmaceutical, and forensic analyses.

CE applications with simultaneous separation of cations and anions

Water quality analysis

Many human activities, such as agriculture and industry, affect the quality of surface and ground water. For this reason, the

analysis of water is highly important and a variety of techniques are currently used to study the composition and characteristics of the water.

In recent years, research groups have also focused their efforts on the analysis of water by the simultaneous separation of certain anions and cations using CE. Wang et al.[9] developed a method for the analysis of river water with simultaneous UV determination of calcium and some anions, such as phosphate, which is abundant in fertilisers and directly impacts water quality when discharged to rivers via surface run off. The authors of this study used 2,6-pyridinedicarboxylic acid (PDCA) as a complexing agent for creating an anionic metal chelate with calcium $[Ca(PDCA)_2]^{2-}$, which can be separated together with the anions in the sample in a single capillary without modification of a standard commercial instrument. Moreover, since PDCA can be used for on-column complexation of calcium, there is no need for a specific sample pre-treatment. Neaga et al.[10] made use of the DOEI approach for the analysis of ground water from 51 domestic wells. The capillary was coated with polyvinyl alcohol to precisely control the EOF and avoid the possible interaction of analytes with the capillary wall. They were able to separate 10 inorganic anions and cations, including nitrates and nitrites, which are of great concern among the inorganic pollutants because they can induce methemoglobinemia in infants and may be causing different types of cancers on chronic exposure. Contactless conductivity detection (C^4D) was used due to the lack of absorbance of some analytes. Mai and Hauser[7] also studied the simultaneous separation of major inorganic cations and anions in tap water. In this case, the authors used dual single-end injection CE in one capillary with two C^4D-cells to obtain separate electropherograms for negatively and positively charged species (Fig. 1). Gaudry et al.[11] designed a new system for the simultaneous determination of cations and anions using DCE. The construction of customised instruments allows different features that cannot be obtained on conventional equipment. For example, in this case, the authors were able to automatically monitor tap water over a period of 48 h, since the system was able to collect and analyse the sample from a water flow unattended. The authors of this work also analysed other environmental samples, including river and lake water samples, determining up to 23 cations and anions. A final application reported in the same work was the analysis of water samples from a zinc processing plant, where samples were taken from various stages of production. Pham et al.[12] also used a custom designed system with C^4D for the automated monitoring of water during the biological removal of ammonium from contaminated groundwater in a sequencing batch reactor, where NO_3 and NO_2 are formed as intermediate products. The authors could experimentally follow the decrease of the ammonium concentration and the formation of the oxidation products nitrite and then nitrate.

The simultaneous separation of cations and anions in natural water samples by CE has frequently been reported in the last few years. One reason is that these samples do not need special pre-treatment before injection in CE and, when needed,
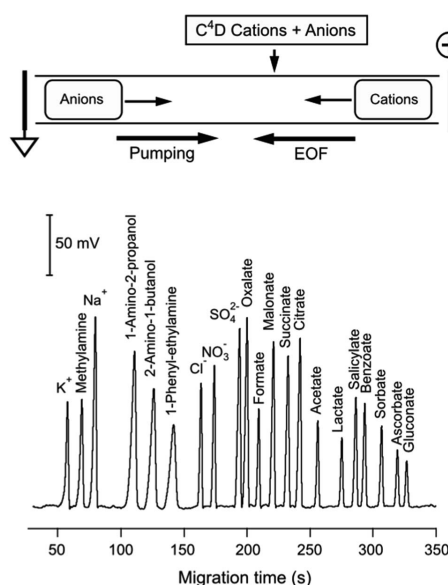

Fig. 1 Simultaneous separation of anions and cations with dual single-end injection, single capacitively coupled contactless conductivity detection (C^4D) and with pressure-assisted capillary electrophoresis (CE) {reprinted from ref. 7 with permission from Elsevier}.

this usually consists of a simple dilution or filtration. Moreover, CE is especially useful for the analysis of aqueous samples.

Medical diagnosis

CE may also be used in clinical laboratories for diagnostic purposes. The simultaneous separation and determination of cations and anions by CE has been proven to be suitable in tests for medical diagnosis of certain diseases. Kubáň et al.[13] conceived a small device able to collect 100–200 µL of exhaled breath condensate in less than 2 min. Samples obtained in this non-invasive way were analysed for their ionic content by DOEI-CE with C^4D. The authors determined up to 15 inorganic cations and anions and organic acids in less than 3 min and observed changes in the concentration of nitrites and other ions in a person diagnosed with mild chronic obstructive pulmonary disease and a person suffering from acute cold and serious cough. Moreover, as the authors mentioned, the method could also be useful for monitoring fast metabolic processes such as lactate build-up following an exhaustive cycling exercise and subsequent elimination (Fig. 2). Kubáň et al.[14] recently developed an approach for non-invasive collection of sweat samples with a moisturised cotton swab and their analysis by DOEI-CE with C^4D. The samples were analysed for the quantification of chloride, sodium and potassium, whose concentrations are affected in individuals suffering from cystic fibrosis. The
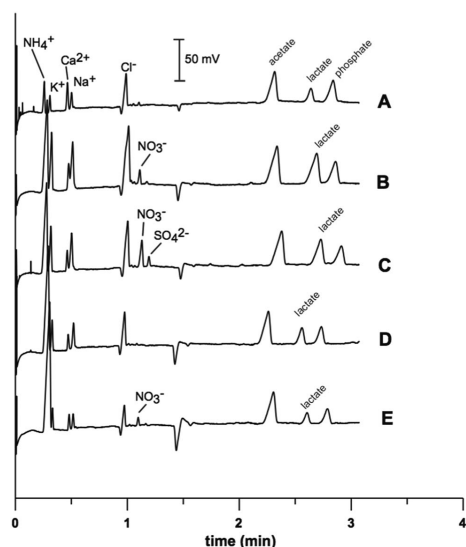
-121-

Fig. 2 Electropherograms of lactate screening together with other cations and anions in exhaled breath condensate before (A) and after 4 (B), 10 (C), 25 (D) and 60 (E) minutes of exhaustive cycling exercise (B) {reprinted from ref. 14 with permission from Elsevier}.

method was able to indicate differences between healthy individuals and cystic fibrosis patients. The results were evaluated using principal component analysis (PCA) in order to render the diagnosis more accurate, *i.e.* to reduce the number of false positive or negative findings.

Because CE can easily be miniaturised and packed into a compact, low power format, and produced as an inexpensive instrument[15] it may be used as a powerful point-of-care screening tool to be easily used by the user at home. The references reviewed in this section demonstrate this possibility. Healthy people and patients with different diseases are already demanding such tools for their everyday lives. The development of smaller and less expensive instruments and new methods which offer information about the health status of the user in a short time may be of high importance in the near future.

Pharmaceutical applications

Approximately, 50% of the active pharmaceutical ingredients of drugs are administered as salts. Although chloride and potassium are the preferred counter-ions for the salt formation, different counter-ions are sometimes chosen depending on the administration path of the drug.[16] The availability of numerous counter-ions makes the salt selection process complex and, for a basic drug, a wide variety of inorganic and organic anions can be chosen. The selection of the correct salt determines the physicochemical stability and bioavailability, which is why it is important to confirm the composition of pharmaceutical salts
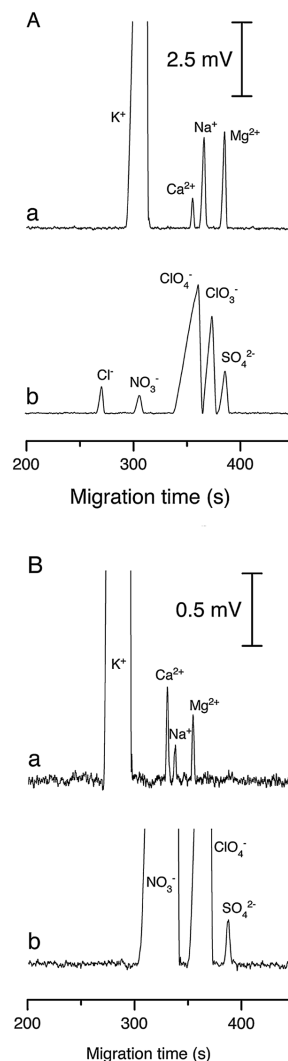

Fig. 3 Dual electropherograms for the analysis of a firecracker. Cations (A-a) and anions (A-b) were determined in the pyrotechnic charge of the firecracker and, similarly, cations (B-a) and anions (B-b) were also determined in the fuse of the same firecracker {reprinted from ref. 19 with permission from Elsevier}.

by analytical methods.[17] As both the cation and the anion in the salt have to be analysed, the analysis of a drug by conventional CE methods would require two different analyses, one for each ionic species. Therefore, in recent years, new methodologies for

the simultaneous determination of drugs and their counter-ions have been developed. Lopez et al.[17] developed a method using DOEI-CE with C[4]D for the analysis of five drugs (chlorpheniramine, metoprolol, clomiphene, catharanthine and vinorelbine) and their respective counter-ions (maleate, tartrate, citrate, sulphate and ditartrate). Using this method, the authors were able to analyse each pharmaceutical composition in less than 10 min. Cunha et al.[16] focussed their research on the simultaneous determination of diclofenac and its common counter-ions (potassium, sodium, and diethylammonium). In this case, the authors chose an EOF of high intensity to perform counter-EOF mode CE with C[4]D using short capillaries for short analyses (less than 1 min). Using this method, it was possible to provide information about the nature of the salt, to study the presence of impurities and to monitor the degradation of active pharmaceutical ingredients after exposure to solar radiation.

These studies show the applicability of the different approaches for the simultaneous separation of drugs and their counter-ions in the quality control of pharmaceutical formulations. The methods have the potential for use in the quality control of pharmaceutical formulation batches before release.

Forensic applications

The simultaneous determination of cations and anions by CE has also been applied to the analysis of forensic samples. In particular, the study of explosives has recently attracted the interest of scientists. In these cases, the aim is to identify the nature of the explosive device from the results of the analysis of residues. Improvised explosive devices (IEDs) are usually made of inorganic salts containing perchlorate, chlorate, or nitrate, which can be identified by CE. Certain organic explosives can also leave significant traces of inorganic ions which may aid in their identification.[18] Kobrin et al.[18] analysed different kinds of post-blast residues on different matrices, such as sand, a metal plate and concrete. Organic explosives and inorganic explosives, including IEDs, were detonated and the residues were sampled and analysed by DOEI-CE with C[4]D in less than 4 min. After PCA analysis the authors were able to identify the type of each detonated explosive.

Fireworks are also suitable for this type of analysis since they are mostly composed of inorganic salts which are soluble in water, and the analysis allows proving if the device meets the manufacturing regulations. Sáiz et al.[19] studied the cationic and anionic compositions of several consumer fireworks by DCE with two C[4]D-cells, providing new information about the composition of the charges and fuses of these explosives devices, and exposing some inaccuracies in the declarations of the compositions given by the manufacturers (Fig. 3).

In both cases, the systems employed were inexpensive, purpose-made, portable instruments, being able to simultaneously separate cations and anions. This highlights the applicability of portable instrumentation for field analysis, where rapid results are needed.

Other applications

Apart from the analysis of water, other environmental applications have attracted the interest of researchers. Huang et al.[20]

analysed airborne particulate matter (PM), which is directly related to mortality and morbidity. The authors of this work studied fine particles with diameters smaller than 2.5 μm, which reach the alveolar region acting as carriers of toxic species. Using the DOEI-CE approach in a system with two C[4]D-cells, the authors were able to determine ten water-soluble ions in PM, which can be carried into the respiratory system. In the same article, the authors repeated the same application using a system conceived for DCE, with two C[4]D-cells, in order to reduce the superposition of peaks.

The simultaneous determination of anions and cations was also covered in the work of Stojkovic et al.[21] in which the authors placed a sample plug of NaCl and KNO_3 in the middle of a capillary, fitted with an array of 16 C[4]D-cells. The authors demonstrated the simultaneous separation of cations and anions while they studied the evolution of peaks originating from the sample plug, offering such a set-up as a novel way for studying the dynamics of electrophoretic separation.

Food quality control and the detection of adulteration in food are of high concern in certain countries. Food and infant formula have been adulterated with melamine with the aim of increasing the apparent protein content. Long-term exposure to melamine and its by-products (ammeline, ammelide and cyanuric acid) can reduce fertility, produce kidney stones and renal failure, and result in fetal toxicity. For this reason Kohler et al.[22] developed a method for the simultaneous determination of melamine, ammeline, ammelide and cyanuric acid, being able to determine the cationic and anionic species using a high EOF in CE with mass spectrometric detection. The method was successfully applied to the analysis of melamine-contaminated powdered milk.

Ito and Okada[23] developed a novel and simple analyte preconcentrating method in which only the freezing of the sample is needed. When an aqueous sample is frozen, solutes are expelled from the ice core while the remaining liquid becomes more concentrated. This makes this pre-concentrating technique especially suitable for the analysis by CE, as it is possible to analyse volume-limited samples. The authors were able to simultaneously separate anions and cations using a high EOF, while a maximum enrichment factor of 1000 was achieved by simple freezing of samples.

Finally, Santos et al.[24] developed a new method for the simultaneous determination of cationic, anionic and neutral alcohols by CE. The method consists of coupling electrochemical derivatization with CE-C[4]D, employing a strong EOF. The alcohols were electrochemically oxidised to carboxylic acids which then can be separated together with other anions. The use of a strong EOF permitted to reverse the mobilities of these anions and simultaneously separate them with cations. The method was successfully applied to the analysis of an antiseptic mouthwash sample in which cations (Na^+), anions (benzoate and saccharinate) and neutral alcohols (in acidic form after derivatization) such as ethanol and *n*-pentanol were all determined by using a single detector.

Conclusions

Different applications of simultaneous separation of anionic and cationic species have been reported for capillary

electrophoresis in the last few years. In many cases customised instrumental set-ups had to be developed and employed for these purposes as the conventional commercial instruments are not always suitable. However, due to the relative simplicity of CE this is not a significant complication and fewer compromises have to be made when specially developed systems can be employed. This is particularly true for dual capillary instruments which are still not overly complex, and indeed an increasing number of applications have been observed for DCE. C^4D was the detection technique of choice in most of the cases. This is due to its suitability for inorganic species, and its relatively low cost and small size also allows the use of multiple detectors. The breadth of the reported applications, including among others, pharmaceutical applications, food analysis and forensic tests, indicates the great but largely untapped potential of simultaneous analysis by CE.

References

1 J. Sáiz, I. J. Koenka, T. D. Mai, P. C. Hauser and C. Garcia-Ruiz, *TrAC, Trends Anal. Chem.*, 2014, **62**, 162–172.

2 O. V. Krokhin, H. Hoshino, O. A. Shpigun and T. Yotsuyanagi, *J. Chromatogr. A*, 1997, **776**, 329–336.

3 S.-Y. Wei, L.-F. Wang, Y.-H. Yang, H.-H. Yeh, Y.-C. Chen and S.-H. Chen, *Electrophoresis*, 2012, **33**, 1571–1581.

4 J. W. Jorgenson and K. D. Lukacs, *Clin. Chem.*, 1981, **27**, 1551–1553.

5 I. Haumann, J. Boden, A. Mainka and U. Jegle, *J. Chromatogr. A*, 2000, **895**, 269–277.

6 A. Padarauskas, V. Olsauskaite and G. Schwedt, *J. Chromatogr. A*, 1998, **800**, 369–375.

7 M. Thanh Duc and P. C. Hauser, *J. Chromatogr. A*, 2012, **1267**, 266–272.

8 K. Bächmann, I. Haumann and T. Groh, *Fresenius' J. Anal. Chem.*, 1992, **343**, 901–902.

9 Q.-P. Wang, Z.-L. Chen, G.-N. Chen and J.-M. Lin, *Int. J. Environ. Anal. Chem.*, 2011, **91**, 255–262.

10 I.-O. Neaga, B. C. Iacob and E. Bodoki, *J. Liq. Chromatogr. Relat. Technol.*, 2014, **37**, 2072–2090.

11 A. J. Gaudry, R. M. Guijt, M. Macka, J. P. Hutchinson, C. Johns, E. F. Hilder, G. W. Dicinoski, P. N. Nesterenko, P. R. Haddad and M. C. Breadmore, *Anal. Chim. Acta*, 2013, **781**, 80–87.

12 P. Thi Thanh Thuy, M. Thanh Duc, N. Thanh Dam, J. Sáiz, P. Hung Viet and P. C. Hauser, *Anal. Chim. Acta*, 2014, **841**, 77–83.

13 P. Kubáň, E.-G. Kobrin and M. Kaljurand, *J. Chromatogr. A*, 2012, **1267**, 239–245.

14 P. Kubáň, M. Greguš, E. Pokojová, J. Skricková and F. Foret, *J. Chromatogr. A*, 2014, **1358**, 293–298.

15 T. D. Mai, T. T. T. Pham, H. V. Pham, J. Sáiz, C. G. Ruiz and P. C. Hauser, *Anal. Chem.*, 2013, **85**, 2333–2339.

16 R. R. Cunha, D. T. Gimenes, R. A. A. Munoz, C. L. do Lago and E. M. Richter, *Electrophoresis*, 2013, **34**, 1423–1428.

17 C. Lopez, R. Nehme, B. Claude, P. Morin, J. P. Max, R. Pena, M. Pelissou and J. P. Ribet, *Chromatographia*, 2012, **75**, 25–32.

18 E. G. Kobrin, H. Lees, M. Fomitšenko, P. Kubáň and M. Kaljurand, *Electrophoresis*, 2014, **35**, 1165–1172.

19 J. Sáiz, M. T. Duc, I. J. Koenka, C. Martin-Alberca, P. C. Hauser and C. Garcia-Ruiz, *J. Chromatogr. A*, 2014, **1372**, 245–252.

20 T. Huang, Q. Kang, X. Zhu, Z. Zhang and D. Shen, *Anal. Methods*, 2013, **5**, 6839–6847.

21 M. Stojkovic, I. J. Koenka, W. Thormann and P. C. Hauser, *Electrophoresis*, 2014, **35**, 482–486.

22 I. Kohler, E. Cognard, I. Marchi, D. Ortelli, P. Edder, J.-L. Veuthey, S. Rudaz and J. Schappler, *Chimia*, 2011, **65**, 389–395.

23 K. Ito and T. Okada, *Anal. Methods*, 2013, **5**, 5912–5917.

24 M. S. Ferreira Santos, F. S. Lopes and I. G. Rolf Gutz, *Electrophoresis*, 2014, **35**, 864–869.

Publication #10:

Background conductivity independent counter flow pre-concentration method for capillary electrophoresis

Published online in Electrophoresis (2017)

Short Communication

Background conductivity independent counter flow pre-concentration method for capillary electrophoresis

Israel Joel Koenka[1], Peter C. Hauser[1,*]

[1]*Department of Chemistry, University of Basel, Spitalstrasse 51, 4056 Basel, Switzerland.*

*Corresponding author.

E-mail address: Peter.Hauser@unibas.ch (P. C. Hauser)

Phone: ++41 61 267 10 03; Fax: ++41 61 267 10 13

Abstract

A pre-concentration method for anions is presented, which relies on a trap created by applying an electric field against a hydrodynamic flow of the sample. The trapping zone is created in front of a cation exchange membrane which allows the isolation of the electrode and thus prevents any interference by electrolysis products. Pre-concentration factors of up to 20 were demonstrated for nitrate and formate as model analyte ions and were linearly related to the sample volume passed through the trap. A discrimination between the ions was found possible by adjustment of the

hydrodynamic flow velocity. The method was also found to be suitable for the preconcentration of an anion (nitrate at 100 µM) in presence of a second anion at a very high concentration (50 mM formate). The detection limits for the four anions chloride, nitrate, perchlorate and formate could be lowered from 4, 4.3, 4.2 and 7.2 µM obtained without trapping respectively to 127, 142, 139 and 451 nM with trapping.

In comparison to chromatography, capillary electrophoresis has the advantages of relative simplicity and a low demand for consumables. This allows its implementation as low cost and portable systems (see for example [1, 2]). A hindrance to wider acceptance are the relatively high limits of detection, which for optical detectors are due to the short available pathlengths. For contactless conductivity detection (C^4D) these also seldom are lower than 1 µM, due to the presence of a background conductivity. For this reason there has been a strong interest in the development of analyte pre-concentration methods. An overview can be found in a recent review [3] and in a systematic guide [4] by Breadmore and coworkers. For capillary electrophoresis so-called stacking methods have been developed. These rely on the local creation of an electric field gradient in the sample zone, which leads to a faster movement of the ions causing them to pre-concentrate, *i.e.* to stack, at the zone boundary. However, with the possible exception of transient isotachophoresis, this is only possible for samples of low conductivity [4]. An alternative method, which is subjected less to this limitation, is counter-flow gradient electrofocusing. This makes use of a hydrodynamic flow in the direction opposite to the electrokinetic movement of the ions. By creating a gradient, or a step, in the electric field, a trapping zone is established as the ions experience forces driving them to the same area from either side. The topic has been reviewed by Shackman and Ross in 2007 [5] and the more recent developments have been summarized by Breadmore *et al.* [3] in 2015.

The field strength can be modified by changing the diameter of the channel, but this also alters the hydrodynamic flow velocity proportionally. Thus it is necessary to create a discontinuity by

-2-

modifying the field with the help of an electrode which is in direct or indirect contact with the trapping zone. As described in the reviews, a variety of in-channel arrangements have been proposed. The challenge lies in the avoidance of interference through electrolysis products created at the electrodes (including the possible bubble creation due to oxygen or hydrogen evolution) and in achieving a robust arrangement on a scale that does not introduce bandbroadening. Good implementations are not easily achieved. Alternatively, as in Pressure Assisted Electrokinetic Injection (PAEKI) [6-8], the trapping is carried out at the inlet of the separation channel. However, this can be expected to be still affected by variations in the background conductivity (see *e.g.* the extensive discussions in [9, 10]).

The device reported herein was designed with the intention of avoiding problems with electrolysis products and bubble formation, effects of varying background conductivities of samples and to obain a sharp sample plug inside the capillary for good resolution in the separation step. A sketch of the trapping cell, made from polymethyl methacrylate (PMMA), is given in Fig. 1A. It has the shape of an isosceles trapezoid and contains a flow through channel of 20 mm length with a diameter of 0.4 mm which has two 90°-turns. At these corners the channel is contacted by two cation exchange membranes (Nafion 117, Sigma-Aldrich, St. Louis, MO, USA). The chambers behind these membranes are filled with a buffer solution consisting of 0.5 M 3-(N-morpholino)propanesulfonic acid (MOPS) + 0.5 M sodium MOPS and contain electrodes made from stainless steel. A separation capillary (fused silica, 365 µm OD, 10 µm ID, 50 cm length, Polymicro Technologies, Phoenix, AZ, USA) is mounted perpendicularly at the halfway point of the channel in the trapping device. As illustrated in Fig. 1B, fluid handling of the system is achieved with a pair of 20 µL syringe pumps (SPS01-020-C360, LabSmith, Livermore, CA, USA), 3 two way valves (AV201-T116, LabSmith) and a 4 port selector valve (AV202-C360, LabSmith) which connects either ports A-C and B-D or A-D and B-C. The system is completed with a high voltage DC module capable of delivering up to 500 V (HMD-

-3-

0.5R10-24-5-ER, Hivolt, Hamburg, Germany) and a second module with a maximum voltage of 30 kV (Spellman CZE2000, Pulborough, UK). A purpose made C^4D cell, similar to the one reported by Tanyanyiwa *et al.* [11], placed 20 cm from the inlet, was used for detection and its signal was captured with an e-corder (eDAQ, Denistone East, NSW, Australia) and processed with the Chart software package (eDAQ). All parts of the system were automatically operated using a purpose made graphical user interface software based on Instrumentino [12, 13].

Trapping of anions is achieved by pumping sample through the channel against a voltage applied through the two cation exchange membranes as illustrated in Fig. 1A. This leads to an accumulation of anions in front of the membrane on the left hand side if their electrokinetic velocity is higher than the hydrodynamic flow velocity. The use of the membranes prevents the creation of bubbles in the trapping channel. The current through the membranes is maintained by the transport of cations. It is thought that the charge of the anions pre-concentrated in front of the membrane is balanced by cations passed through the membrane. The fact that the trapping voltage is applied through the membranes directly across the sample solution also leads to the creation of consistent field strengths regardless of the conductivity of the sample.

The process is started by filling the channel with sample solution, followed by a period in which both the hydrodynamic flow and the electric field are applied. The flow through arrangement allows a flexible choice of sample volume. Subsequent to the trapping step the volume of the trapping zone is moved with the help of a syringe pump to the inlet of the separation capillary, where part of it is then injected hydrodynamically by pressurization, followed by flushing of the channel with the electrophoretic background electrolyte. The separation of the trapping zone from the capillary inlet assures a high integrity of the sample plug which enters the capillary. Analysis by zone electrophoresis is then carried out by application of the high voltage across two separate electrodes.

-4-

In Fig. 2 results obtained for formate and nitrate are reported, having mobilities of $56.6 \cdot 10^{-9}$ and $74.1 \cdot 10^{-9}$ $m^2 \cdot s^{-1} \cdot V^{-1}$ respectively (as calculated from the ionic conductivities tabulated in [14]). In Fig. 2A the enhancement factors for the two ions are plotted against different applied hydrodynamic flow rates while keeping the applied voltage constant. It can be seen that the enhancement factors are found to drop for flow rates higher than approximately 400 and 560 $\mu m \cdot s^{-1}$ for formate and nitrate, respectively. The values match very well the expected limits in the flow rates for which trapping should be possible. These were calculated from the mobilities of the ions and the applied field strength of 75 $V \cdot cm^{-1}$ as 424 and 555 $\mu m \cdot s^{-1}$ for the two ions. This clearly demonstrates that the implementation of the concept works. The fact that some enhancement is observed for both ions also for higher flow rates than these maxima must be due to imperfections caused by the laminarity of the hydrodynamic flow and distortion of the electric field in the angled arrangement of the trapping zone in front of the membrane. Sets of experiments were also carried out for field strengths of 35, 150 and 250 $V \cdot cm^{-1}$ and the highest possible flow rates for maximal trapping were also found to correlate well with the expected values.

In Fig. 2B it is shown that the enhancement factor scales linearly with the volume of the sample passed through the cell. The experiment was carried out with a flow velocity of 318 $\mu m \cdot s^{-1}$ and again an applied field strength of 75 $V \cdot cm^{-1}$. Under these conditions both, formate and nitrate are efficiently trapped. It is, however, also possible to selectively trap the ion with the higher mobility, namely nitrate. The mixture of formate and nitrate was passed through the cell at the higher flow velocity of 477 $\mu m \cdot s^{-1}$, which according to prediction and the results of Fig. 2A is too high for efficient trapping of formate. As can be seen in Fig. 2C, nitrate is trapped as efficiently as for the lower flow rate, but as expected, formate is only trapped to a small extent. Why the enhancement factor for formate even drops slightly with increasing volume is not clear.

-5-

The effect of the composition of the solution was then tested. Pre-concentration experiments were carried out for solutions containing 100 µM potassium nitrate and up to 50 mM sodium formate. In all cases, nitrate was successfully pre-concentrated, despite the high background conductivity of the solutions due to the formate salt. An electropherogram for a pre-concentrated standard solution of 100 µM potassium nitrate and 50 mM sodium formate can be seen in Fig. 3A. An expanded view of the nitrate peak is shown in the inset together with the peak for nitrate for the solution not subjected to the trapping experiment demonstrating the increase in concentration achieved for the high ionic background.

Finally, it was examined if the system can be employed for lowering the LODs for CE-C^{4}D by examining the behaviour for the four anions chloride, nitrate, perchlorate and formate. Without carrying out the trapping step LODs of 4, 4.3, 4.2 and 7.2 µM were determined for the 4 anions respectively under the CE-C^{4}D conditions employed. Trapping from a volume of 150 µL with an applied field strength of 150 V·cm^{-1} and a flow velocity of 663 µm·s^{-1} resulted in LODs of 127, 142, 139 and 451 nM. The separation of the ion mixture following pre-concentration from 500 nM, which is well below the LOD without pre-concentration, is shown in Fig. 3B. Note, that the flow velocity of 663 µm·s^{-1} corresponds to a volumetric flow rate of 5 µL·min^{-1} for the set-up employed which means that the trapping experiment for the 150 µL of standard solution had a duration of 30 min.

In conclusion, a fully automated pre-concentration system based on balancing hydrodynamic and electrokinetic flows was built and integrated into a miniaturized capillary electrophoresis instrument. In contrast to the electrokinetic stacking methods employed in capillary electrophoresis, the method has the advantage of working even for high conductivity samples and a discrimination between slow and fast ions could be achieved by adjustment of the flow rate. The results are preliminary and there is room for improvement of the pre-concentration factors and the trapping

-6-

times. Although only anions were tested thus far, the same principle should be applicable for cations as well, using anion-exchange membranes and reverse voltages.

Acknowledgements

References

[1]   Gregus, M., Foret, F., Kubáň, P., *J. Chromatogr. A* 2016, *1427*, 177-185.

[2]   Koenka, I. J., Küng, N., Kubáň, P., Chwalek, T., Furrer, G., Wehrli, B., Müller, B., Hauser, P. C., *Electrophoresis* 2016, *37*, 2368-2375.

[3]   Breadmore, M. C., Tubaon, R. M., Shallan, A. I., Phung, S. C., Keyon, A. S. A., Gstoettenmayr, D., Prapatpong, P., Alhusban, A. A., Ranjbar, L., See, H. H., Dawod, M., Quirino, J. P., *Electrophoresis* 2015, *36*, 36-61.

[4]   Breadmore, M. C., Sänger-Van De Griend, C. E., *LCGC N. Am.* 2014, *32*, 174-186.

[5]   Shackman, J. G., Ross, D., *Electrophoresis* 2007, *28*, 556-571.

[6]   Feng, Y.-L., Zhu, J., *Anal. Chem.* 2006, *78*, 6608-6613.

[7]   Xu, Z., Li, A., Wang, Y., Chen, Z., Hirokawa, T., *J. Chromatogr. A* 2014, *1355*, 284-290.

[8]   D'Ulivo, L., Feng, H. T., *Electrophoresis* 2015, *36*, 1024-1027.

[9]   Hirokawa, T., Koshimidzu, E., Xu, Z., *Electrophoresis* 2008, *29*, 3786-3793.

[10]   Gstoettenmayr, D., Quirino, J., Ivory, C. F., Breadmore, M. C., *J. Chromatogr. A* 2015, *1408*, 236-242.

-7-

[11]   Tanyanyiwa, J., Galliker, B., Schwarz, M. A., Hauser, P. C., *Analyst* 2002, *127*, 214-218.
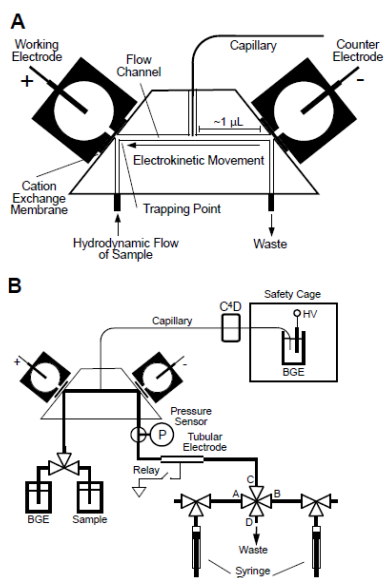
[12]   Koenka, I. J., Sáiz, J., Hauser, P. C., *Comput. Phys. Commun.* 2014, *185*, 2724-2729.

[13]   Koenka, I. J., Sáiz, J., Hauser, P. C., *Chimia* 2015, *69*, 172-175.

[14]   Lide, D. R. E., *CRC Handbook of Chemistry and Physics*, CRC Press, Boca Raton 1995.

Figure Captions:

Fig. 1   A) Pre-concentration cell. B) Microfluidic system. HV = high voltage, BGE = background

electrolyte.

Fig. 2   A) Enhancement factors for nitrate and formate as a function of the applied flow velocity

for an applied field strength of 75 V·cm^{-1} and a volume of 15 µL. Standard solution: 50 µM

potassium nitrate, 100 µM sodium formate. The two vertical lines represent the theoretical

maximal flow rates at which trapping is possible. Injection: 20 s at 100 kPa. Separation

voltage: 25 kV. Background electrolyte: 30 mM histidine, 30 mM acetic acid.

B) Enhancement factors for nitrate and formate as a function of the volume of sample

passed through the trapping cell for an applied flow velocity of 318 µm·s^{-1} and an applied

field strength of 75 V·cm^{-1}. Other conditions as for Fig. 2A.

C) Enhancement factors for nitrate and formate as a function of the volume of sample

passed through the trapping cell for an applied flow velocity of 477 µm·s^{-1} and an applied

field strength of 75 V·cm^{-1}. Other conditions as for Fig. 2A.

-9-
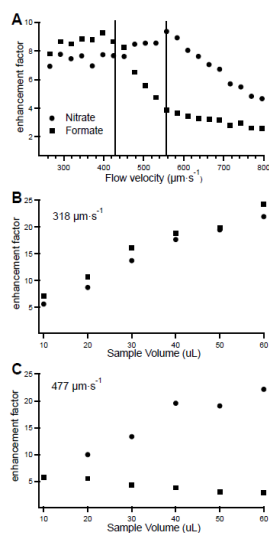
Fig. 3   A) Separation of a pre-concentrated high conductivity standard solution. Hydrodynamic flow velocity: 265 $\mu m \cdot s^{-1}$. Field strength: 35 $V \cdot cm^{-1}$. Standard solution: 15 μL of 100 μM potassium nitrate, 50 mM sodium formate. BGE: 300 mM histidine, 300 mM acetic acid. Other conditions as for Fig. 2A. A magnification of the pre-concentrated nitrate peak (full line) is overlaid on the non-concentrated nitrate peak (dotted line) in the inset.

B) Separation of 500 nM chloride, nitrate, perchlorate and formate following pre-concentration. Hydrodynamic flow velocity: 663 $\mu m \cdot s^{-1}$. Field strength: 150 $V \cdot cm^{-1}$. Volume of standard solution: 150 μL. Other conditions as for Fig. 2A.

-10-

-136-
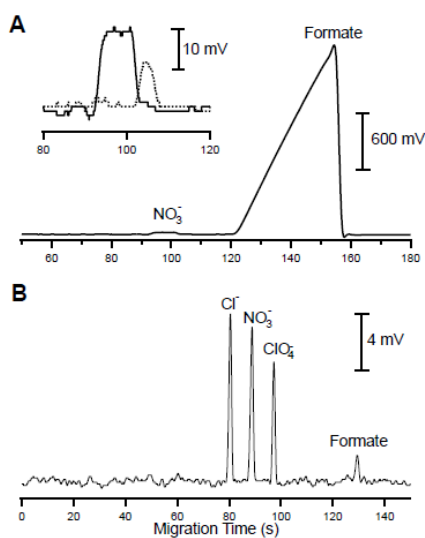
3　References

[1] Stevens, T. S., Cortes, H. J., *Anal. Chem.* 1983, *55*, 1365-1370.

[2] *High Performance Capillary Electrophoresis*, Agilent Technologies, Germany 2000.

[3] Caslavska, J., Koenka, I. J., Hauser, P. C., Thormann, W., *Electrophoresis* 2016, *37*, 699-710.

[4] Thormann, W., Zhang, C. X., Caslavska, J., Gebauer, P., Mosher, R. A., *Anal. Chem.* 1998, *70*, 549-562.

[5] Caslavska, J., Thormann, W., *J. Microcolumn Sep.* 2001, *13*, 69-83.

[6] Sáiz, J., Koenka, I. J., Mai, T. D., Hauser, P. C., García-Ruiz, C., *TrAC, Trends Anal. Chem.* 2014, *62*, 162-172.

[7] Shariff, K., Ghosal, S., *Anal. Chim. Acta* 2004, *507*, 87-93.

[8] Mai, T. D., Hauser, P. C., *Talanta* 2011, *84*, 1228-1233.

[9] Svobodová, J., Beneš, M., Hruška, V., Ušelová, K., Gaš, B., *Electrophoresis* 2012, *33*, 948-957.

[10] Tanyanyiwa, J., Galliker, B., Schwarz, M. A., Hauser, P. C., *Analyst* 2002, *127*, 214-218.

[11] Koenka, I. J., Küng, N., Kubáň, P., Chwalek, T., Furrer, G., Wehrli, B., Müller, B., Hauser, P. C., *Electrophoresis* 2016, *37*, 2368-2375.

[12] Koenka, I. J., Sáiz, J., Rempel, P., Hauser, P. C., *Anal. Chem.* 2016, *88*, 3761-3767.

[13] Gregus, M., Foret, F., Kubáň, P., *J. Chromatogr. A* 2016, *1427*, 177-185.

[14] Mark, D., Haeberle, S., Roth, G., von Stetten, F., Zengerle, R., *Chem. Soc. Rev.* 2010, *39*, 1153-1182.

[15] Manz, A., Graber, N., Widmer, H. M., *Sensors Actuators B: Chem.* 1990, *1*, 244-248.

[16] Becker, H., Locascio, L. E., *Talanta* 2002, *56*, 267-287.

[17] Castro, E. R., Manz, A., *J. Chromatogr. A* 2015, *1382*, 66-85.

[18] Landers, J. P., *Handbook of Capillary and Microchip Electrophoresis and Associated Microtechniques, Third Edition*, CRC Press 2007.

[19] Lim, J., Maes, F., Taly, V., Baret, J.-C., *Lab on a Chip* 2014, *14*, 1669-1672.

[20] Yuen, P. K., *Lab on a Chip* 2008, *8*, 1374-1378.

[21] Bhargava, K. C., Thompson, B., Malmstadt, N., *Proceedings of the National Academy of Sciences* 2014, *111*, 15013-15018.

[22] Kubáň, P., Nguyen, H. T. A., Macka, M., Haddad, P. R., Hauser, P. C., *Electroanalysis* 2007, *19*, 2059-2065.

[23] Kappes, T., Galliker, B., Schwarz, M. A., Hauser, P. C., *Trac-Trends in Analytical Chemistry* 2001, *20*, 133-139.

[24] Kappes, T., Schnierle, P., Hauser, P. C., *Anal. Chim. Acta* 1999, *393*, 77-82.

[25] Thanh Duc, M., Minh Duc, L., Sáiz, J., Hong Anh, D., Koenka, I. J., Hung Viet, P., Hauser, P. C., *Anal. Chim. Acta* 2016, *911*, 121-128.

[26] Nguyen, T. A. H., Pham, T. N. M., Doan, T. T., Ta, T. T., Sáiz, J., Nguyen, T. Q. H., Hauser, P. C., Mai, T. D., *J. Chromatogr. A* 2014, *1360*, 305-311.

[27] Mai, T. D., Schmid, S., Muller, B., Hauser, P. C., *Anal. Chim. Acta* 2010, *665*, 1-6.

[28] Stojkovic, M., Thanh Duc, M., Hauser, P. C., *Anal. Chim. Acta* 2013, *787*, 254-259.

[29] Stojkovic, M., Koenka, I. J., Thormann, W., Hauser, P. C., *Electrophoresis* 2014, *35*, 482-486.

[30] Breadmore, M. C., Shallan, A. I., Rabanes, H. R., Gstoettenmayr, D., Keyon, A. S. A., Gaspar, A., Dawod, M., Quirino, J. P., *Electrophoresis* 2013, *34*, 29-54.

[31] Breadmore, M. C., Tubaon, R. M., Shallan, A. I., Phung, S. C., Abdul Keyon, A. S., Gstoettenmayr, D., Prapatpong, P., Alhusban, A. A., Ranjbar, L., See, H. H., Dawod, M., Quirino, J. P., *Electrophoresis* 2015, *36*, 36-61.

[32] Kazarian, A. A., Hilder, E. F., Breadmore, M. C., *J. Sep. Sci.* 2011, *34*, 2800-2821.

[33] Breadmore, M. C., Saenger-van de Griend, C. E., Majors, R. E., *LC GC North America* 2014, *32*, 174.

[34] D'Ulivo, L., Feng, Y.-L., *Electrophoresis* 2015, *36*, 1024-1027.

[35] Feng, Y. L., Zhu, J. P., *Anal. Chem.* 2006, *78*, 6608-6613.

[36] Feng, Y. L., Lian, H. Z., Zhu, J. P., *J. Chromatogr. A* 2007, *1148*, 244-249.

[37] Feng, Y. L., Zhu, J. O., *Electrophoresis* 2008, *29*, 1965-1973.

[38] Yan, N., Zhou, L., Zhu, Z. F., Zhang, H. G., Zhou, X. M., Chen, X. G., *J. Chromatogr. A* 2009, *1216*, 4517-4523.

[39] Zhang, H. J., Zhu, J. P., Feng, Y. L., *Anal. Sci.* 2010, *26*, 1157-1162.

[40] Zhang, H. J., Gavina, J., Feng, Y. L., *J. Chromatogr. A* 2011, *1218*, 3095-3104.

[41] Zhang, H. J., Zhu, J. P., Aranda-Rodriguez, R., Feng, Y. L., *Anal. Chim. Acta* 2011, *706*, 176-183.

[42] Aranda-Rodriguez, R., Jin, Z. Y., Zhu, J. P., Feng, Y. L., *Anal. Sci.* 2012, *28*, 231-236.

[43] Chien, R. L., Burgi, D. S., *Anal. Chem.* 1992, *64*, 1046-1050.

[44] Burgi, D. S., *Anal. Chem.* 1993, *65*, 3726-3729.

[45] Breadmore, M. C., *Electrophoresis* 2007, *28*, 254-281.

[46] Breadmore, M. C., Wuethrich, A., Li, F., Phung, S. C., Kalsoom, U., Cabot, J. M., Tehranirokh, M., Shallan, A. I., Abdul Keyon, A. S., See, H. H., Dawod, M., Quirino, J. P., *Electrophoresis* 2017, *38*, 33-59.

[47] Aebersold, R., Morrison, H. D., *J. Chromatogr.* 1990, *516*, 79-88.

[48] Aranas, A. T., Guidote, A. M., Quirino, J. P., *Anal. Bioanal. Chem.* 2009, *394*, 175-185.

[49] Zhao, Y. P., Lunte, C. E., *Anal. Chem.* 1999, *71*, 3985-3991.

[50] Gillogly, J. A., Lunte, C. E., *Electrophoresis* 2005, *26*, 633-639.

[51] Shackman, J. G., Ross, D., *Electrophoresis* 2007, *28*, 556-571.

[52] Huang, Z., Ivory, C. F., *Anal. Chem.* 1999, *71*, 1628-1632.

[53] See, H. H., Hauser, P. C., *Anal. Chem.* 2011, *83*, 7507-7513.

[54] See, H. H., Stratz, S., Hauser, P. C., *J. Chromatogr. A* 2013, *1300*, 79-84.

[55] Bier, M., Palusinski, O. A., Mosher, R. A., Saville, D. A., *Science* 1983, *219*, 1281-1287.

[56] Mosher, R. A., Saville, D. A., Thormann, W., *The Dynamics of Electrophoresis*, VCH Publishers, Weinheim 1992.

[57] Breadmore, M. C., Kwan, H. Y., Caslavska, J., Thormann, W., *Electrophoresis* 2012, *33*, 958-969.

[58] Caslavska, J., Thormann, W., *Electrophoresis* 2006, *27*, 4618-4630.

[59] Sáiz, J., Duc, M. T., Koenka, I. J., Martín-Alberca, C., Hauser, P. C., García-Ruiz, C., *J. Chromatogr. A* 2014, *1372*, 245-252.

[60] Bui, D. A., Hauser, P. C., *Sensors and Actuators B-Chemical* 2016, *235*, 622-626.

[61] Koenka, I. J., Sáiz, J., Hauser, P. C., *Comput. Phys. Commun.* 2014, *185*, 2724-2729.

[62] Koenka, I. J., Sáiz, J., Hauser, P. C., *Chimia* 2015, *69*, 172-175.

[63] Sáiz, J., Koenka, I. J., García-Ruiz, C., Müller, B., Chwalek, T., Hauser, P. C., *Electrophoresis* 2015, *36*, 1941-1944.

[64] Torres, N. T., Och, L. M., Hauser, P. C., Furrer, G., Brandl, H., Vologina, E., Sturm, M., Buergmann, H., Mueller, B., *Environmental Science-Processes & Impacts* 2014, *16*, 879-889.

[65] Torres, N. T., Hauser, P. C., Furrer, G., Brandl, H., Mueller, B., *Environmental Science-Processes & Impacts* 2013, *15*, 715-720.

[66] Koenka, I. J., Mai, D. T., Hauser, P. C., Sáiz, J., *Anal. Methods* 2016, *8*, 1452-1456.

[67] Koenka, I. J., Hauser, P. C., *Electrophoresis* 2017, published online, 10.1002/elps.201700071.

4 Curriculum Vitae

Mr. *Israel Joel* **KOENKA**

Date of Birth: August 4th 1983

Nationality: Israeli

Address: Gyöngy u. 2 – 9163 Fehértó – Hungary

Mobile Tel: +36 20 233 1243

Email: joel.koenka@unibas.ch, yoel.koenka@gmail.com

EDUCATION & QUALIFICATIONS

2013 - 2016 PhD student at the University of Basel, Switzerland.

Specialty: Analytical and Bioanalytical Sciences

2009 - 2012 MSc studies at the Technion IIT (Israel Institute of Technology), Israel; Recepient of the special Schulich scholarship.

2006 - 2009 BSc studies at the Technion IIT; Full scholarship from the Technion Excellence program.

Specialty: Molecular Bio-Chemistry

WORK EXPERIENCE

2013-2014 Students lab assistant at the University of Basel.

2007-2011 Teaching assistant at the Technion IIT for the courses "Chemical Thermodynamics", "Physical Chemistry" and "Solid State Physics".

2001 -2006 Embedded systems programmer at the Israeli Defense Force (IDF), Israel.

LANGUAGE & COMPUTER COMPETENCES

Languages: English: *proficient user*

German: *independent user (telc Certificate, level B1)*

Hebrew: *mother language*

Hungarian: *basic user*

Informatics :   Much experience programming in C/C++, Python, Java and Matlab.

Moderate experience with PHP, HTML and LaTeX.

Experience programming in Windows, Linux and Android environments.

5   List of publications, patents and posters

1. Publications and patents between 2013-2017 (in order of appearance)

1.   Marko Stojkovic, **Israel Joel Koenka**, Wolfgang Thormann, Peter C. Hauser

Contactless conductivity detector array for capillary electrophoresis

Electrophoresis (Feb. 2014), 35(4), 482–486

2.   **Israel Joel Koenka**, Jorge Sáiz, Peter C. Hauser

Instrumentino: An open-source modular Python framework for controlling Arduino based experimental instruments

Computer Physics Communications (Oct. 2014), 185(10), 2724–2729

3.   Jorge Sáiz, **Israel Joel Koenka**, Thanh Duc Mai, Peter C. Hauser, Carmen García-Ruiz

Simultaneous separation of cations and anions in capillary electrophoresis

Trends in Analytical Chemistry (Nov. 2014), 62, 162–172

4.   Jorge Sáiz, Mai Thanh Duc, **Israel Joel Koenka**, Carlos Martín-Alberca, Peter C. Hauser, Carmen García-Ruiz

Concurrent determination of anions and cations in consumer fireworks with a portable dual-capillary electrophoresis system

Journal of Chromatography A (Dec. 2014), 1372, 245-252

5.   **Israel Joel Koenka**, Jorge Sáiz, Peter C. Hauser

Instrumentino: An Open-Source Software for Scientific Instruments

Chimia (Apr. 2015), 69(4), 172-175

6. Jorge Sáiz, **Israel Joel Koenka**, Carmen García-Ruiz, Beat Müller, Thomas Chwalek, Peter C. Hauser

   Micro-injector for capillary electrophoresis

   Electrophoresis (Aug. 2015), 36(16), 1941-1944

7. **Israel Joel Koenka**, Thanh Duc Mai, Peter C. Hauser, Jorge Sáiz

   Simultaneous separation of cations and anions in capillary electrophoresis - Recent applications

   Analytical Methods (Feb. 2016), 8(7), 1452-1456

8. Jitka Caslavska, **Israel Joel Koenka**, Peter C. Hauser, Wolfgang Thormann

   Validation of CE modelling with a contactless conductivity array detector

   Electrophoresis (Feb. 2016), 37(5-6), 699–710

9. Thanh Duc Mai, Minh Duc Le, Jorge Sáiz, Hong Anh Duong, **Israel Joel Koenka**, Hung Viet Pham, Peter C. Hauser

   Triple-channel portable capillary electrophoresis instrument with individual background electrolytes for the concurrent separations of anionic and cationic species

   Analytica Chimica Acta (Mar. 2016), 911, 121-128

10. **Israel Joel Koenka**, Jorge Sáiz, Paul Rempel, Peter C. Hauser

    Microfluidic Breadboard Approach to Capillary Electrophoresis

    Analytical Chemistry (Apr. 2016), 88(7), 3761–3767

11.   **Israel Joel Koenka**, Nina Küng, Pavel Kubáň, Thomas Chwalek,

Gerhard Furrer, Bernhard Wehrli, Beat Müller, Peter C. Hauser

Thermostatted dual-channel portable capillary electrophoresis instrument

Electrophoresis (Sep. 2016), 37(17-18), 2368-2375

12.   Jorge Sáiz, Thanh Duc Mai, **Israel Joel Koenka**, Peter C. Hauser

Patent file number EP16200715:

DEVICE AND METHOD FOR CAPILLARY ELECTROPHORESIS

Submitted to the European patent office (Nov. 2017)

13.   **Israel Joel Koenka**, Andres Koller, Peter C. Hauser

Patent file number 00083/17:

ION   CONCENTRATING   APPARATUS,   CAPILLARY   ELECTROPHORESIS
ARRANGEMENT AND METHOD OF CONCENTRATING IONS

Submitted to the Swiss patent office (Jan. 2017)

14.   **Israel Joel Koenka**, Peter C. Hauser

Background conductivity independent counter flow pre-concentration method
for capillary electrophoresis

Published online in Electrophoresis (Feb. 2017)

2. Posters and talks

1.   **Israel Joel Koenka**, Jorge Sáiz, Peter C. Hauser

"Instrumentino: An open-source modular Python framework for controlling Arduino based experimental instruments"

- o   Poster: SCS Fall Meeting 2014, Zurich, Switzerland (Sep. 2014)
- o   Talk: SCS Fall Meeting 2014, Zurich, Switzerland (Sep. 2014) * Best oral presentation prize
- o   Talk: PITTCON, New-Orleans, USA (Mar. 2015)
- o   Poster: ANAKON, Graz, Austria (Mar. 2015)

2.   **Israel Joel Koenka**, Jorge Sáiz, Paul Rempel, Carmen García-Ruiz, Peter C. Hauser

"Breadboard CE - Prototyping electrophoretic separations"

- o   Talk: PITTCON, New-Orleans, USA (Mar. 2015)
- o   Talk: ANAKON, Graz, Austria (Mar. 2015)

3.   **Israel Joel Koenka**, Nina Küng, Pavel Kubáň, Thomas Chwalek, Gerhard Furrer, Bernhard Wehrli, Beat Müller, Peter C. Hauser

"Building a CE for Environmental Samples"

- o   Talk: PCC Seminar, Basel, Switzerland (Nov. 2015)